SIMPLIFIED DESIGN AND INTEGRITY ASSESSMENT OF PRESSURE COMPONENTS AND STRUCTURES

MD. MOSHARRAF HOSSAIN

SIMPLIFIED DESIGN AND INTEGRITY ASSESSMENT OF PRESSURE COMPONENTS AND STRUCTURES

By

Md. Mosharraf Hossain ©

A thesis submitted to the School of Graduate Studies
In fulfillment of the requirement for the degree of
Doctor of Philosophy in Engineering

Faculty of Engineering & Applied Science
Memorial University

August 2009
St. John's, NL, Canada

ABSTRACT

Standard analysis methods of mechanical components and structures are based on elastic analysis, elastic-plastic analysis and limit analysis. The determination of limit load using a simplified method is considered to be an attractive alternative over the conventional limit analysis methods i.e., analytical methods, experimental methods and numerical methods. Simplified methods are considered to be effective if they are able to estimate the lower bound limit load of a general class of mechanical components and structures within a minimum number of linear elastic analysis iteration without compromising with the quality of the result.

In this thesis, a simplified method is proposed in order to estimate the limit load of a general class of mechanical components and structures. The proposed m_α-tangent method makes use of statically admissible stress fields based on a single linear elastic analysis or on an assumed distribution to estimate the limit load. The method is applied to a number of mechanical components and structures ranging from standard example problems to typical pressure vessel components. The results are in good agreement with the corresponding analytical and inelastic finite element analysis results. The underlying features of the m_α-tangent method enabled its application into three major areas: analysis of cracked components, stress categorization and fitness-for-service assessment.

The determination of load carrying capacity is an important step in the integrity assessment of mechanical components and structures containing crack-like flaws. The m_α-tangent method is extended in order to estimate the limit load of components and

structures with cracks. The proposed method enables the determination of limit load using a single linear elastic analysis. The method is applied to a number of cracked component configurations and the results compare well with those obtained from the corresponding analytical and inelastic finite element analysis results.

The ASME Boiler and Pressure Vessel Code can be applied to design pressure vessels and piping systems by using the design by analysis (DBA) approach. It provides guidelines for the classification of linear elastic stresses into primary, secondary and peak stress. Although these guidelines cover a wide range of pressure containing components, the guidelines are sometimes difficult to employ for three dimensional components with complex geometry. In this thesis, a simplified method is proposed in order to categorize the elastic stresses in pressure vessel components and structures using a single linear elastic finite element analysis. It uses the m_α-tangent method, an assessment of constraint in the component based on limit load multiplier estimates, as a stress classification tool. The proposed method is applicable to both mechanical and thermal loads and is able to partition the elastic stresses into primary (P), primary plus secondary (P+Q) and peak (F) stress. The proposed method is a direct and alternative approach over conventional approaches i.e., stress linearization and interaction / discontinuity analysis. The method is applied to several practical pressure vessel components from simple to relatively complex geometric configurations and the results compare favorably with those obtained by the conventional techniques.

Thermal hot spot and corrosion are the typical of damages occurring in operational pressurized components and structures. Fitness-for-service (FFS) assessment of these components and structures need to be performed periodically in order to demonstrate the

operational safety and structural integrity. In this thesis, a simplified method, based on the m_α-tangent method, is proposed in order to perform Level 2 FFS assessment of aging pressure vessel components and piping systems containing thermal hot spot and corrosion damage. The method is demonstrated through a number of examples and the results are verified by Level 3 inelastic finite element analysis.

The potential benefits of using the above mentioned simplified methods over the conventional methods is that the simplified methods are applicable to a wide range of mechanical components and structures; they require minimum expertise from the analyst to perform the analysis; they are economically viable to use on a daily or regular basis; they are computationally effective as they do not require any iterative procedure; and they are very rapid and easy to implement in practice.

ACKNOWLEDGEMENTS

I would like to express my deep gratitude to my supervisor, Dr. R. Seshadri for his intellectual guidance, tireless support and valuable technical discussions during the course of my doctoral program. His vast knowledge and immense expertise in diversified areas provided me with working in industrial projects. I would also like to thank Dr. A. S. J. Swamidas and Dr. S. M. R. Adluri for their help and support. I would also like to thank Dr. S. E. Bruneau for his support and encouragement. I am also thankful to Dr. W. D. Reinhardt, Atomic Energy of Canada Limited (AECL), for valuable technical discussions. The financial support provided by the School of Graduate Studies and the Faculty of Engineering and Applied Science, Memorial University are gratefully acknowledged. I also thank the Associate Dean of Graduate Studies, and acknowledge Ms. Moya Crocker, office of the Associate Dean, for her administrative assistance during the course of my program.

I would like to extend my acknowledgements to my friends in the Asset Integrity Management Research Group for their cooperation. I would like to thank all my friends for their support and encouragement. I also would like to thank Ms. Lisa O'Brien and Ms. Heather O'Brien, Canada Research Chairs' office, for their administrative assistance during the course of my program. Last but not least, I owe my deepest thanks to my wife Shakila Ibrahim; for her continuous support, encouragement and understanding through all four years. I also owe my thanks to my family members for their inspiration and understanding through all these years.

TABLE OF CONTENTS

LIST OF TABLES

LIST OF FIGURES

NOMENCLATURE

List of Symbols

a	Crack length, Half width of a rectangular damage area
b	Half length of a rectangular damage area
A_1, A_2	Bar cross-sectional area
d_0	Nominal outside diameter
$\dot{D}$	Increment of plastic dissipation per unit volume
E	Modulus of elasticity
E_0	Initial modulus
E_j	Joint efficiency
E_s	Secant modulus
$f(s_{ij})$	Yield function
F	Peak stress
h	Shell thickness
h_c	Thickness of corroded area
k	Yield stress in pure shear
L	Length of beam
L_1, L_2	Bar length
m	Exact limit load multiplier
m^0	Upper bound multiplier
m'	Lower bound multiplier from Mura's formulation

m_α	Improved lower bound multiplier
m^*	Kinematically admissible multiplier
m_L	Classical lower bound limit load multiplier
m_u	Classical upper bound limit load multiplier
m_d^0	Upper bound multiplier for damaged component
m_u^0	Upper bound multiplier for undamaged component
M	Bending moment
p	Internal pressure
P	Primary stress, Normal force
p_d	Design pressure
P_m	Primary membrane stress
q	Modulus adjustment index
Q	Secondary stress
Q_b	Secondary bending stress
r_1, r_2, r_3	Fillet radius
R, r	Radius
R_i	Inner radius
R_0	Outer radius
R^0	Ratio of m^0/m
R_L	Ratio of m_L/m
R_α	Ratio of m_α/m
RSF^*	Allowable RSF

RSF_T	*RSF* based on the m_α-tangent multiplier
RSF_α	RSF based on m_α-multiplier
RSF_L	RSF based on classical lower bound multiplier
s_{ij}	Deviatoric stress field
s_{ij}^0	Statically admissible deviatoric stress field under applied load $m^0 T_i$
$\bar{s}_{ij}^0$	Statically admissible deviatoric stress field under applied load T_i
S_{eq}	Equivalent stress
S_T	Surface of the body where surface traction is prescribed
S_v	Surface of the body where velocity is applied
t, t_n	Nominal wall thickness
t_r, t_{rn}	Required minimum wall thickness
T	Temperature
T_i	Applied surface traction
$\dot{u}$	Velocity field
V	Volume of the component
V_C	Volume of corrosion damage
V_H	Volume of hot spot
V_R	Reference volume
V_T	Total volume
V_U	Undamaged adjacent volume
w	Width
x_c	Decay length in the circumferential direction

x_l	Decay length in the meridional direction

Greek Symbols

α	Thermal coefficient of expansion
δ_{ij}	Kronecker delta
ΔT	Temperature difference between hot spot and remaining vessel
ε	Strain
$\dot{\varepsilon}$	Strain rate
$d\varepsilon_{ij}^{P}$	Plastic strain increment
$\dot{\varepsilon}_{ij}^{*}$	Kinematically admissible strain rate
v_i^{*}	Kinematically admissible velocity field
φ^{o}	Point function introduced in the yield criterion
$d\lambda$	Positive scalar of proportionality in the flow rule
μ	Plastic flow parameter
ν	Poisson's ratio
σ_{ij}	Stress tensor
$\sigma_{\max}$	Maximum stress
σ_{eq}	von Mises equivalent stress
σ_{ref}	Reference stress
σ_y	Yield stress
$\sigma_1, \sigma_2, \sigma_3$	Principal stress
ζ	Ratio of m^0/m_L

Subscripts

bar	Two-bar structure
c	Circumferential direction
C	Corroded part of the component
Comp	Component
d	Design pressure
D	Damaged part of the component
e	von Mises equivalent
f	Final quantity
H, h	Parameters inside the hot spot
i	Tensorial index, initial quantity
j	Tensorial index
k	Element numbers
L	Limit, Lower bound
u	Upper bound quantity
U	Undamaged part of the component
α	Parameters based on m_α and m_α -tangent method
y	Yield

Superscripts

0	Statically admissible quantities
b	Bending component
F	Peak component
m	Membrane component
T	Tangent
*	Kinematically admissible quantities

Acronyms

API	American Petroleum Institute
ASME	American Society of Mechanical Engineers
CA	Corrosion Allowance
DBA	Design by Analysis
EMAP	Elastic Modulus Adjustment Procedure
FEA	Finite Element Analysis
FEM	Finite Element Method
FFS	Fitness-for-Service
LTA	Locally Thinned Area
MAWP	Maximum Allowable Working Pressure

NFEM	Nonlinear Finite Element Method
R-Node	Redistribution Node
RSF	Remaining Strength Factor
SCL	Stress Classification Line
SINTAP	Structural Integrity Assessment Procedures
SMYS	Specified Minimum Yield Strength
TBM	Two Bar Model

CHAPTER 1

INTRODUCTION

1.1 General Background

Mechanical and structural designers are continuously working on to develop innovative and reliable design solutions. The main objective in designing mechanical components and structures is to ensure that the structure is able to serve the intended purpose safely at minimum capital and operating costs. In order to design such a structure, the designer should focus on the efficient utilization of material and consider all potential failure modes associated with the structure during its service life. Among the various failure modes that govern the failure of a mechanical component or structure, plastic collapse is considerably important and should be properly addressed.

Standard analysis methods for mechanical components and structures are based on elastic analysis, elastic-plastic analysis and limit analysis. Among these methods, limit analysis

is of considerable interest to the structural engineers as it simplifies the analysis using an elastic perfectly plastic material model and provides a guaranteed margin of safety against load carrying capacity of the structure. Limit analysis could be defined as the determination of load that results in cross-sectional plasticity in the structure, which leads to uncontained plastic flow (plastic collapse). Limit analysis is considered as a viable tool for design, analysis and assessment of mechanical components and structures.

In practice, limit load could be determined either by using analytical methods, numerical methods, experimental methods or by using simplified methods. Analytical methods are based on bounding theorems in plasticity. Application of these methods is generally limited to standard and simple structures. These methods are not suitable for practical complicated three dimensional components and structures. Numerical methods, on the other hand, are applicable to a wide range of practical components and structures. These methods include finite element analysis (FEA), where an elastic perfectly plastic material model is considered. The finite element method is generally accepted by the Codes and Standards (e.g., ASME Boiler and Pressure Vessel Code, 2007) as an alternative method for limit analysis. Inelastic FEA is carried out in an incremental and iterative manner. It requires substantial effort / expertise from the analyst to carryout the analysis. It involves numerical difficulties and demands significant computational time especially in case of complex three dimensional component configurations and loading conditions. It requires detailed information about the material properties at various operating conditions. In addition, the analysis and interpretation of inelastic FEA results require in-depth knowledge and understanding of nonlinear analysis techniques.

Experimental methods are widely accepted as a tool for limit analysis given that the experiments are to be carried out very precisely. In order to perform such experiments for practical complex components and structures, skilled personnel as well as costly experimental setups / instrumentation is required. In practical term, each experiment involves considerable capital investment and hence is not economically viable to perform in a daily basis. Therefore, in-practice, the experimental methods are of very limited use.

In order to overcome the above mentioned limitations of the conventional limit analysis methods, the development of robust and simplified methods is of considerable interest. In recent years, significant efforts have been directed to develop robust and simplified methods. The idea behind the simplified method is that it is able to estimate the limit load by using linear elastic analysis. The potential benefits of using simplified method over the convention methods is that the simplified method is applicable to a wide range of practical components and structures, it requires minimum expertise from the analyst to perform the analysis, it is economically viable to use on a daily or regular basis, it is computationally effective as it does not require any iterative procedure, and it is very rapid and easy to implement in practice.

The integrity assessment of cracked components and structures is of paramount importance in industrial applications. One of the most important elements of the integrity assessment is the estimation of load carrying capacity of the component or structure. Simplified methods are shown to be very effective in determining the limit load of components and structures with crack like flaws.

In conventional design approach, a safety factor is considered to limit the maximum calculated stress level to some percentage of either the yield or ultimate strength of the material at the operating temperature. Design-by-analysis (DBA) using ASME stress categorization approach is a direct application to linear elastic analysis results. ASME Boiler and Pressure Vessel Code, Section III (2007) and Section VIII, Div. 2 (2007) provide guidelines for interpreting the elastic stresses obtained from linear elastic analysis. In these guidelines, the stresses are divided into different categories and allowable stress limits are imposed on each of these categories and specific combinations of the same. The categorization of elastic stresses in pressurized components and structures is a challenging task even with the finest computing facilities and available numerical techniques. Conventional indirect approaches for categorization of stresses are stress linearization and interaction / discontinuity analysis. Use of simplified method for stress categorization is considered to be an attractive alternative over the conventional approaches as the simplified method does not require any stress classification lines or planes; and hence is a direct approach over conventional indirect approaches. The simplified method makes use of statically admissible stress field based on von Mises or Tresca yield criterion to categorize the stresses.

A fitness-for-service assessment of mechanical components and structures is of paramount importance in oil and gas, nuclear and petrochemical industries. The determination of load carrying capacity of the in-service mechanical components and structures is an important goal in structural integrity assessment. Simplified method is considered to be a viable tool for fitness-for-service assessment of aging pressure vessel

components and structures undergoing damage. The simplified method is useful for plant engineers to use on a daily or regular basis.

1.2 Objective of Research

The aim of the present research work is to develop robust and simplified methods in order to design and conduct integrity assessment of mechanical components and structures. The main set of objectives of this thesis is to:

1. Develop a simplified method to estimate the limit load of a general class of mechanical components and structures containing crack-like flaws and those without flaws.

2. Categorize the linear elastic stresses induced in mechanical components and structures by using simplified method, conforming to the available Codes and Standards used for design.

3. Develop simplified method based procedure for Level 2 fitness-for-service (FFS) assessment of pressure vessels and piping systems containing thermal hot spot or corrosion damage.

4. Apply the proposed methods to typical mechanical components and structures and validate the simplified methods by comparing the results with those obtained from the conventional techniques.

1.3 Scope of Research

Limit analysis plays an important role in designing mechanical components and structures. Estimation of limit load by using simplified method is of considerable interest due to its simplicity and effectiveness, in terms of computational effort and time, over the conventional limit analysis techniques. A simplified method is one, which is able to estimate the lower bound limit load of a general class of mechanical components and structures at a minimum number of linear elastic iterations, without compromising with the quality of the results. In this thesis, significant effort has been directed to develop a simplified method for estimation of limit loads of a general class of mechanical components and structures. The method makes use of statically admissible stress field, based on a single linear elastic analysis, in order to estimate the limit loads. Simple equations are deduced that enable rapid determination of reasonably accurate limit loads. The formulation of the proposed method is based on the variational principles in plasticity. The proposed method is applicable to a general class of mechanical components and structures. The method is suggested as a viable tool for limit analysis.

Determination of load carrying capacity is an important goal in structural integrity assessment. Limit analysis plays an important role in integrity assessment of mechanical components and structures containing defects. Crack-like flaws are considered to be a severe threat to the integrity of in-service components and structures. Components containing crack-like flaws could fail either by brittle fracture or ductile tearing depending on the loading and corresponding stress state. The limit load of these components and structures are needed to be determined in order to address the failure by

ductile tearing. Therefore, a simplified method which is able to estimate the load carrying capacity of cracked components and structures is of considerable importance from structural integrity standpoint. In this thesis, a simplified method is proposed for estimations of limit loads of mechanical components and structures containing crack-like flaws.

In designing mechanical components and structures based on ASME design-by-analysis (DBA) approach, elastic stresses are partitioned into primary, secondary and peak stress categories in order to apply the appropriate stress limits for each of these stress categories and for specific combinations of the same. Each of these stress categories and their specific combinations are associated with distinct type of failure modes: primary stress limits are intended to prevent the gross distortion and plastic collapse, primary plus secondary stress limits are intended to prevent the excessive plastic deformation leading to incremental collapse, and the cumulative usage factor from all cycles of primary plus secondary plus peak stress is limited to a specific value, less than or equal to one, to prevent fatigue failure.

In practice, categorization of stresses is a complex task especially in case of complicated three dimensional mechanical components and structures. In this thesis, an attempt has been made to categorize the elastic stresses into primary, primary plus secondary and peak stress by using a single linear elastic finite element analysis, in light of available Codes and Standards (e.g., ASME Boiler and Pressure Vessel Code, Section III and Section VIII Div. 2, 2007). The proposed simplified method makes use of statically admissible stress field based on a single linear elastic analysis. The proposed method is a direct and alternative approach over conventional stress categorization concepts e.g.,

stresses linearization and interaction / discontinuity analysis. The proposed method is applicable to both two and three dimensional pressure vessel components and structures with complex geometries. The proposed method can be applied to both mechanical and thermal loading cases, without requiring two separate analyses.

Fitness-for-service (FFS) assessments are performed in operating plants in order to demonstrate the integrity of in-service components and structures undergoing damage. Thermal hot spots and corrosion are the typical of damages occurring in in-service pressure vessels and piping systems. FFS assessments of these components and structures need to be performed periodically in order to determine the suitability of the component for the prevailing operating conditions and for the assessment of remaining life. Therefore, appropriate assessment methods are needed to assess the serviceability as well as remaining life of the aging components and structures under various operating conditions. In this thesis, a simplified method, based on the m_α-multiplier, is proposed for Level 2 FFS assessment of pressure vessels and piping systems containing thermal hot spot and corrosion damage. The proposed method gives an improved estimate of the remaining strength factor (RSF) of the damaged pressure vessel components and structures. The method is applicable to a wide range of components and structures including the structures experiencing significant stress gradient in and around the damaged spot.

1.4 Organization of the Thesis

This thesis is composed of eight chapters. The first chapter addresses the general background, objective and scope of the proposed research work. The chapter also covers a brief review of state-of-the-art limit load estimation methods and purpose of the present research work.

Chapter 2 presents a comprehensive review of the literature pertaining to the current research work. The chapter covers theoretical aspects of elasticity and plasticity, including failure theories and bounding theorems in plasticity. The chapter also covers a brief review of different limit load multipliers.

Chapter 3 discusses the upper bound and classical lower bound limit load multipliers along with the review of extended variational theorems in limit analysis. The derivation of the m_α method is also presented in this chapter. This method is used as a basis for the development of the proposed simplified method for lower bound limit load estimation.

Chapter 4 presents the proposed simplified method, called the m_α-tangent method, which has been developed for estimation of limit loads of a general class of mechanical components and structures. The m_α-tangent method overcomes the limitations of the m_α method and hence is applicable to any practical mechanical components and structures. The proposed method makes use of statically admissible stress field based on a single linear elastic analysis to estimate the limit load. The method makes use of the "limiting tangent" in order to relate the initial elastic state of a component or structure to that of the exact limit state. The theoretical background, formulation and potential areas

of application of the method are presented in a systematic manner. A number of example problems are worked out to demonstrate the method, and the results are verified by comparing them with those obtained by the conventional analytical and numerical methods.

Chapter 5 presents the extension of the m_α-tangent method, which has been proposed to estimate the limit load of components and structures containing crack-like flaws. Three different procedures are proposed, which covers a wide range of practical components and structures containing crack-like flaws. The method is demonstrated through a number of examples and the results are compared with those obtained from the conventional techniques.

Chapter 6 presents a simplified method to categorize the elastic stresses induced in pressure vessels and piping systems. The method makes use of equivalent stresses (von Mises or Tresca) in order to categorize the stresses. The proposed method is able to categorize the stresses into primary, secondary plus secondary and peak stress, in light of ASME B&PV Code Section III (2007) and Section VIII Div. 2 (2007). The proposed method is a direct and alternative approach over conventional stress categorization approaches, e.g., stress linearization and interaction / discontinuity analysis. The method is applicable to both mechanical and thermal loading cases. The proposed method is demonstrated through a number practical pressure vessel component configuration. The results are compared with those obtained from the conventional techniques.

Chapter 7 discusses the simplified method, based on the m_α-multiplier, which has been developed for Level 2 FFS assessment of pressurized components and structures

containing thermal hot spot and corrosion damage. The proposed method gives an improved estimate of the remaining strength of the damaged pressure vessel components and structures. The method is applicable to a wide range of pressurized components and structures especially the components experiencing significant stress gradient in and around the damage spot. The proposed method is demonstrated through a number of practical examples and the results are verified by Level 3 inelastic finite element analysis.

Chapter 8 summarizes and concludes the contributions and findings present in this thesis. The chapter also presents the original contributions to this thesis along with some guidelines for future work.

CHAPTER 2

LITERATURE REVIEW

2.1 Introduction

The theoretical concepts pertaining to the research work of this thesis are presented in this chapter. The current research work covers an extensive volume of literature particularly in the area of elasticity, plasticity and limit analysis. A brief review of the basic theories of elasticity, plasticity and limit analysis including limit load multipliers is covered. The variational principles in limit analysis are also presented in brief. These theories and concepts are used extensively in the research work presented in this thesis.

2.2 Elastic Analysis and Design Concepts

The theory of elasticity deals with the behavior of solid bodies, which are able to recover their original shape upon removal of the applied loads. The elastic analysis of a mechanical component or structure essentially means the determination of stress and strain fields that simultaneously satisfies the equilibrium equations, compatibility conditions and constitutive relationships. The equilibrium equations are basic physical laws that represent a balance between the applied external forces and/or moments with that of the internal resistive forces and/or moments. On the other hand, compatibility conditions are the geometric relationships that express the continuity of the structure. Stresses are related to the strains by appropriate constitutive relationships.

For a linear elastic solid body, the constitutive relationship is expressed by generalized Hooke's law. The most general relationship between the stresses and strains could be expressed by $\sigma_{ij} = C_{ijkl}\varepsilon_{kl}$, where σ_{ij} is the stress tensor, ε_{kl} is the strain tensor and C_{ijkl} are the material dependent elastic constants.

In case of isotropic material, where all possible symmetries are considered, the elastic strains are related to the stresses according to the following relationship, $\varepsilon_{ij} = \frac{1+\nu}{E}\sigma_{ij} - \frac{\nu}{E}\sigma_{kk}\delta_{ij}$, where ε_{ij} is the strain tensor, σ_{ij} is the stress tensor, E is the Young's modulus, ν is the Poisson's ratio and δ_{ij} is the Kronecker's delta.

In designing mechanical components and structures by using the theory of elasticity, the maximum stress based on certain specified conditions is limited to the *allowable stress* of

the material. The allowable stress is usually defined on the basis of design *safety factor* and *yield strength* of the material at operating temperature.

2.3 Plasticity Concepts

The theory of plasticity deals with the behavior of solid bodies, where the deformation of the body does not fully recover upon removal of the applied loads. The underlying principles and mathematical interpretations of the theory of plasticity and its field of applications are available in a number standard text by Mendelson (1968), Calladine (2000), Hill (1950), Kachanov (1971). In contrast to the theory of elasticity, the stress-strain relationship in plastic range is generally expressed by *Prandtl-Reuss* equation and is characterized as the *flow rule*. In the plastic range, the strains are dependent on the history of loading. Therefore, in order to determine the final strain, the incremental strains must be accumulated over the full loading history. Theory of plasticity is the basis for limit analysis. The limit analysis is an idealized form of elastic-plastic analysis, where an elastic perfectly plastic material model is assumed without considering any strain hardening.

2.3.1 Theories of Failure

In a uniaxial state of stress, the initiation of yielding of the material can be readily determined by simple tensile test. However, when a material is subject to multiaxial state of stresses, then an appropriate yield criterion is needed in order to identify the beginning

of yielding of the material. These yield criteria are generally termed as failure theories. The yield criteria that are pertaining to the current research work are discussed below.

(a) Tresca Yield Criterion (Maximum Shear Stress Theory)

Historically, the first yield criterion for general states of stress was presented by Tresca (Calladine, 2000). The Tresca yield criterion states that the yielding of a material will occur when the maximum shear stress in a multiaxial state of stress reaches the value of the maximum shear stress occurring under simple tension test at onset of yielding. The maximum shear stress is equal to half the difference between the maximum and minimum principal stresses. For simple tension, only one principal stress exists ($\sigma_1 \neq 0$) and the other two principal stresses are equal to zero ($\sigma_2 = \sigma_3 = 0$). If the principal stresses (σ_1, σ_2 and σ_3) are arranged in such a way that $\sigma_1 > \sigma_2 > \sigma_3$, then according to Tresca yield criterion, yielding will occur when $|\sigma_1 - \sigma_3| = \sigma_y$, where σ_y is the yield strength of the material. The Tresca yield criterion takes the form of a *hexagon* in two-dimensional stress space. The size of the hexagon depends on the yield strength of the material. The Tresca yield criterion is used extensively in design because it often simplifies the analysis and design, and is slightly conservative compared to the von Mises yield criterion.

(b) von Mises Yield Criterion (Distortion Energy Theory)

R. von Mises proposed an alternative to Tresca's yield criterion (1912). The formal basis of the von Mises yield criterion is as follows. The *strain energy* is the energy that stored

in the material due to elastic deformation. This deformation can be the combination of volume change and angular distortion without volume change. The energy that is stored in the body due to angular distortion is called the *shear strain energy* or *distortion energy*. The shear strain energy is considered to be the primary cause of failure in ductile material.

The von Mises yield criterion states that the yielding of a material will occur when the distortion energy density in a multiaxial state of stress is equal to the value of the distortion energy that occurs in a simple tensile specimen at the onset of yielding. The von Mises yield criterion can now be expressed as, $\frac{1}{2}[(\sigma_1-\sigma_2)^2+(\sigma_1-\sigma_3)^2+(\sigma_3-\sigma_2)^2]=\sigma_y^2$, where σ_y is the yield strength of the material. The von Mises yield criterion takes the shape of an *ellipse* in two-dimensional stress space. The size of the ellipse depends on the yield strength of the material. It can be seen that the von Mises yield criterion is related to the root-mean-square (R.M.S.) value of the principal stress differences, while the Tresca yield criterion considers only the largest absolute value.

(c) Yield Surface in Three-Dimensional Stress Space

In case of three-dimensional principal stress space, the experimental observation shows that the hydrostatic pressure does not affect the yield behavior of the material as there is no change in shape. This insensitivity of the yield behavior to hydrostatic pressure is the basis for plastic *incompressibility* of the material. Therefore, under hydrostatic pressure loading the state of stress is expected to be purely elastic.

Generally, the yield criterion depends on the complete three-dimensional stress state at the point under consideration. The state of initial yielding of a material can be represented by the following relationship $f(\sigma_{ij}) = K$, where σ_{ij} is the stress tensor in three-dimensional stress space and K is a known quantity. This equation is called the *yield function*. The hypersurface represented by the yield function is called the *yield surface*. Any point on this surface essentially indicates the beginning of yielding. In order to define the yield surface, consider a three-dimensional stress space, where the coordinate axes are represented by three principal stresses $(\sigma_1, \sigma_2, \sigma_3)$. The line having equal subtended angle with the principal coordinate axes represent the hydrostatic stress state ($\sigma_1 = \sigma_2 = \sigma_3 = \sigma_m$), on which the *deviatoric* stress components are equal to zero.

In case of Tresca yield criterion, the shape of the yield surface takes the form of a *hexagonal prism* with the axis $\sigma_1 = \sigma_2 = \sigma_3 = \sigma_m$. On the other hand, the yield surface based on the von Mises yield criterion takes the form of a *cylinder* with the centre line $\sigma_1 = \sigma_2 = \sigma_3 = \sigma_m$. The size of the yield surface depends on the yield strength of the material.

2.3.2 The Plastic Flow Rule

When a material is loaded within the elastic range, the strains are linearly related to the stresses by Hooke's law. In that case, the strains can be computed directly from the current state of stress regardless of the loading history. But in plastic range, the relationship between stresses and strains are nonlinear and the final strain depends on the

history of loading. Therefore, the total strains can be computed by summing the increments of plastic strain throughout the loading history. The onset of yielding is defined by the appropriate yield criterion and the subsequent plastic strain increment is prescribed by the corresponding plastic *flow rule*. The most general form of the plastic flow rule for ideal plasticity is as follows,

$$d\varepsilon_{ij}^{P} = d\lambda \frac{\partial f(\sigma_{ij})}{\partial \sigma_{ij}} \tag{2.1}$$

where $d\varepsilon_{ij}^{P}$ is the plastic strain increment at any instant of loading, $d\lambda$ is the plastic flow parameter, f is a yield function and σ_{ij} is the stress tensor.

The plastic flow parameter $d\lambda$ is equal to zero when the material behaves elastically i.e., $f(\sigma_{ij}) < K$ and takes a positive value when the material behaves plastically i.e., $f(\sigma_{ij}) = K$. The direction cosine of the normal to the yield surface is proportional to $\partial f(\sigma_{ij})/\partial \sigma_{ij}$. Therefore, Eq. (2.1) implies that the plastic flow vector is directed along the normal to the yield surface when plastic flow takes place.

As mentioned earlier, onset of plastic flow is characterized by the appropriate yield criterion. For instance, von Mises yield criterion can be expressed as, $f(s_{ij}) = \frac{1}{2} s_{ij} s_{ij} - k^2$. The *associated* flow rule corresponding to von Mises yield criterion can be expressed as, $d\varepsilon_{ij}^{P} = s_{ij} d\lambda$, where s_{ij} is the deviatoric stress tensor. The plastic strains and stresses are related by the infinitesimal strain increments and deviatoric stresses. Therefore, it is

convenient to divide the strains and strain rates by increment of time and write the equilibrium equations.

2.3.3 Bounding Theorems in Plasticity

Most of the practical engineering components and structures are complicated in nature and hence the complete plastic analyses of these structures are generally more involved and time consuming. The complexities arise from the irreversibility of plastic flow and its dependency on the history of loading. Since the failure prevention is the primary objective of any structural design, therefore, it is justified to concentrate on the collapse state of the structure, which results in a considerable saving of effort.

The plasticity theory offers the well known bounding theorems in order to estimate the collapse load of the structure. There are two approaches, the equilibrium approach for lower bound estimate and the geometry approach for upper bound estimate. The load at plastic collapse is termed as limit load of the structure. In the classical limit analysis, material nonlinearity is included by assuming perfectly plastic material model, while the geometric nonlinearity is not taken into account.

(a) Classical Lower Bound Theorem

The statement of the classical lower bound theorem is as follows: "If any stress distribution throughout the structure can be found, which is everywhere in equilibrium

internally and balances the external loads and at the same time does not violate the yield condition, those loads will be carried safely by the structure" (Calladine, 2000).

Therefore, the load estimated by the lower bound theorem will be less than or at most equal to the exact limit load. In lower bound theorem, the equilibrium equations (statically admissible stress field) and yield condition are satisfied without considering the mode of deformation of the structure.

(b) Classical Upper Bound Theorem

The classical upper bound theorem states that "If an estimate of the plastic collapse load of a body is made by equating the internal rate of dissipation of energy to the rate at which external forces do work in any postulated mechanism of deformation of the body, the estimate will be either high, or correct" (Calladine, 2000).

In upper bound theorem, only the mode of deformation (kinematically admissible velocity fields) and energy balance are considered without considering the equilibrium equations. Applying the principle of virtual work, the upper-bound theorem can be expressed as,

$$\int_{S_T} T_i \dot{u}_i dS \leq \int_{V_T} \dot{D} dV \qquad (2.2)$$

where T_i are the surface tractions acting on surface S_T, $\dot{u}_i$ are the rates of displacement, $\dot{D}$ are the corresponding plastic dissipation rates per unit volume and V_T is the total volume.

2.4 Limit State and Admissible Limit Load Multipliers

Consider a structure with volume V and surface S (Figure 2.1), which is in equilibrium under surface traction T_i applied on surface S_T and the geometric constraint v_i=0 applied on surface S_v. It is assumed that the surface traction is applied in proportional loading, that is, the external traction is assumed to be mT_i, where m is a monotonically increasing parameter. For sufficiently small values of m, the structure will be in a purely elastic state. As m gradually increases, plastic flow starts to occur at a certain point in the structure. If the value of m continues to increase, the plastic region spreads further and the structure will reach to a state of impending plastic collapse.

The set of loads corresponding to the impending plastic collapse state is called the limit load of the structure and the corresponding value of m is the *safety factor*. Therefore, the safety factor is the ratio of the limit load to the actual applied load.

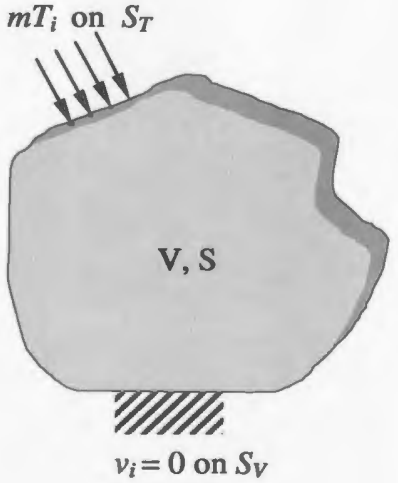

Figure 2.1 A closed domain V bounded by surface S

2.4.1 Classical Statically Admissible Multiplier

A given stress field, σ_{ij}^0 is said to be statically admissible when it is in equilibrium internally, balances the external load $m_s T_i$, and nowhere violates the yield criterion. The multiplier m_s corresponding to such a stress field is called the statically admissible multiplier. Therefore, a statically admissible stress field should satisfy the following conditions,

$$\sigma_{ij,j}^0 = 0 \qquad \text{in } V, \tag{2.3}$$

$$\sigma_{ij}^0 n_j = m_s T_i \qquad \text{on } S_T, \tag{2.4}$$

$$f(s_{ij}^0) = \frac{1}{2} s_{ij}^0 s_{ij}^0 - k^2 \leq 0 \quad \text{in } V, \tag{2.5}$$

where k is the yield stress in pure shear and s_{ij}^0 is the statically admissible deviatoric stress tensor which can be defined as,

$$s_{ij}^0 = \sigma_{ij}^0 - \delta_{ij}\sigma^0 \tag{2.6}$$

$$\sigma^0 = \frac{1}{3}\sigma_{kk}^0 \tag{2.7}$$

where δ_{ij} is the Kronecker delta. Note that Eqs. (2.3 and 2.4) are the equilibrium equations and Eq. (2.5) is the yield function.

2.4.2 Classical Kinematically Admissible Multiplier

A given velocity field, v_i^* is said to be *kinematically admissible* if it satisfies the displacement (velocity) boundary conditions and also the rate of total external work done by the applied loads on this velocity field is positive. Therefore, a kinematically admissible velocity field should satisfy the following conditions,

$$\delta_{ij} v_{i,j}^* = 0 \qquad \text{in } V \tag{2.8}$$

$$v_i^* = 0 \qquad \text{on } S_v \tag{2.9}$$

$$\int_{S_T} T_i v_i^* dS > 0 \tag{2.10}$$

where δ_{ij} is the Kronecker delta. Here, Eq. (2.8) is the condition of incompressibility. The generalized strain-rate vector associated with a given kinematically admissible velocity field can be defined by $\dot{\varepsilon}^*$, where the asterisk is used to indicate that it is not necessarily the actual strain-rate vector but kinematically admissible. If von Mises yield criterion is applied, plastic strains occur when deviatoric stresses are on the yield surface i.e., $\frac{1}{2} s_{ij} s_{ij} = k^2$, where k is the yield stress in pure shear. The kinematically admissible multiplier, m^* can now be expressed as,

$$m^* = \frac{k \int_V (2 \dot{\varepsilon}_{ij}^* \dot{\varepsilon}_{ij}^*)^{1/2} dV}{\int_{S_T} T_i v_i^* dS} \tag{2.11}$$

where

$$\dot{\varepsilon}_{ij}^{*} = \frac{1}{2}(v_{i,j}^{*} + v_{j,i}^{*}) \quad \text{in } V, \tag{2.12}$$

According to the classical limit theorem, the following relation holds,

$$m_s \leq m \leq m^{*} \tag{2.13}$$

where m is the actual collapse load multiplier.

2.5 Closure

A review of the theory of elasticity, plasticity and limit load multipliers is presented in this chapter. The derivation of the admissible limit load multipliers is also presented. These fundamental concepts have been used in the research work presented in this thesis. In the next chapter, the variational theorems in limit analysis and the derivation of the improved lower bound limit load multiplier, the m_α method, is presented. The next chapter also presents a brief review of the limit load analyses methods.

CHAPTER 3

REVIEW OF LIMIT LOAD MULTIPLIERS

3.1 Introduction

Limit analysis plays an important role in design and integrity assessment of mechanical components and structures. Limit load is the load at which uncontained plastic flow (plastic deformation) occurs in a perfectly plastic structure, and the structure is on the verge of collapse. Limit load is a quantitative measure of the load carrying capacity of such a structure. Limit analysis is especially attractive as it simplifies the inelastic analysis by assuming an elastic perfectly plastic material model.

Lower bound limit load is the load that a structure is able to carry out safely during its service life. There is no permanent deformation of the structure. It is the maximum load that a structure is expected to experience in its service life. Lower bound limit load is especially attractive as it provides a guaranteed margin of safety against load controlled plastic failure modes. The limit load multiplier scales the applied load proportionally to that level where the structure reaches to its limit state. The exact limit load multiplier is available only by performing a plastic limit analysis. Several estimates and bounds of the exact limit load multiplier can be obtained from an elastic analysis. Some of these are discussed below.

3.2 Classical Lower Bound Multiplier

The lower bound multiplier can be directly obtained by applying the lower bound theorem of plasticity. Assuming that some stress distribution throughout the component or structure can be found, which is everywhere in equilibrium internally, balances the external loads and at the same time does not violate the yield condition. Then the corresponding applied loads will be less than or equal to the exact limit load, and will be carried safely by a sufficiently ductile material. If σ_y is the yield strength of the elastic-perfectly plastic material, then the classical lower bound multiplier (m_L) can be expressed as

$$m_L = \frac{\sigma_y}{\sigma_{\max}}; \quad P_L = P\, m_L \tag{3.1}$$

where P is the applied load and P_L is the limit load.

Statically admissible stress distributions can be constructed by "inspection", or by using a closed form linear elastic solution. When a finite element analysis is performed, the stress distribution inside each element is approximate. Therefore, m_L obtained from linear elastic FEA is a mesh dependent estimate that is expected to converge to the exact value as the mesh is refined successively.

3.3 Upper Bound Multiplier

In limit analysis, the statically admissible stress field (equilibrium set) cannot lie outside the yield surface and the stress associated with a kinematically admissible strain rate field (compatibility set) in calculating the plastic dissipation should lie on the yield surface. Mura et al. (1965) proposed an approach that eliminates such a requirement and replaced it by the concept of *integral mean of yield* based on a variational formulation. The integral mean of yield criterion can be expressed as,

$$\int_{V_T} \mu^0 \left[f(\bar{s}_{ij}^0) + (\varphi^0)^2 \right] dV = 0 \tag{3.2}$$

where $\bar{s}_{ij}^0$ is the statically admissible deviatoric stress for impending plastic flow; φ^0 is a point function which takes on a value of zero if $\bar{s}_{ij}^0$ is at yield and remains positive below yield. The flow parameter μ^0 is defined through the associated flow rule as,

$$\dot{\varepsilon}_{ij} = \mu \frac{\partial f}{\partial s_{ij}} \tag{3.3}$$

where $\mu^0 \geq 0$ (statically admissible set) and $\dot{\varepsilon}_{ij}$ is the strain rate. Now, $\bar{s}_{ij}^0 = m^0 \, s_{ij}^0$ where s_{ij}^0 corresponds to the applied traction, T_i. The von Mises yield criterion can be expressed as,

$$f(s_{ij}) = \frac{3}{2} \bar{s}_{ij} \bar{s}_{ij} - \sigma_y^2 \tag{3.4}$$

Assuming an unspecified but constant flow parameter μ^0 and performing the necessary mathematical manipulations Eq. (3.4) becomes (Seshadri and Mangalaramanan, 1997),

$$m^0 = \frac{\sigma_y \sqrt{V_T}}{\sqrt{\int_{V_T} (\sigma_{eq})^2 \, dV}} \; ; \; \varphi^0 = 0 \tag{3.5}$$

where σ_{eq} is the von Mises equivalent stress and V_T is the total volume. Proof of the upper-boundedness of m^0 is presented by Reinhardt and Seshadri (2003).

3.4 Extended Variational Theorems in Limit Analysis

The variational formulation, proposed by Mura et al. (1963, 1965), is an alternate approach to the classical limit theorem. Seshadri and Mangalaramanan (1997) proposed the m_α-method based on Mura's variational theorem, which provides better lower bound limit load over Mura's lower bound estimate. The m_α-method adopted the elastic modulus adjustment procedure (EMAP) to estimate improved lower bound limit load. Further discussion on these methods is presented in the following sections of this chapter.

Mura et al. showed by using the variational principles that the safety factor, the statically admissible multiplier and the kinematically admissible multiplier for a component or structure made of elastic perfectly plastic material model and subjected to prescribed surface tractions are actually extremum values of the same functional under different constraint conditions.

In limit analysis, the statically admissible stress field (equilibrium set) cannot lie outside the yield surface and the stress associated with a kinematically admissible strain rate field (compatibility set) in calculating the plastic dissipation should lie on the yield surface. Mura et al. proposed an approach that eliminates such a requirement and replaced it by the concept of *integral mean of yield* based on a variational formulation. The integral mean of yield criterion can be expressed as,

$$\int_{V_T} \mu^0 [f(\bar{s}_{ij}^0) + (\varphi^0)^2] dV = 0 \qquad (3.6)$$

where the superscript "0" refers to the statically admissible equilibrium stress fields and μ^0 is the plastic flow parameter. The deviatoric stress $\bar{s}_{ij}^0$ corresponds to the impending limit state, where $\bar{s}_{ij}^0 = m^0 s_{ij}^0$. Here, m^0 is the limit load multiplier and s_{ij}^0 is the deviatoric stress field that is in equilibrium with the applied loads. The parameter φ^0 is a point function that takes a value of zero if $\bar{s}_{ij}^0$ is at yield and remains positive below yield.

A lower bound limit load multiplier m' is derived from Mura's extended variational principle, which is smaller than the unknown actual collapse load multiplier *m*. Mura's lower bound multiplier can be expressed as,

$$m' = \frac{m^0}{1 + \max[\{f(\bar{s}_{ij}^0) + (\varphi^0)^2\}/2k^2]} \leq m \tag{3.7}$$

The von Mises yield criterion is given by, $f(\bar{s}_{ij}) = \frac{3}{2} s_{ij} s_{ij} - \sigma_y^2$ and the associated flow rule can be expressed as, $\dot{\varepsilon}_{ij} = \mu(\partial f(s_{ij})/\partial s_{ij})$ where $\mu \geq 0$. Mura et al. have shown that m^0, μ^0 and φ^0 can be determined by rendering the functional F stationary in,

$$F = m^0 - \int_{V_T} \mu^0 [f(s_{ij}^0) + (\varphi^0)^2] dV \tag{3.8}$$

which leads to the set of equations,

$$\frac{\partial F}{\partial m^0} = 0, \quad \frac{\partial F}{\partial \mu^0} = 0, \quad \frac{\partial F}{\partial \varphi^0} = 0 \tag{3.9}$$

For von Mises yield criterion, the functional takes the form,

$$F = m^0 - \int_{V_T} \mu^0 \left[\frac{3}{2} (m^0)^2 s_{ij}^0 s_{ij}^0 - \sigma_y^2 + (\varphi^0)^2 \right] dV \tag{3.10}$$

Assuming a constant flow parameter μ^0 and setting $\delta F = 0$, the above functional can be solved for $\varphi^0 = 0$ as,

$$m^0 = \frac{\sigma_y \sqrt{V_T}}{\sqrt{\int_{V_T} (\sigma_{eq})^2 dV}} \tag{3.11}$$

where σ_{eq} are the equivalent stress and V_T is the total volume of the component or structure. Eq. (3.2) for m' can now be written in terms of the maximum equivalent stress σ_M^0 in a component or structure as,

$$m' = \frac{2m^0\sigma_y^2}{\sigma_y^2 + (m^0)^2(\sigma_M^0)^2} \tag{3.12}$$

3.5 The m_α- Method

The lower bound limit load multiplier (m') obtained from Mura's extended variational theorem was shown to be less than that obtained by applying classical lower bound theorem. As an attempt for improved estimation of lower bound limit loads, Seshadri and Mangalaramanan (1997) proposed the m_α-method by invoking the notion of *reference volume* to account for localized plastic collapse and the technique of *leapfrogging* to reach to the limit state. The iteration variable ζ was introduced in such a way that an infinitesimal changes to the elastic modulus of various elements in successive elastic analysis would induce a corresponding change of $\Delta\zeta$. As ζ increases with iterations therefore, m^0 and m' should ideally converge uniformly to exact value of the safety factor, m.

3.5.1 Local Plastic Collapse - The Reference Volume

When plastic collapse occurs in the localized region of a component or structure, the value of upper bound multiplier m_1^0 will be overestimated if it is calculated based on the

total volume, V_T, as in Eq. (3.6). Furthermore, the corresponding value of m' will be underestimated. The reference volume was introduced in order to identify the *kinematically active* portion of the component or structure that participates in plastic action. If V_R is the reference volume, then $V_R \leq V_T$ and hence the upper bound multiplier can be written as,

$$m_1^0(V_R) = \frac{\sigma_y \sqrt{V_R}}{\sqrt{\sum_{k=1}^{\alpha} (\sigma_{ek}^0)^2 \Delta V_k}} \tag{3.13}$$

where

$$V_R = \sum_{k=1}^{\alpha} (\Delta V_k), \quad \text{and} \quad \alpha < N \tag{3.14}$$

The elements are arranged in following sequences,

$$(\sigma_{e1}^0)^2 \Delta V_1 > (\sigma_{e2}^0)^2 \Delta V_2 > \ldots\ldots\ldots > (\sigma_{en}^0)^2 \Delta V_n \tag{3.15}$$

Mura's lower bound multiplier can be expressed in terms of the iteration variable ζ as,

$$m'(\zeta) = \frac{2m^0(\zeta)\sigma_y^2}{\sigma_y^2 + [m^0(\zeta)]^2 [\sigma_M^0(\zeta)]^2} \tag{3.16}$$

where $\sigma_M^0(\zeta)$ is the maximum equivalent stress at iteration number "*i*". The quantities m', m^0 and σ_M^0 are all functions of ζ. Differentiating the both sides of the above equation with respect to ζ, we get,

$$\frac{dm'}{d\zeta} = \frac{\partial m'}{\partial m^0}\frac{dm^0}{d\zeta} + \frac{\partial m'}{\partial \sigma_M^0}\frac{d\sigma_M^0}{d\zeta} \tag{3.17}$$

In terms of finite difference, Eq. (3.12) can be expressed as,

$$\Delta m' = \left.\frac{\delta m'}{\delta m^0}\right|_{\zeta_i} .(\Delta m^0) + \left.\frac{\delta m'}{\delta \sigma_M^0}\right|_{\zeta_i} .(\Delta \sigma_M^0) \tag{3.18}$$

where $\zeta = \zeta_i$ corresponds to the i^{th} iteration. For a limit type state (ζ_∞), we define,

$$\begin{aligned} \Delta m' &= m_\alpha - m_i' \\ \Delta m^0 &= m_\alpha - m_i^0 \\ \sigma_M^0 &= \frac{\sigma_y}{m_\alpha} - \sigma_{Mi}^0 \end{aligned} \tag{3.19}$$

where m_α is the value to which m' and m^0 are expected to converge. Combining Eq. (3.13) and (3.14) and carrying out the necessary algebraic manipulations, the following quadratic equation can be obtained,

$$Am_\alpha^2 + Bm_\alpha + C = 0 \tag{3.20}$$

where

$$\begin{aligned} A &= \left(m_i^0 \sigma_{Mi}^{-0}\right)^4 + 4\left(m_i^0 \sigma_{Mi}^{-0}\right) - 1 \\ B &= -8m_i^0\left(m_i^0 \sigma_{Mi}^{-0}\right)^2 \\ C &= 4\left(m_i^0\right)^3 \sigma_{Mi}^{-0} \end{aligned} \tag{3.21}$$

and $\sigma_{Mi}^{-0} = \dfrac{\sigma_{Mi}^0}{\sigma_y}$

The coefficients *A, B, C* and finally, the value of m_α can be evaluated from the results of any linear elastic FEA. Although the m_α-method was intended for two iterations at first, increasing iterations would give better estimates provided certain conditions are satisfied. To ensure real roots for Eq. (3.20), the discriminant must be greater than zero, i.e.,

$$m_i^o \sigma_{Mi}^{-o} \leq 1 + \sqrt{2} \tag{3.22}$$

3.5.2 Expression for Lower Bound Multiplier m_α

Reinhardt and Seshadri (2003) derived an expression for the lower bound limit load multiplier m_α from the equation $m' = f(m_L, m^0)$. If m_L and m^0 are derived from a series of stress and strain distributions that converge to the collapse state, then m' is assumed to follow a line that ends at $m = m_L = m' = m^0$. From current iteration ζ, estimate of the final solution is made by linear extrapolation along the tangent to the curve $m'(\zeta)$. The differentiation of the equation $m' = f(m_L, m^0)$ with respect to the iteration variable ζ is as follows,

$$\frac{dm'}{d\zeta} = \left(\frac{\delta m'}{\delta m^0}\right)_{\zeta_i} \frac{dm^0}{d\zeta} + \left(\frac{\delta m'}{\delta \frac{1}{m_L}}\right) d\frac{\frac{1}{m_L}}{d\zeta} \tag{3.23}$$

It is postulated that the trajectory ends at $m = m_L = m' = m^0$ and by doing so, m_α is expected to give a reasonable estimate of the multiplier *m* if the values of m_L and m^0 are

sufficiently close to the exact limit load multiplier m. In terms of finite difference, Eq. (3.18) can be written as,

$$m' - m_\alpha = 2\frac{1-\left(\frac{m^0}{m_L}\right)^2}{\left[1+\left(\frac{m^0}{m_L}\right)^2\right]^2}\left(m^0 - m_\alpha\right) - 4\frac{\left(m^0\right)^3}{m_L\left[1+\left(\frac{m^0}{m_L}\right)^2\right]^2}\left(\frac{1}{m_L}-\frac{1}{m_\alpha}\right) \tag{3.24}$$

Solving the above equation for m_α, we get

$$m_\alpha = 2m^0\frac{2\left(\frac{m^0}{m_L}\right)+\sqrt{\frac{m^0}{m_L}\left(\frac{m^0}{m_L}-1\right)^2\left(1+\sqrt{2}-\frac{m^0}{m_L}\right)\left(\frac{m^0}{m_L}-1+\sqrt{2}\right)}}{\left(\left(\frac{m^0}{m_L}\right)^2+2-\sqrt{5}\right)\left(\left(\frac{m^0}{m_L}\right)^2+2+\sqrt{5}\right)} \tag{3.25}$$

The m_α-method has been shown to provide reasonable estimate of limit loads of various mechanical components and structures.

3.6 Review of Limit Load Analysis Methods

Seshadri and Fernando (1992) have developed the Redistribution Node (R-ode) method in order to determine the lower bound limit load of mechanical components and structures, using the elastic modulus adjustment procedure (EMAP) and by adopting the concepts of reference stress in creep analysis. The R-Node method makes use of two linear elastic finite element analyses to identify the load controlled location(s) in the structure and the limit load of the structure is achieved by using the load controlled

stresses. The R-Node method is further extended by Seshadri and Marriott (1993) to categorize the linear elastic stresses in mechanical components and structures. Seshadri and Mangalaramanan (1997) have used the R-Node method for minimum weight design of pressure vessel components and structures. Famous and Seshadri (2005) have used the R-Node method to estimate the limit load of components and structures subjected to multiple loadings. Other applications of the R-Node method are available in the monograph by Seshadri (1998).

Seshadri and Mangalaramanan (1997) have developed the upper bound multiplier m_1^0 using the integral mean of yield criterion (Mura *et al.*, 1965) and further details are available in Section 3.3 of this thesis. The m_1^0 multiplier is shown to be greater than the classical lower bound multiplier (m_L) and lower than the classical upper bound multiplier (m_U) (Reinhardt and Seshadri, 2003). The m_1^0 multiplier is based on the total volume of the component or structure. If plastic collapse occurs over a localized region of the component or structure, the m_1^0 multiplier will be overestimated. In order to overcome this limitation, Pan and Seshadri (2001) have proposed the m_2^0 multiplier by invoking the concept of reference volume.

Seshadri and Indermohan (2004) have developed the m_β method by making use of the integral mean of yield criterion in order to estimate the limit load of mechanical components and structures. The m_β multiplier relies on the entire stress distribution rather than the maximum stress in the component or structure.

3.7 Closure

Mura's variational formulation and the corresponding limit load multipliers have been presented in this chapter. The classical lower bound multiplier and upper bound multiplier based on Mura's variational formulation is also presented. The derivation of the improved lower bound limit load estimation method, the m_α-method, has also been presented in detail. The chapter also covered a brief review of the simplified methods in limit analysis. The following chapter represents the m_α-tangent method, which has been developed under the scope of this thesis to estimate the limit load of a general class of mechanical components and structures. The formal basis of the proposed simplified method is the m_α-method, which has been developed by Seshadri and Mangalaramanan (1997).

CHAPTER 4

THE m_α-TANGENT METHOD

4.1 Introduction

The assessment of load carrying capacity under applied loads is an important goal in designing mechanical components and structures. Limit load analysis is performed in order to determine the load at which uncontained plastic flow (plastic collapse) occurs in the component or structure. Lower bound limit loads are especially relevant from design standpoint since they provide a guaranteed margin of safety against load controlled plastic failure modes, or the related primary stress limits contained in the ASME Boiler and Pressure Vessel Code (2007). The concept of reference stress (Webster and Ainsworth, 1994), used extensively in the United Kingdom in high temperature integrity assessment procedures and inelastic fracture evaluations (Ainsworth et al., 2000), is related to the limit load.

The conventional method for limit analysis includes analytical method, experimental method, and numerical method e.g., nonlinear finite element method. Analytical methods have a very limited application in real-life as these methods are based on simplified assumptions and are particularly applicable to standard classical problems and simple structures. It is practically impossible to apply the analytical methods in order to estimate the limit load of complex three dimensional mechanical components and structures.

On the other hand, experimental methods are widely used as a practical tool for limit load estimation. These methods are accepted by the structural design community as a viable tool for limit load estimation. However, these methods are not always cost effective as they require expensive set-ups as well as experienced professional to run the experiment precisely.

Nonlinear finite element methods are widely used in determining the limit load. These methods are accepted by the Code (ASME B&PV Code, 2007) as a standard method to estimate the limit load of mechanical components and structures. However, these methods are not effective in terms of computational effort and time, especially when applied to practical three dimensional components and structures subjected to complex loading. These methods work on iterative procedure and sometimes face convergence problems.

4.2 Simplified Method in Limit Analysis

There are several practical advantages of using limit analysis as a tool for mechanical structural design. Limit analysis provides a guaranteed margin of safety over the load

carrying capacity of the structure. As discussed earlier, conventional methods of limit analyses have their own limitations in terms of applicability and cost effectiveness. As a result, simplified methods drew significant attention of structural design community to use these methods as an alternative tool over the conventional limit analysis techniques. The simplified methods are shown to be effective in terms computational effort and time. Significant efforts have been directed over the recent years in order to develop robust and simplified methods to estimate the limit loads. A simplified method is one, which is able to estimate the lower bound limit load of a general class of mechanical components and structures at a minimum number of linear elastic iteration without compromising with the quality of the result.

In this thesis, significant effort have been directed to develop a robust and simplified method in order to estimate the limit load of a general class of mechanical components and structures. The proposed m_α-tangent method makes use of statically admissible stress field based on a single linear elastic analysis or assumed fields to estimate the limit load. The formulation of the method is based on the variational principles in plasticity. The method is shown to be rapid and easy to implement in practice.

The method is demonstrated through a number of mechanical components and structures ranging from standard example problems to typical pressure vessel component configurations. The results are in good agreement with the corresponding analytical and inelastic finite element analysis results. The detailed derivation of the m_α-tangent method is presented in the following sections of this chapter.

4.3 Beyond the m_α-Method

The m_α multiplier method was developed by Seshadri and Mangalaramanan (1997) on the basis of variational considerations. The m_α multiplier depends on the parameters m^0 and m_L, and can be expressed as

$$m_\alpha = 2m^0 \frac{2\left(\frac{m^0}{m_L}\right)^2 + \sqrt{\frac{m^0}{m_L}\left(\frac{m^0}{m_L}-1\right)^2\left(1+\sqrt{2}-\frac{m^0}{m_L}\right)\left(\frac{m^0}{m_L}-1+\sqrt{2}\right)}}{\left(\left(\frac{m^0}{m_L}\right)^2+2-\sqrt{5}\right)\left(\left(\frac{m^0}{m_L}\right)^2+2+\sqrt{5}\right)} \tag{4.1}$$

The m_α multiplier is an improved estimate of the analytical limit load multiplier compared to the bounds m_L and m^0. Although it is often found to be an improved lower bound, it could not be established as a lower bound in general. The issue of lower-boundedness of m_α has been discussed by Reinhardt and Seshadri (2003). Rewriting the expression for m_α by normalizing with the (usually unknown) exact multiplier (m), the following equation can be obtained

$$R_\alpha = 2R^0\left[\frac{2\zeta^2+\sqrt{\zeta(\zeta-1)^2(1+\sqrt{2}-\zeta)(\zeta-1+\sqrt{2})}}{(\zeta^2+2-\sqrt{5})(\zeta^2+2+\sqrt{5})}\right] \tag{4.2}$$

where $\zeta = m^0/m_L$, $R_0 = m^0/m$ and $R_\alpha = m_\alpha/m$. Due to normalization, R_α=1 represents the boundary between the upper bound region ($R_\alpha > 1$) and lower bound region ($R_\alpha < 1$) as shown in Figure 4.1. The value of m_α becomes imaginary when $m^0/m_L > 1+\sqrt{2}$, as would be the case for components with notches and cracks.

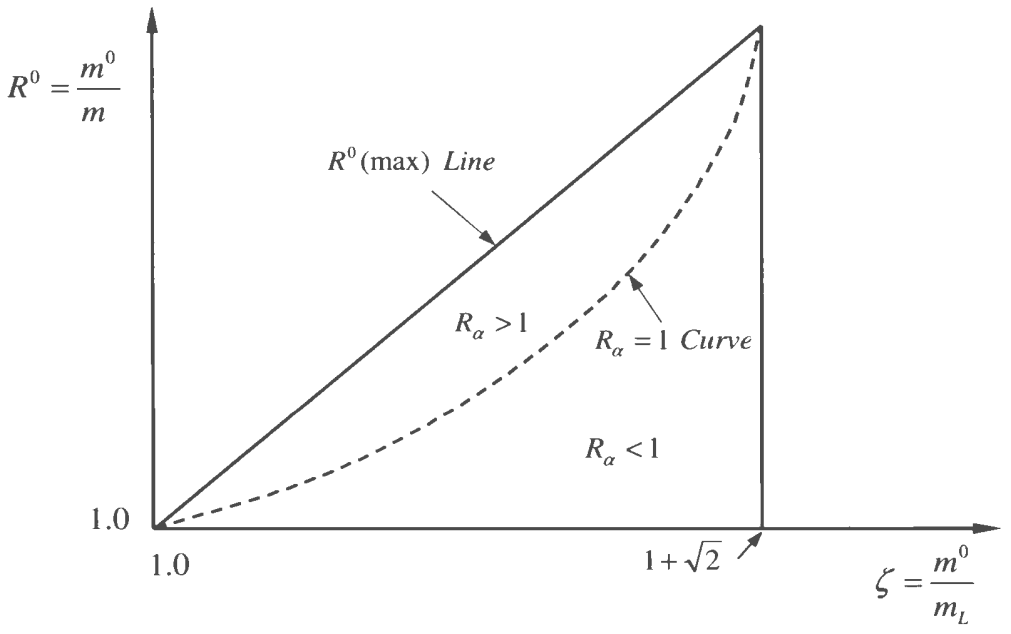

Figure 4.1 Regions of lower and upper bounds of m_α

In Eq. (4.2), the exact multiplier (m) for a component being analyzed is generally unknown. As well, m^0/m_L which is equal to $((\sigma_e)_{\max}/\sigma_{ref})$ is a measure of the theoretical stress-concentration factor of the notch. The region bounded by $m^0(max)$, $1 \le m^0/m_L \le 1+\sqrt{2}$ and $1 \le m^0/m \le 1+\sqrt{2}$ is designated as the "m_α triangle".

Due to the behavior of the two bounds in response to local stress concentration that was discussed above, the ratio m^0/m_L can become large for components with notches and cracks, and fall outside the domain where m_α is defined. Therefore, the m_α multiplier method is not applicable if a component falls outside the "m_α triangle". In order to overcome these limitations, the m_α–tangent method is developed in the present thesis. The m_α–tangent method can take practically any value of m^0/m_L, which extended the

domain of application of the proposed m_α–tangent method beyond the "m_α triangle". Therefore, the m_α–tangent method is applicable to a general class of mechanical components and structures containing significant amount of peak stresses. The underlying concepts, formulation, and detail derivation of the proposed m_α–tangent method is presented in the following sections of this chapter.

4.4 The Constraint Map

General pressure vessel components subjected to mechanical and thermal loads are made up of primary, secondary and peak stresses. The plot of m^0/m versus m^0/m_L in the context of iterative EMAP (Elastic Modulus Adjustment Procedure) represents the trajectory signifying a progressive loss of constraint from an initial elastic state to a plastic collapse state (Seshadri and Adibi-Asl, 2007), which is called "constraint map" (Figure 4.2).

It should be noted that the upper bound multiplier m^0 is based on the overall statically admissible stress distribution in the component whereas the classical lower bound multiplier m_L depends on the maximum stress in the component. Therefore, m_L is sensitive to peak stresses whereas m^0 is almost insensitive to peak stresses and hence is invariant while blunting of peak stresses. The ratio m^0/m_L represents a combination of primary, secondary and peak stresses. At the origin, the stresses are purely primary (limit state), and therefore load controlled. The ratio $m^0/m_L>1$ points to the existence of secondary and peak stresses, in addition to primary stresses.

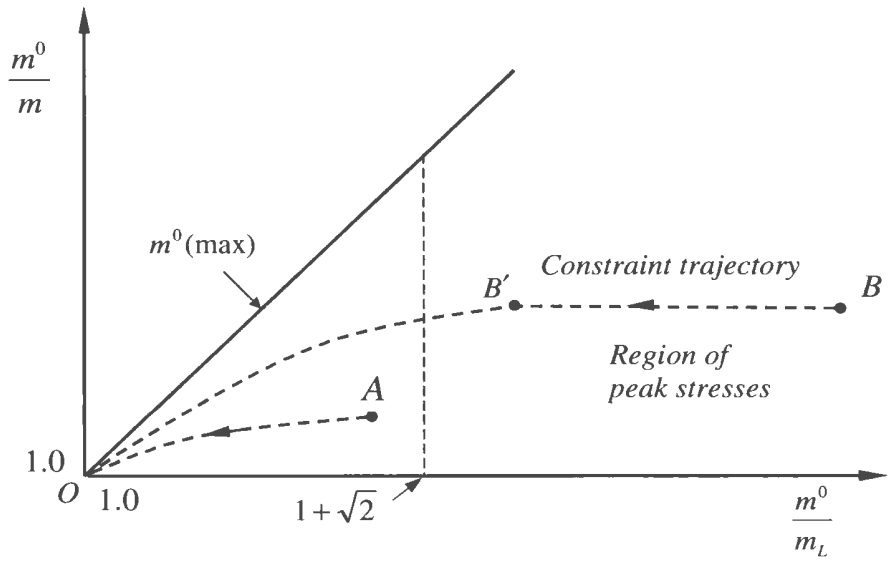

Figure 4.2 The constraint map

The ratio m^0/m represents a combination of primary and secondary stresses for which $m^0/m>1$. A trajectory that proceeds towards the origin with a continuous reduction in the magnitudes of m^0/m_L and m^0/m, points to a corresponding reduction in the degree of "statical indeterminacy". In this context, the plot of m^0/m_L versus m^0/m is a "constraint map" in which the m^0, m_L and m are essentially "scalar measures".

Points A and B in Figure 4.2 represent the state of static indeterminacy of a given component or structure. The constraint trajectory AO and $BB'O$ can be generated for a general class of mechanical components and structures. For most of the components BB' is nearly horizontal and represents the blunting of peak stresses. Therefore, m^0 is almost invariant while m_L increases as m^0/m_L decreases. If m^0/m_L is less than $1+\sqrt{2}$, which corresponds to point A in Figure 4.2, the peak stress in the component is expected to be either zero or negligible.

According to Figure 4.2, if we proceed from B to B' along the constraint trajectory, the peak stress will be gradually redistributed due to their deformation controlled nature. The peak stress of the component is redistributed by suitably adjusting the elastic modulus of the elements, in a finite element discretization scheme, stressed above reference stress level (where $\sigma_{ref} = \sigma_y/m^0$).

The modulus adjustment formula is as follows:

$$E^{i+1} = \left(\frac{\sigma_{ref}}{\sigma_{eq}^{i}} \right)^{q} E^{i} \tag{4.3}$$

This formula describes how the elastic modulus at a location with the equivalent stress σ_{eq} (e.g., von Mises equivalent stress) is updated from i^{th} to the $(i+1)^{th}$ linear elastic iteration while plotting the constraint trajectory. It should be noted that the constraint trajectory and the location of point A, B, and B' (Figure 4.2) are problem dependent, i.e., it depends on the geometry, loading, and boundary conditions of the component under consideration. The formal basis for $1+\sqrt{2}$ will be discussed in the following sections of this chapter.

4.5 Reference Two-Bar Model (TBM)

General pressure vessel component configurations can be related to the reference two-bar structure by using the "integral mean of yield" criterion. Seshadri and Adibi-Asl (2007) have derived the "scaling equations" as follows (Figure 4.3):

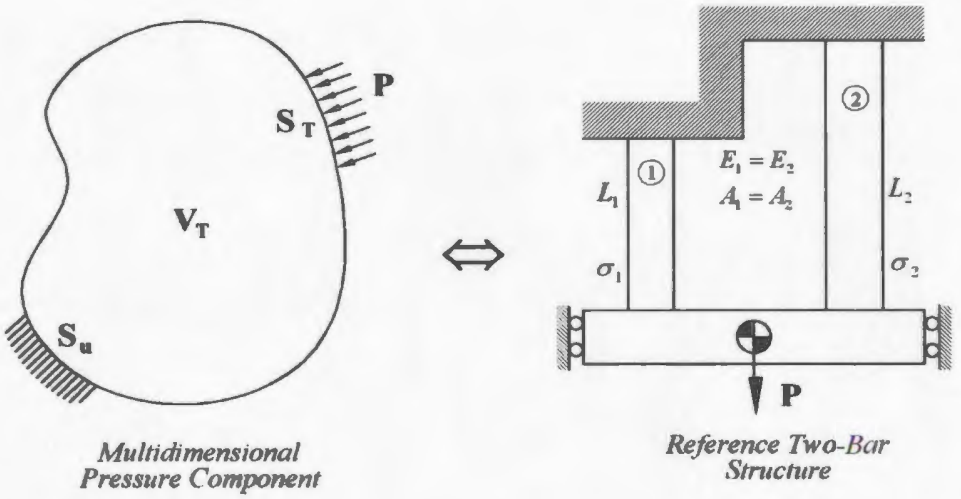

Figure 4.3 Reference two-bar structure (Seshadri and Adibi-Asl, 2006)

$$\frac{m^0_{Comp}}{m_{L,Comp}} = \frac{m^0_{Bar}}{m_{L,Bar}} \left(= \frac{1}{\sqrt{\lambda}} \right) \tag{4.4}$$

$$\frac{m^0_{Comp}}{m_{Comp}} = \frac{m^0_{Bar}}{m_{Bar}} \left(= \frac{\lambda + 1}{2\sqrt{\lambda}} \right) \tag{4.5}$$

where $\lambda = L_1/L_2 = \sigma_2/\sigma_1$.

L_1 and L_2 are the lengths of the bars, and σ_1 and σ_2 are the respective stresses.

Once m^0_{Comp} and $m_{L,Comp}$ are determined on the basis of a linear elastic FEA, the value of λ can be determined by using Eq. (4.4). Based on this λ an estimate of m_{Comp} can be obtained by using Eq. (4.5). It should be noted that $m_{Bar} = \dfrac{2\sigma_y}{\sigma_1 + \sigma_2}$, where σ_1 is identified with the maximum equivalent stress, $(\sigma_e)_{\max}$. Therefore, the ratio (m^0_{Bar} / m_{Bar}) will represent a combination of primary, secondary and peak stresses along the TBM trajectory.

4.6 The Concept of the m_α-Tangent

The m_α multiplier method (Seshadri and Mangalaramanan, 1997) was developed on the basis of variational concepts in plasticity. The method has explicit dependency on the upper bound multiplier, m^0, and the classical lower bound multiplier, m_L. The upper bound multiplier, m^0, depends on the entire stress distribution in a component or structure whereas m_L depends on the magnitude of maximum stress. Therefore, for components with sharp notches and cracks, the value of m^0/m_L will be high due to the presence of peak stresses.

With respect to Figure 4.4, the following can be stated:

(1) when m approaches m_L, the domain of statically admissible m^0 is bounded by the 45-deg (R^0(max)) line and the positive x-axis.

(2) when m approaches m^0, the domain of statically admissible m^0 is represented by the line $m=m^0$.

(3) the exact solution (m) locus would lie somewhere between the positive x-axis and the 45-deg line (R^0(max)).

(4) the tangent to the $R_\alpha=1$ curve at the limit state ($m_L=m^0=m$) will locate the m_α-tangent, which can then be used to estimate the multiplier m.

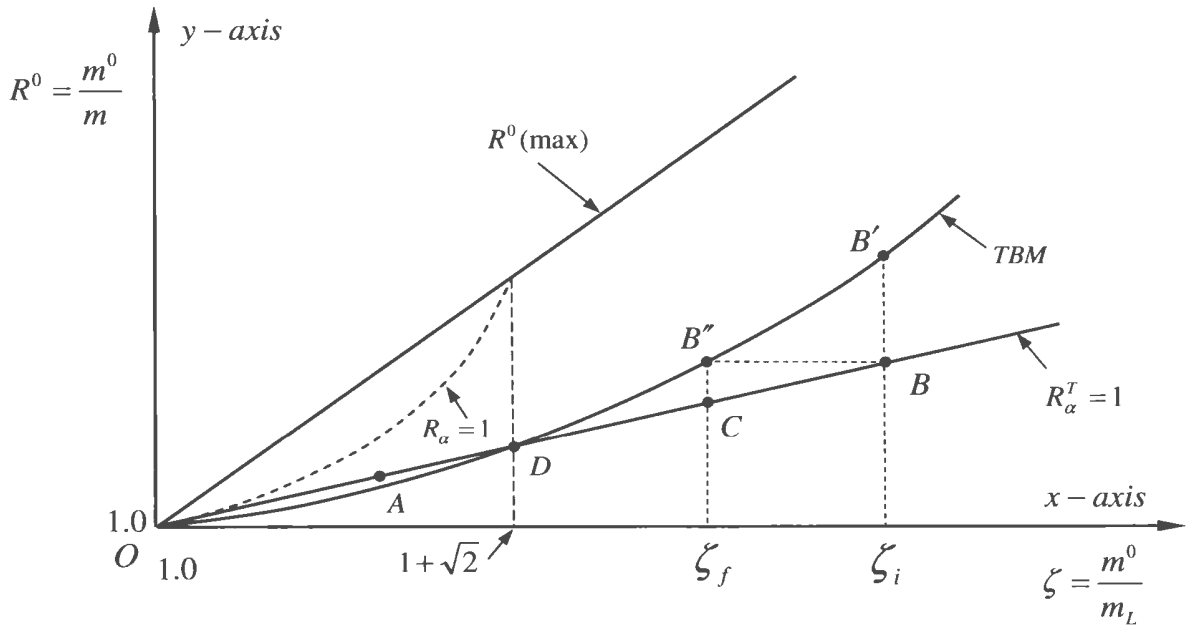

Figure 4.4 The m_α-tangent construction

The determination of the m_α-tangent multiplier is as follows. Equation (4.2) describes R_α as a function of two variables, R^0 and ζ, where $\zeta=m^0/m_L$. For $R_\alpha=1$, Eq. (4.2) can be represented by a curve in two-dimensional space as shown in Figure 4.4. The slope of the tangent at the limit state, where $m_\alpha = m^0 = m_L = m$, can be obtained as:

$$\left.\frac{dR_\alpha}{d\zeta}\right|_{\zeta=1} = 1-\frac{1}{\sqrt{2}} \tag{4.6}$$

Therefore, the slope of the tangent ($R_\alpha^T = 1$) line at the converged limit state is $Tan(\theta) = 0.2929$.

The equation corresponding to $R_\alpha^T = 1$ can be obtained as:

$$\frac{m^0}{m} = 1 + (\zeta - 1)\ Tan(\theta) \tag{4.7}$$

The exact limit load multiplier (m) for most of the practical components and structures being analyzed is not known a priori. For the m_α-tangent method, R^0 can be defined by making use of the tangent (R_α^T-line in Figure 4.4) for any value of ζ. Both R^0 and ζ are greater than one, except at the limit state for which $R^0 = \zeta = 1$. It should be noted that the reduction of m^0 along the $R_\alpha^T = 1$ trajectory implicitly accounts for the reference volume. Therefore, m^0 will converge to the exact multiplier as the trajectory approaches to the origin.

4.7 Peak Stresses

Secondary and peak stresses are set up by redundant kinematic constraints (or static indeterminacy) in a component. ASME Boiler and Pressure Vessel Codes (2007) explicitly recognize these stress and related constraint effects. Figure 4.5 shows the stress distribution in the ligament adjacent to the notch tip, where x-axis represents the distance ahead of the notch tip, and y-axis represents the equivalent stress. As can be seen from this figure, the magnitude of the peak stress (σ_F) at the notch tip is considerably high; however, it is assumed that the peak stresses are very localized and that the following expression is valid (Adibi-Asl and Seshadri, 2007):

$$\int_A \sigma_F dA \approx 0 \tag{4.8}$$

where A is the representative area on which σ_F acts.

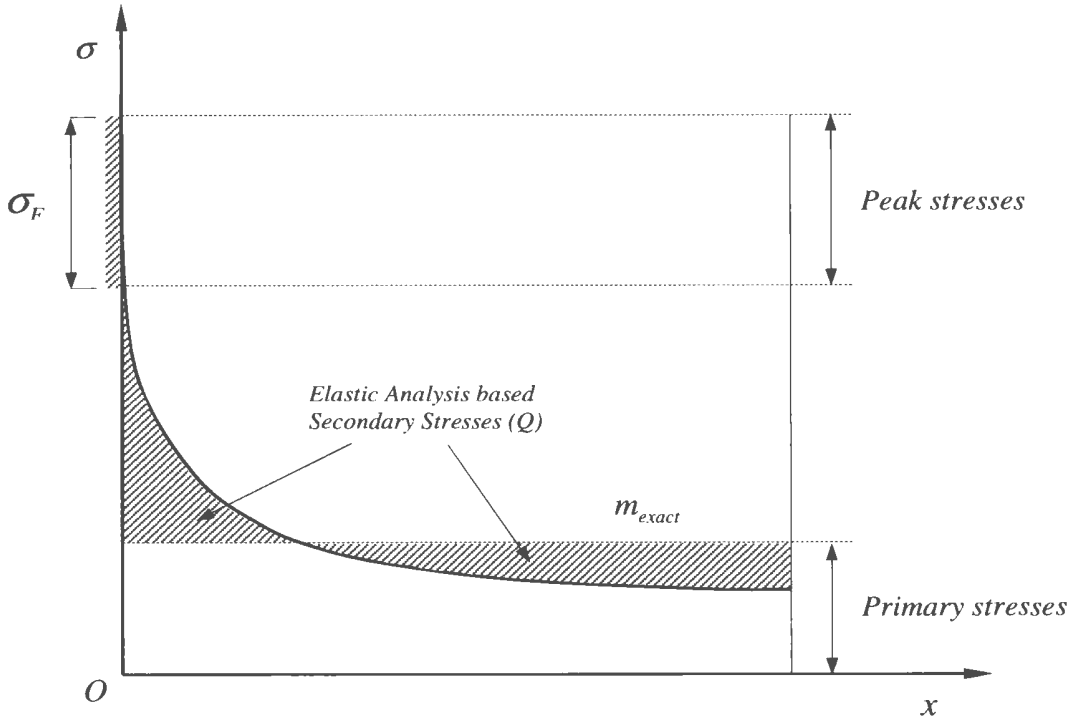

Figure 4.5 Stress distribution ahead of notch tip

With respect to the constraint map, $R_\alpha^T = 1$ line can be identified as shown in Figure 4.4. This line is tangential to the $R_\alpha = 1$ curve at the origin (m^0/m=1, m^0/m_L=1). The curve $\frac{m^0}{m} = \frac{1+\lambda}{2\sqrt{\lambda}}$ for the reference two-bar model (TBM) can also be located as shown in Figure. 4.4.

4.8 Significance of $\zeta^* = 1+\sqrt{2}$

The point D (Figure 4.4) can be determined by finding the intersection of the $R_\alpha^T = 1$ line and the reference two-bar model equation, i.e.,

$$\frac{m^0}{m} = 1 + (\zeta - 1)\ Tan(\theta) = \frac{1+\lambda}{2\sqrt{\lambda}} \tag{4.9}$$

where $\lambda = \frac{1}{\zeta^2}$ and $Tan(\theta) = 1 - \frac{1}{\sqrt{2}}$.

The intersection points work out to be $\zeta^* = 1.0$ and $1+\sqrt{2}$. The $R_\alpha^T = 1$ line represents a combination of primary and secondary stresses that exists in the pressure vessel components. On the other hand, the TBM trajectory represents the combination of primary, secondary and peak stresses. Therefore, at point *D* the peak stresses are negligible.

4.9 The m_α–Tangent Method

Once the $R_\alpha^T = 1$ line is identified, the value of m_α^T can be readily estimated by using the following relationship

$$m_\alpha^T = \frac{m^0}{1 + 0.2929(\zeta - 1)} \tag{4.10}$$

where $\zeta = \frac{m^0}{m_L}$.

The slope of the $R_\alpha^T = 1$ line is equal to $Tan(\theta) = \left(1 - \frac{1}{\sqrt{2}}\right)$. The value of m^0 and ζ can be determined from statically admissible distributions obtained from linear elastic FEA.

Two cases are considered next:

Case-I: $\zeta \leq 1+\sqrt{2}$, (negligible peak stresses)

For this case, point *A* (Figure 4.4) is assumed to lie on the $R_\alpha^T = 1$ line. The value of m_α^T can be obtained from Eq. (4.10). This case usually applies to well-designed pressure vessel components with gentle geometric transitions.

Case-II: $\zeta > 1+\sqrt{2}$, (presence of peak stresses)

This case applies to components that develop flaws or cracks in service, or to components with sharp notches. The aim here is to blunt the peak stresses prior to evaluating m_α^T. With respect to Figure 4.4, the initial linear elastic FEA locates point *B* on the $R_\alpha^T = 1$ line and point B' on the TBM locus corresponding to $\zeta_i = \dfrac{m_i^0}{m_{L,i}}$. The subscript "$i$" refers to the initial point *B* and B'. The calculation procedure is as follows:

1. Perform a linear elastic analysis.

2. Locate point *B* and B'. Point *B* represents the combination of primary and secondary stresses whereas point B' represents the combination of primary, secondary and peak stresses.

3. Construct a horizontal line from point *B* to B'' signifying an invariant m_i^0 (blunting of peak stresses). Designate the value of m^0/m_L at B'' as ζ_f, which can be obtained by solving the equation

$$\frac{m_i^0}{m} = 1 + 0.2929(\zeta_i - 1) = \frac{\zeta_f^2 + 1}{2\zeta_f} \tag{4.11}$$

The roots of Eq. (4.11) are

$$\zeta_f = (1 + C) \pm \sqrt{(1 + C)^2 - 1} \tag{4.12}$$

where $C = 0.2929(\zeta_i - 1)$

4. The value of m_α^T can be evaluated by the equation

$$m_\alpha^T = \frac{m_i^0}{1 + 0.2929(\zeta_f - 1)} \tag{4.13}$$

For some geometric transitions for which $\zeta > 1 + \sqrt{2}$, redistribution of secondary stresses could occur along with peak stresses. In such cases, the value of m_i^0 is not constant during the blunting of peak stresses, and there is a gradual reduction in its magnitude. These cases are usually attributed to components undergoing highly localized plastic flow such as beam and frame structures. In this thesis, all the problems are solved by assuming a constant value of m_i^0.

4.10 Applications

A number of example problems, ranging from simple to relatively complex geometric configurations, are worked out in this section to demonstrate the proposed m_α-tangent method. The results obtained from the proposed method are compared with those obtained from the corresponding analytical and inelastic finite element analysis results.

4.10.1 Thick Walled Cylinder

A thick walled cylinder with inner radius, R=65 mm (2.56 in.) and wall thickness, t=25 mm (0.984 in.) is modeled in plane-strain condition. The modulus of elasticity of the material is 200 GPa (29×10^6 psi) and yield strength is 300 MPa (43.5×10^3 psi). The cylinder is subjected to an internal pressure of 50 MPa (7.25×10^3 psi).

The finite element model of the cylinder is developed in plane-strain condition by taking advantage of symmetry. The geometry and finite element model of the cylinder is shown in Figure 4.6. Linear elastic FEA for this problem leads to a statically admissible stress distribution, on the basis of which m_L=1.702 and m^0=2.264. The corresponding ζ=1.330 lies within the m_α-triangle. Using Eq. (4.10) the value of the limit load multiplier is m_α^T=2.065. Elastic-plastic FEA estimates the limit load multiplier m_{NFEA} =2.254. The results are shown in Table 4.1.

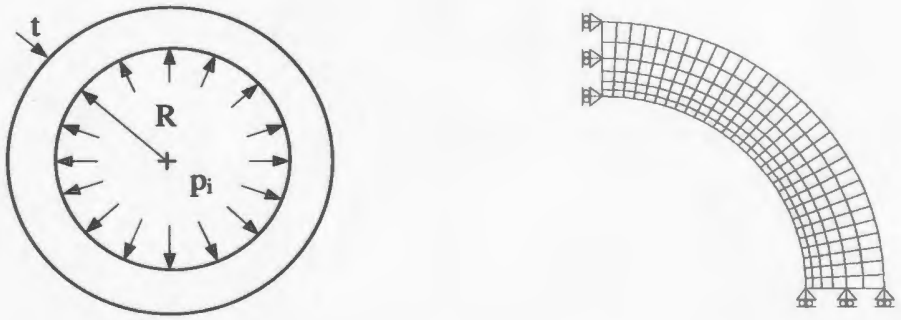

(a) (b)

Figure 4.6 Thick walled cylinder (a) Geometry (b) Finite element model (plane strain)

Table 4.1 Limit load multipliers for thick walled cylinder

Method	m^0	m_L	ζ	m_α^T	m_{NFEA}	$m_{Analytical}$*
Linear elastic FEA	2.264	1.702	1.330	2.065	2.254	2.255

*Analytical result from (Mendelson, 1968)

4.10.2 Plate with a Hole

Consider next a thin plate with a hole (Figure 4.7) with the following dimensions: plate width, $2W$=150 mm (5.905 in.); length, $2L$=300 mm (11.811 in.); hole radius, r=20 mm (0.787 in.). Applied load in the vertical direction is p=100 MPa (14.5×10^3 psi). The material properties are as follows: yield strength, σ_y=150 MPa (21.75×10^3 psi); modulus of elasticity, E=150 GPa (21.75×10^6 psi), and Poisson's ratio, υ=0.3.

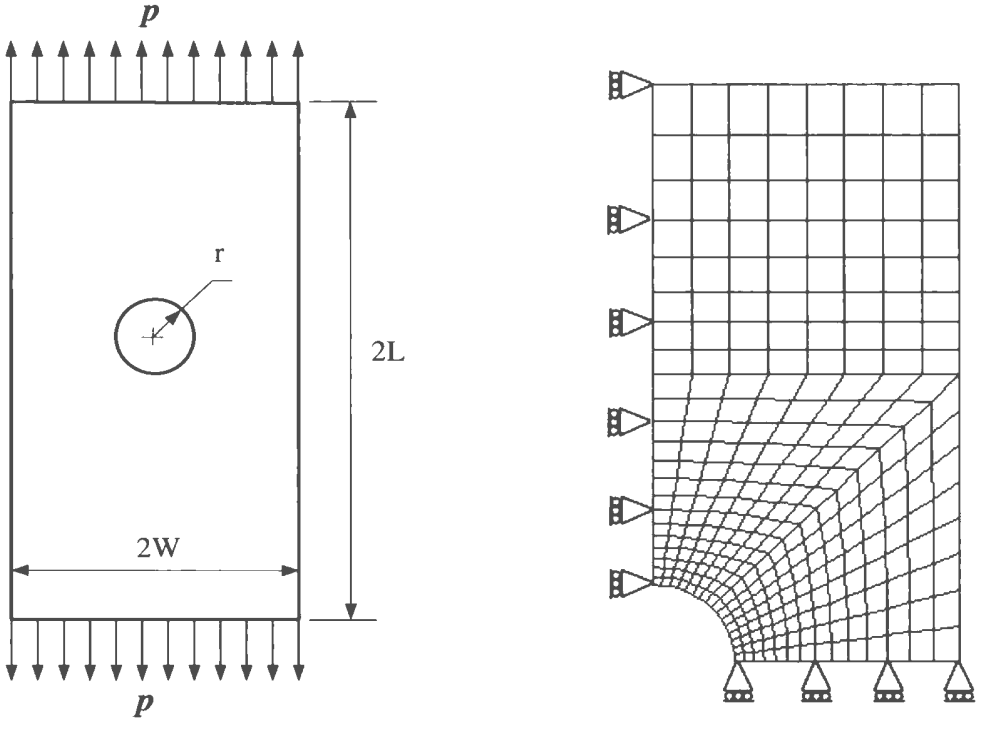

(a) (b)

Figure 4.7 Plate with a hole (a) Geometry (b) Finite element model (plane stress)

Table 4.2 Limit load multipliers for plate with a hole

Method	m^0	m_L	ζ_f	m_α^T	m_{NFEA}
Linear elastic FEA	1.416	0.527	2.604	0.963	1.099

Linear elastic FEA leads to the location of point B (Figure 4.4). The value of m_i^0=1.416, $m_{L,i}$=0.527 and ζ_i=2.687. Since $\zeta_i > 1+\sqrt{2}$, peak stresses are present in the component. ζ_f is evaluated so that m^0 at B and B'' are equal (Eq. (4.12)). The value of ζ_f=2.604. The m_α^T, based on ζ_f, as obtained from Eq. (4.13), is 0.963. The corresponding elastic-plastic estimate is 1.099. The results are shown in Table 4.2.

Convergence study has been performed for this example problem to verify the sensitivity of the m_α^T estimate with respect to the mesh density. It was observed that the current result changes within the range of 1 to 3% while using relatively coarser or finer mesh.

4.10.3 Indeterminate Beam

An indeterminate beam (Figure 4.8) with length, L= 508 mm (20 in.); height, h=25.4 mm (1 in.) and width, w=25.4 mm (1 in.) is modeled. The modulus of elasticity of the material is 206.85 GPa (30×10^6 psi) and yield strength is 206.85 MPa (30×10^3 psi). The beam is subjected to uniformly distributed load of 1.0 MPa (145 psi).

An initial linear elastic finite element analysis is performed. From the results of the initial linear elastic FEA, m^0=2.648 and m_L=0.636 is evaluated. Since ζ_i=4.164 is greater than

$1+\sqrt{2}$, significant amount of peak stresses are present in the component. Now, ζ_f is evaluated so that m^0 at B and B'' are equal (Eq. (4.11)). The value of $\zeta_f = 3.573$; and the value of m_α^T based on ζ_f, as obtained from Eq. (4.13), is 1.510. Then a complete elastic-plastic finite element analysis is performed, which gives the limit load multiplier m_{NFEA} = 1.538. The analytical solution of the problem gives the limit load multiplier $m_{Analytical}$ = 1.510. The analysis results are tabulated in Table 4.3.

Table 4.3 Limit load multipliers for indeterminate beam

Method	m^0	m_L	ζ_f	m_α^T	m_{NFEA}	$m_{Analytical}$ †
Linear elastic FEA	2.648	0.636	3.573	1.510	1.538	1.510

†Analytical result from (Mendelson, 1968)

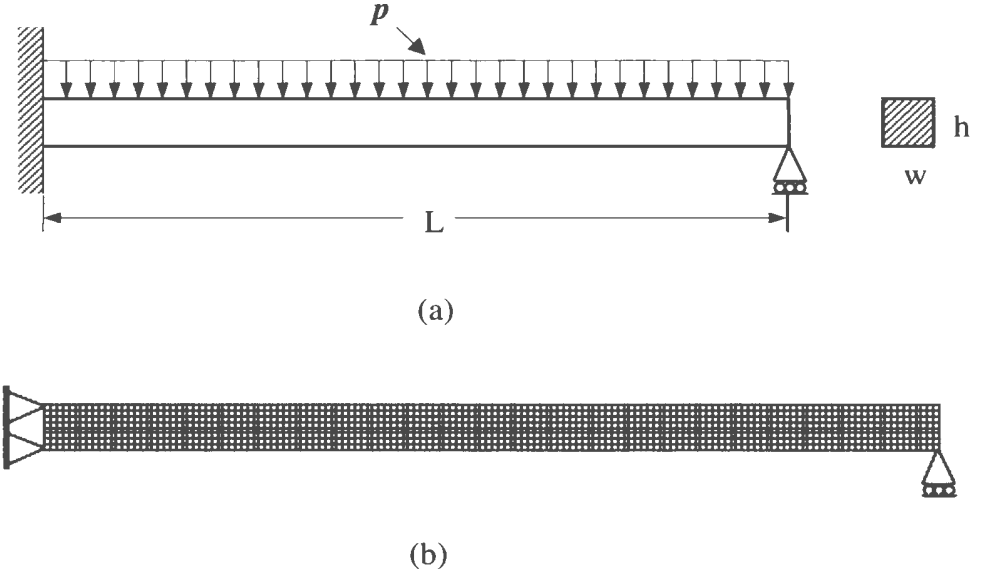

Figure 4.8 Indeterminate beam (a) Geometry (b) Finite element model (plane stress)

4.10.4 Unreinforced Axisymmetric Nozzle

In this example, an axisymmetric cylindrical nozzle on a hemispherical head (Figure 4.9) is modeled. Inside radius of the head is R=914.4 mm (36 in.), and the nominal wall thickness is t=82.55 mm (3.25 in.). Inside radius of the nozzle is r=136.525 mm (5.375 in.) and nominal wall thickness is t_n=25.4 mm (1 in.). The required minimum wall thickness of the head and the nozzle are t_r=76.835 mm (3.025 in.) and t_{rn}=24.308 mm (0.957 in.), respectively.

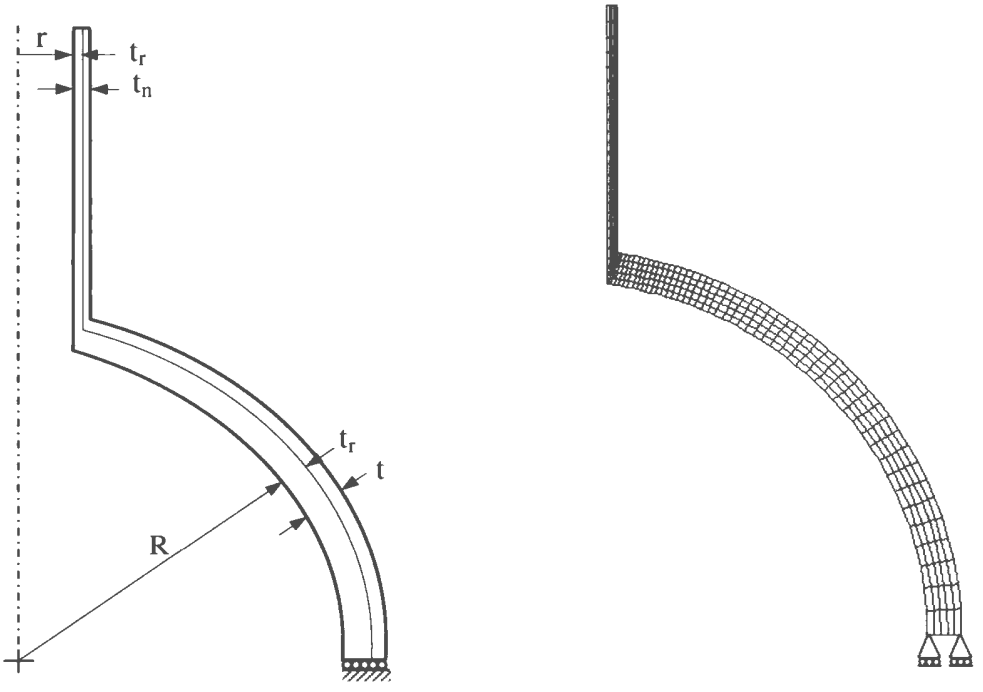

(a) (b)

Figure 4.9 Unreinforced nozzle on a hemispherical head (a) Geometry (b) Finite element model (axisymmetric)

Table 4.4 Limit load multipliers for unreinforced nozzle

Method	m^0	m_L	ζ	m_α^T	m_{NFEA}
Linear elastic FEA	1.847	0.896	2.061	1.410	1.672

The modulus of elasticity of the material is 262 GPa (38×10^6 psi) and yield strength is 262 MPa (38×10^3 psi). The hemispherical head is restrained at the vessel end, away from the nozzle, in the meridional direction but allowed to move in the radial direction. The structure is subjected to an internal pressure of 24.132 MPa (3500 psi).

From the results of the initial elastic FEA, m^0=1.847 and m_L=0.896 is evaluated. Since ζ_i=2.061 is less than $1+\sqrt{2}$, therefore peak stresses are either negligible or zero. The value of m_α^T is obtained from Eq. (4.10) as 1.410. The elastic-plastic finite element analysis gives the limit load multiplier m_{NFEA} = 1.672. The analyses results are tabulated in Table 4.4.

4.10.5 Reinforced Axisymmetric Nozzle

A reinforced axisymmetric cylindrical nozzle on a hemispherical head is considered here. Inside radius of the head is R=914.4 mm (36 in.), and nominal wall thickness is t=82.55 mm (3.25 in.). Inside radius of the nozzle is r=136.525 mm (5.375 in.) and nominal wall thickness is t_n=25.4 mm (1 in.). The required minimum wall thickness of the head and the nozzle are t_r=76.835 mm (3.025 in.) and t_{rn}=24.308 mm (0.957 in.), respectively.

The nozzle is reinforced with an appropriate reinforcement scheme. The schematic diagram and typical finite element mesh of the model is shown in Figure 4.10. The

geometric transitions of the reinforcement are modeled with fillet radius, r_1=10.312 mm (0.406 in.), r_2= 83.312 mm and r_3= 115.214 mm (4.536 in.). The other dimensions include, T_2=54.61 mm (2.15 in.) and θ=45°. The distribution of reinforcement is bounded by the reinforcement zone boundary specified by the circle of radius, L_n=143.51 mm (5.65 in.). The other geometric dimensions are the same as the previous example.

The modulus of elasticity of the material is 262 GPa (38×10^6 psi) and yield strength is 262 MPa (38×10^3 psi). The hemispherical head is restrained at the vessel end, away from the nozzle, in the meridional direction but allowed to move in the radial direction. The structure is subjected to an internal pressure of 24.132 MPa (3500 psi).

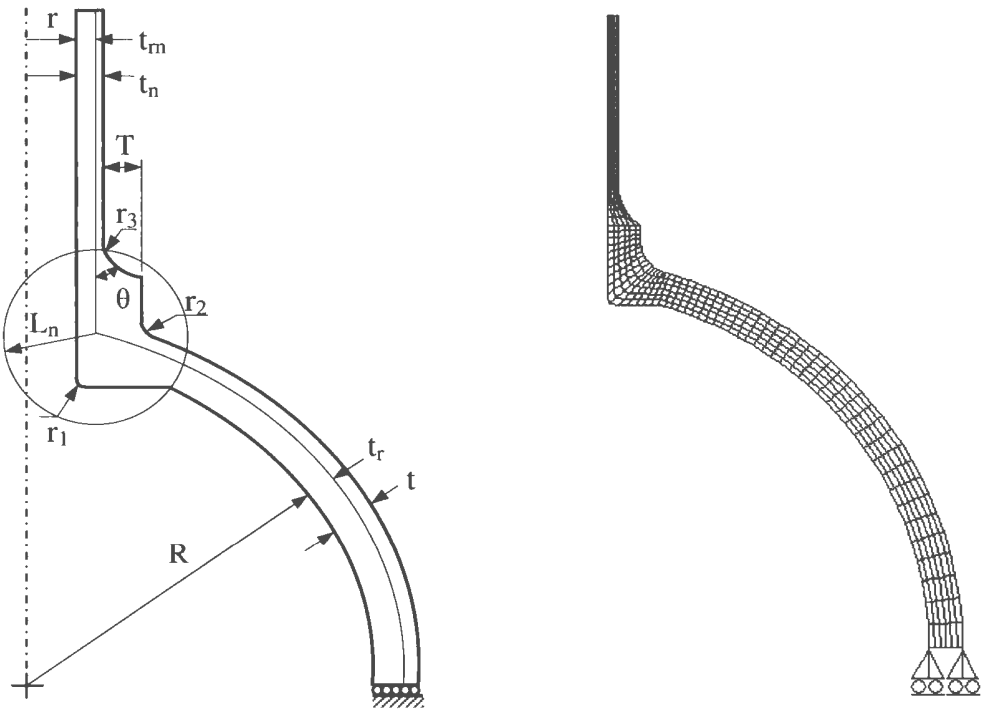

(a) (b)

Figure 4.10 Reinforced nozzle on a hemispherical head (a) Geometry (b) Finite element model (axisymmetric)

Table 4.5 Limit load multipliers for reinforced nozzle

Method	m^0	m_L	ζ	m_α^T	m_{NFEA}
Linear elastic FEA	1.891	1.176	1.608	1.605	1.874

From the results of the initial elastic FEA, m^0=1.891 and m_L=1.176 is evaluated. Since ζ_i=1.608 is less than $1+\sqrt{2}$, therefore peak stresses are either negligible or zero. The value of m_α^T is obtained from Eq. (4.10) as 1.605. The elastic-plastic finite element analysis gives the limit load multiplier m_{NFEA} = 1.874. The analysis results are shown in Table 4.5.

4.10.6 Oblique Nozzle

Limit load analysis of a vessel with oblique nozzle has been studied both experimentally and numerically by Sang. et al. (2005) to find the limit pressure. The geometry consists of a cylindrical vessel with a closed nozzle connected with an angle of 30 deg. The schematic diagram of the model and corresponding finite element model is shown in Figure 4.11. The inside diameter of the vessel D_i=600 mm (23.622 in.) and outside diameter of the nozzle d_o=325 mm (12.795 in.). The wall thickness of both vessel and nozzle is t=6 mm (0.236 in.). The length of the vessel is L=2400 mm (94.488 in.) and the length of the nozzle along the centerline l=600 mm (23.622 in.). The dimensions of the heads of the vessel and the nozzle are H_i=175 mm (6.890 in.) and h_i=106 mm (4.173 in.), respectively. The saddles are located at a distance A=400 mm (15.748 in.).

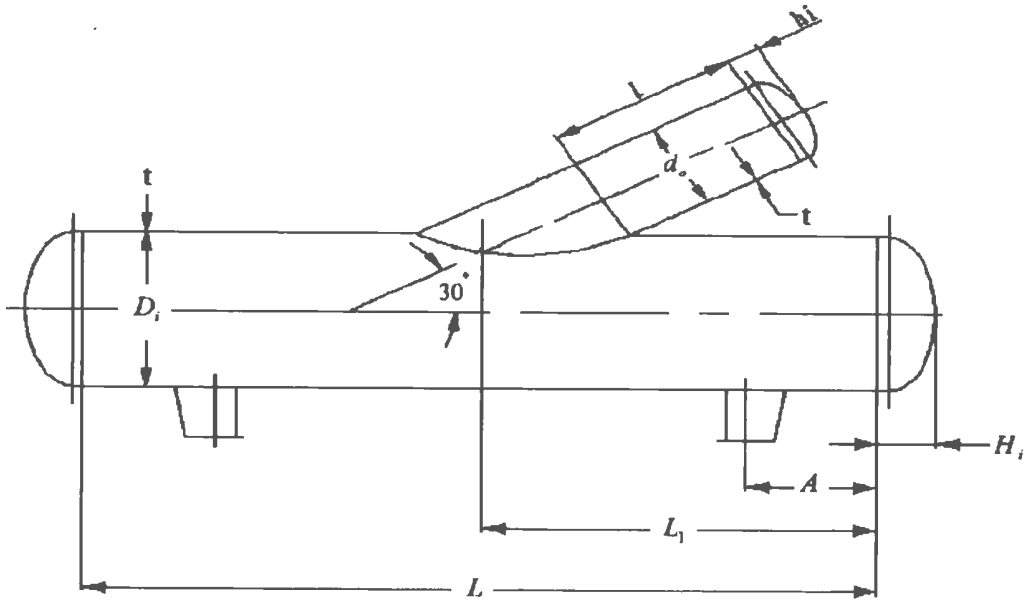

(a)

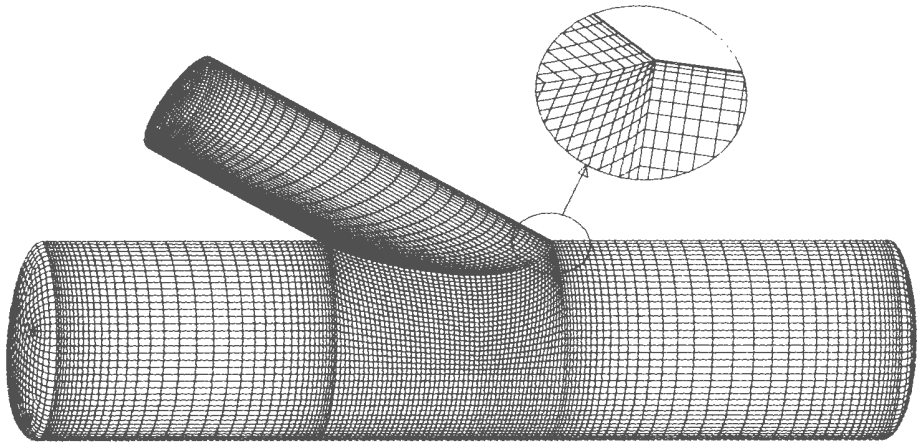

(b)

Figure 4.11 Oblique nozzle on a cylindrical vessel from Sang. et al. (2005) (a) Geometry, (b) Finite element model

Table 4.6 Limit load multipliers for oblique nozzle

Method	m^0	m_L	ζ_f	m_α^T	m_{NFEA}
Linear elastic FEA	4.804	0.411	8.139	1.554	1.805

Modulus of elasticity and yield strength of the material is 400 GPa (58.015×10^6 psi) and 339.4 MPa (49.226×10^3 psi) respectively. The structure is subjected to an internal pressure of 1.0 MPa (145 psi). The finite element model of the geometry is developed with three dimensional isoparametric solid elements. Due to the symmetry about the longitudinal plane, one-half of the vessel was modeled.

An initial linear elastic finite element analysis is performed. From the results of the initial elastic FEA, m^0=4.804 and m_L=0.411 is evaluated. Since ζ_i=11.688 is greater than $1+\sqrt{2}$, therefore significant amount of peak stresses are present in the structure. Now, ζ_f is evaluated so that m^0 at B and B'' are equal (Eq. (4.11)). The value of $\zeta_f = 8.139$ and the value of m_α^T based on ζ_f, as obtained from Eq. (4.13), is 1.554. Then a complete elastic-plastic finite element analysis is performed, which gives the limit load multiplier m_{NFEA} = 1.805. The results are summarized in Table 4.6.

4.11 Lower Boundedness of the m_α^T - Multiplier

The detailed derivation of the m_α-tangent method and its application to practical complex three dimensional mechanical component configurations have been presented in the previous sections of this chapter. The method makes use of the "limiting tangent" in

order to relate the initial elastic state of a component or structure to that of the exact limit state. The proposed method is developed as a viable tool for estimating the limit load of a general class of mechanical components and structures by using a single linear elastic analysis. The limit load multiplier m_α^T is evaluated by making use of the limiting tangent; upper bound multiplier m^0 and classical lower bound multiplier m_L. All necessary information can be extracted from the initial linear elastic analysis. The limiting tangent approximates the value of m^0/m with respect to a give value of m^0/m_L.

Several example problems are worked out in the previous section of this chapter, ranging from simple to relatively complex geometric configurations, and the results are found to be lower bound to the corresponding analytical and inelastic finite element analysis results. The exact locations of m^0/m for all of the example problems are shown on the m_α-tangent plot in Figure 4.12. It should be noted that the value of m is calculated on the basis of inelastic finite element analysis results. In Figure 4.12, the limiting tangent line essentially represents the value of m^0 / m_α^T for any component under consideration. It could be observed from the plot that the value of m^0 / m_{NFEA}, for different components, lies under the limiting tangent line.

Therefore, it is clear from the Figure 4.12 that the limit load estimated by the proposed m_α-tangent method is lower bound to the inelastic finite element analysis results for all worked out examples. Therefore, the proposed method is expected to give lower bound solution to the exact limit loads for a general class of mechanical components and structures.

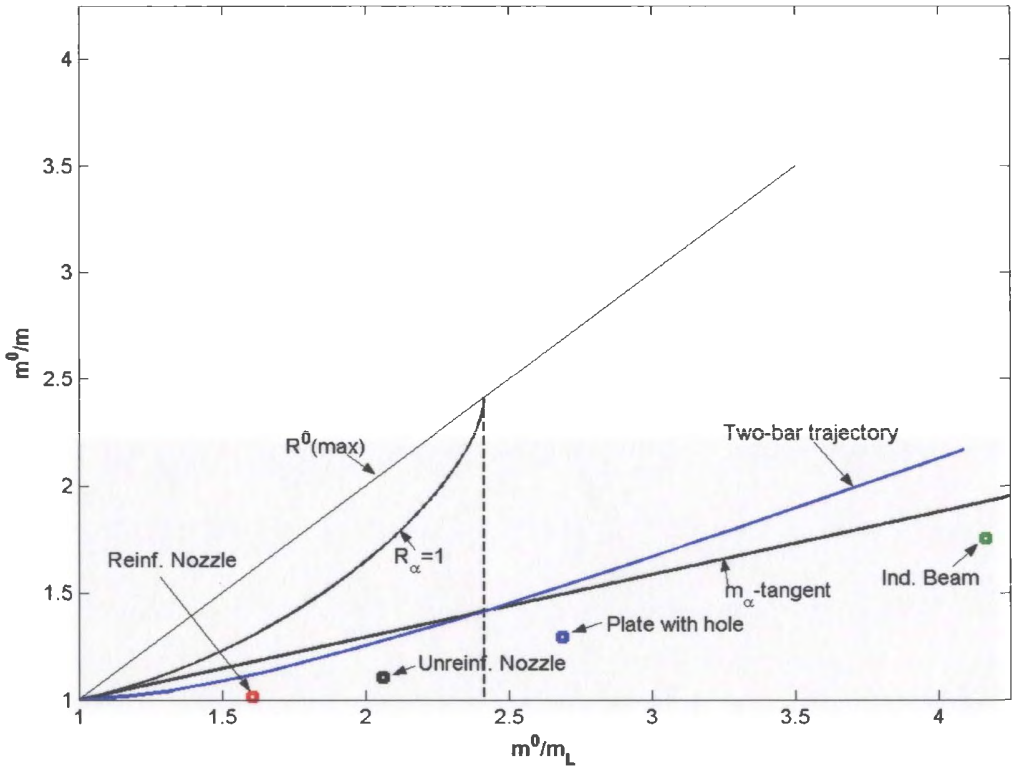

Figure 4.12 The location of different components, on the m_α-tangent plot, based on inelastic FEA results.

4.12 Discussion

The estimates of m_α^T for all the worked out example problems are found to be lower bound to the corresponding analytical or inelastic finite element analysis results. With reference to Figure 4.4, points such as B' on the two-bar model (TBM) locus are indicative of the existence of peak stresses and therefore, convexity (viewed from the origin) of the linear elastic stress distribution. This is the case for $\zeta > 1+\sqrt{2}$. For values

of ζ less than $1+\sqrt{2}$, the peak stresses are either zero or negligible. The aspect of convexity of stress distribution is a possible explanation for lower bound values of limit load multiplier m_{α}^{T}.

In recent times, inelastic finite element analysis has been successfully used to solve complex problems. For three dimensional nonsymmetric problems, however the computational time can be excessive. Furthermore, computational issues associated with volumetric and shear locking can arise. Iterative EMAP has been shown to converge within 10 iterations to an acceptable limit load, and has recently found applications in non-cyclic methods for plastic shakedown determination (Adibi-Asl and Reinhardt, 2008) and fitness-for-service (FFS) assessments.

4.13 Conclusion

Simplified methods are shown to be very useful in determining the limit loads of mechanical components and structures. These methods are easy to implement in practice and overcomes the potential difficulties encountered in conventional inelastic finite element analysis. The m_{α}-tangent method is proposed as a simplified tool to estimate the limit load for a general class of mechanical components and structures. The phrase "m_{α}-tangent" refers to the use of the limiting tangent that relates the initial elastic state of a component or structure to that of the exact limit state. A simple expression is deduced that enables the rapid determination of limit loads.

By using the proposed method, reasonably accurate estimate of limit load can be obtained on the basis of a single linear elastic analysis. The proposed method is applied to components and structures including standard example problems as well as typical pressure vessel component configurations. The results obtained are in reasonably good agreement with the respective analytical and elastic-plastic finite element analysis results. The method is suitable for Level-2 "fitness-for-service" (FFS) assessments of mechanical components and structures, which will be discussed in Chapter 7 of this thesis.

4.14 Closure

A new and simplified method, called the m_α-tangent method, has been developed in this chapter of the thesis. The theoretical background, formulation and detail derivation of the proposed method is presented in a systematic way. The method is shown to be able to estimate the limit load of a general class of mechanical components and structures using a single linear elastic analysis. The current form of the method is applicable to components and structures without sharp notches or cracks. The method has been extended in the next chapter of this thesis to estimate the limit load of components and structures containing crack-like flaws.

CHAPTER 5

ANALYSIS OF CRACKED COMPONENTS

5.1 Introduction

Determination of load carrying capacity is an important step in integrity assessment of mechanical components and structures. The load carrying components and structures generally fail due to either excessive yielding or dominant fracture. In case of components with crack-like flaws, failure can be due to either ductile tearing (net-section collapse) or brittle fracture. Net section collapse becomes more important in case of high toughness materials where brittle fracture is unlikely. On the other hand, brittle fracture becomes very important in case of materials with high strength. Linear elastic fracture mechanics (LEFM) is no longer valid in this case and a nonlinear formulation must be

considered. However, both modes of failure must be taken into account in order to assess the integrity of components and structures containing crack-like flaws.

Limit analysis is performed in order to determine the load carrying capacity of a component or structure. Closed form solutions for determination of limit loads of cracked bodies are limited to simple geometric configurations and loading conditions. For complex situations, numerical methods such as finite element method are more appropriate. Inelastic finite element analysis is extensively used for complex geometric configurations and loading conditions; however, it can often be expensive in terms of computational effort and time.

For small-scale yielding at the crack tip, the load-deflection behavior is linear, and therefore, linear elastic fracture mechanics (LEFM) is applicable in this case. When the plasticity spreads around the crack tip and significant plastic deformation occurs, the concept of limit load becomes more appropriate. Therefore, any effort directed towards developing robust and simplified methods that are cost effective and reasonably accurate would be of importance from integrity assessment standpoint.

Extensive investigations have been carried out over the past few decades in order to assess the integrity of in-service components and structures containing flaw or damage. Some of the available practices and procedures are API 579 (2000), R5 and R6 procedure (2004) and SINTAP (1999). These procedures are mostly semi-empirical and obtained from numerous experimental data. In order to perform more accurate assessment, advanced numerical simulation and analysis techniques need to be incorporated. This will facilitate more accurate modeling and analysis of the real-life scenario.

In this chapter of the thesis, a simplified method is proposed in order to estimate the limit load of components and structures containing crack-like flaws. The proposed simplified method is an extension of the m_α-tangent method. A reasonably accurate estimate of the limit load can be obtained by using a single linear elastic finite element analysis. The method is applied to a number of cracked component configurations including component with multiple cracks and pipe with extended inner axial crack. The results compare well with those obtained from the conventional inelastic finite element analysis.

5.2 Integrity Assessment of Cracked Components and Structures

Integrity assessment of mechanical components and structures is an effort to assess whether a structure is fit to withstand the service conditions safely and reliably throughout its predicted lifetime. The philosophy behind the design of any structural component is to ensure that the strength of the material, of which the component is made of, is higher than the maximum applied stress in service. If the former appears to be greater than the latter, then the component is considered to be fit for service, otherwise, modification in design or the use of another material with a higher strength is required to be considered.

The fracture mechanics based fitness-for-service (FFS) assessment enables the assessment of crack-like flaws in order to ensure the structural integrity. FFS can be used to demonstrate whether a given flaw can be left as it is and so avoid unnecessary repairs or replacements. In order to perform the integrity assessment of components and

structures containing crack-like flaws, it is required to obtain the detail material data, estimate applied as well as residual stresses either experimentally or by simulated modeling, detect size and location of the flaw in the structure by non-destructive testing, and finally assess the fitness of the structure for continued service.

In order to address the brittle fracture, assessment needs to be performed that requires the information about the size and shape of the existing flaws, material tensile properties, fracture toughness and applied stress. To carry out a brittle fracture assessment, the above information should be implemented into one of the available assessment procedures, e.g., failure assessment diagram (FAD). The outcome of the assessment is normally presented as maximum tolerable crack-like flaw size, permissible applied load and minimum fracture toughness for the material used.

In order to perform the integrity assessment of components and structures containing crack-like flaws, the following two criteria needs to be considered:

- **Susceptibility to brittle fracture**: A cracked component or structure is prone to brittle fracture if the applied loading exceeds materials resistance to brittle fracture. This phenomenon is pronounced in case of components made up of high strength material.

- **Susceptibility to plastic collapse**: A cracked component or structure is susceptible to local plastic collapse if the reference stress on the ligament ahead of the crack exceeds a factor of yield or flow stress. This phenomenon occurs in case of high toughness material.

5.2.1 Failure Assessment Diagram (FAD)

The failure assessment diagram (FAD) is used for the evaluation of components and structures containing crack-like flaws. The FAD gives a technically based assessment procedure for the cracked components where the failure of the structure is measured by using two distinct criteria i.e., brittle fracture and plastic collapse. When the material is brittle in nature (high strength material) and the flaw size is relatively small, then brittle fracture is the possible mode of failure of the component.

On the other hand, when the material is ductile in nature (high toughness material) and the flaw size is relatively large, then plastic collapse (ductile tearing) is the possible mode of failure of the component. In order to assess the integrity of the component or structure containing crack-like flaws, both modes of failure needs to be considered and addressed properly.

In order to perform the integrity assessment of components and structures containing crack-like flaws, the results from a stress analysis (σ_{ref}), stress intensity factor (K_I) and limit load solutions, the material yield strength (σ_y) and fracture toughness (K_{IC}) are combined to calculate a toughness ratio (K_r) and load ratio (L_r). These parameters are used in the FAD to assess the cracked components and structures.

The failure assessment diagram (FAD) was first proposed in R6 procedure (Harrison et al., 1976) for integrity assessment of structures containing crack-like defects. The FAD method uses two parameters, toughness ratio K_r and load ratio L_r, in order to predict the failure of cracked component, which are defined by

$$K_r = K / K_{mat} \quad \Leftrightarrow \quad K_r = \frac{K_I}{K_{IC}} \tag{5.1}$$

$$L_r = P / P_L \quad \Leftrightarrow \quad L_r = \frac{\sigma_{ref}}{\sigma_Y} \tag{5.2}$$

where K_r is the ratio of the linear elastic stress intensity factor (K) and the fracture toughness of the material (K_{mat}), and L_r is the ratio of the applied load (P) and limit load (P_L) of the structure. By evaluating these two parameters using Eq. (5.1) and Eq. (5.2), failure could be avoided if the point (K_r, L_r) lies within the failure assessment diagram (safe region) as shown in Figure 5.1.

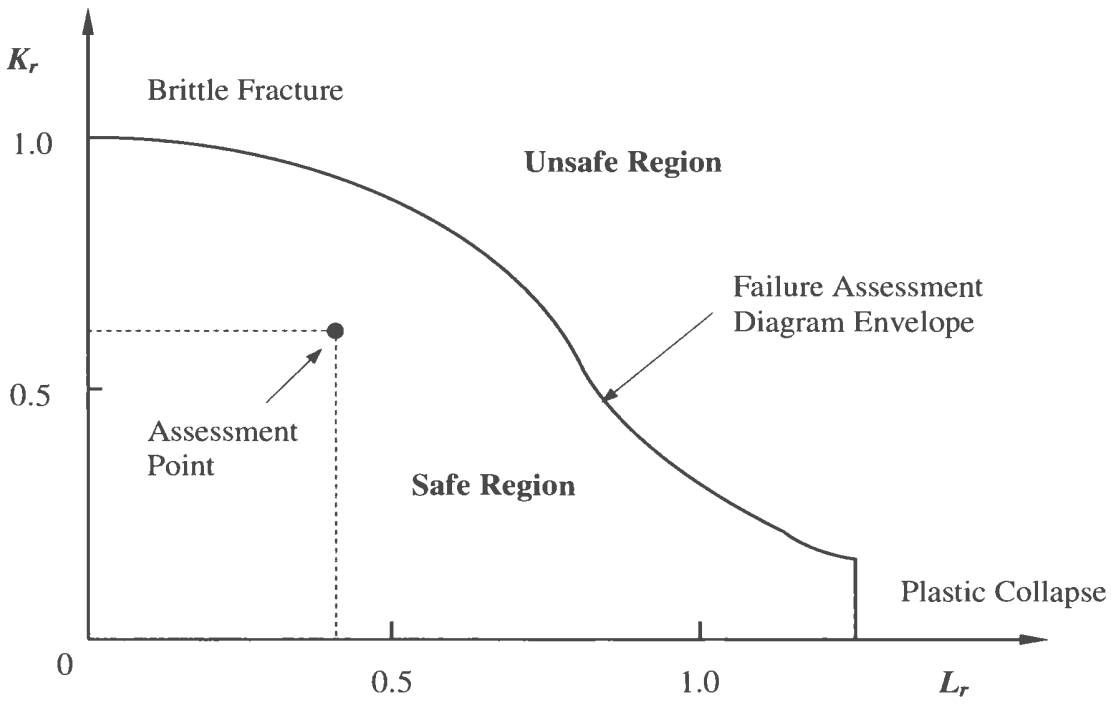

Figure 5.1 Failure assessment diagram (FAD)

To conduct a brittle fracture assessment, both brittle fracture and plastic collapse parameters are implemented in the failure assessment diagram (FAD). This is considered to be an essential tool in order to assess the integrity of components or structures containing crack like flaws. Both failure modes (brittle fracture & ductile tearing) should be considered for fracture evaluation (structural integrity assessment). Note that the failure assessment curves are independent of geometry and material strain-hardening properties (Ainsworth and O'Dowd, 1995).

5.3 Estimation of Limit Load for Cracked Components

The materials generally used for pressure vessel construction are sufficiently ductile. Therefore, the number of catastrophic failure by brittle fracture is very small. However, the possibility of brittle fracture in large complex structures must be taken into account, and assessment should be performed using appropriate assessment method. Generally, brittle fracture occurs in a pressurized component or structure due to the presence of residual stresses and / or high triaxiality at the ligament ahead of the crack-tip as the pressure vessel materials are generally sufficiently ductile. On the other hand, plastic collapse (ductile tearing) is the possible mode of failure if the material is sufficiently ductile. Therefore, limit load plays an important role in the integrity assessment of components or structures containing crack-like flaws.

5.3.1 Blunting of Peak Stresses

Secondary and peak stresses are set up due to static indeterminacy in a component or structure. ASME Boiler and Pressure Vessel Code (2007) explicitly recognize these stress and related constraint effects. Figure 5.2 shows the stress distribution in the ligament adjacent to the crack tip, where x-axis represents the distance ahead of the crack tip, and y-axis represents the equivalent stress.

As can be seen from this figure, the magnitude of the peak stress (σ_F) at the crack tip is considerably high; however, it is assumed that the peak stresses are very localized and that the following expression is valid (Adibi-Asl and Seshadri, 2007)

$$\int \sigma_F \, dA \approx 0 \tag{5.3}$$

where A is the representative area on which σ_F acts.

An explanation of this concept is presented by Adibi-Asl and Seshadri (2007). The shaded area in Figure 5.2 represents the elastic analysis based secondary stresses (Q) that are essentially self-limiting, and tend to redistribute around the redistribution node (R-Node) (Seshadri, 1991). Therefore, theoretically it does not have any effect on the limit load of a component. The primary stresses, which are "load-controlled" in nature, do not redistribute upon plastic-deformation or inelastic action, as shown in Figure 5.2. The following section is dedicated to address the treatment of peak stress ahead of the crack tip in the context of limit load determination.

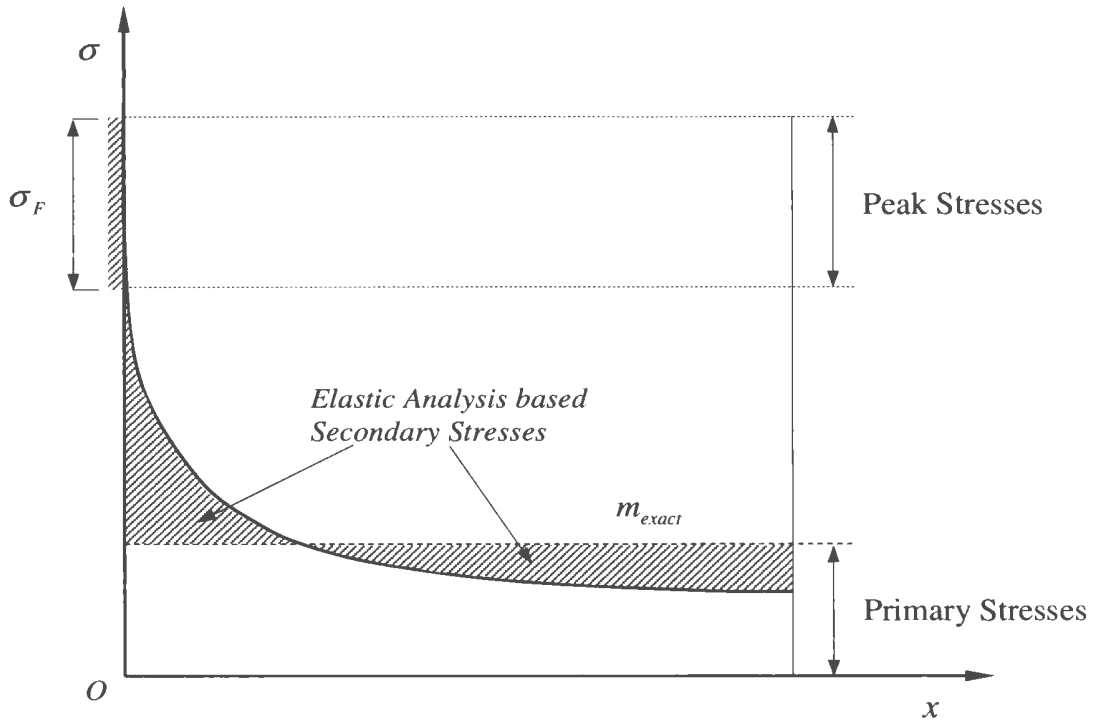

Figure 5.2 Stress distribution ahead of crack tip

The stress distribution, ahead of a crack, based on linear elastic analyses can be represented by the plots as shown in Figure 5.2. By modifying the elastic modulus of the material around the crack tip (i.e., singular elements that surrounded the crack tip in a finite element discretization scheme), stress distributions can be plotted as shown in Figure 5.3. In this figure, E_s is the modified value of elastic modulus around the crack tip. At a specific value of $E_s = E_s^*$, the stress distribution ahead of crack becomes almost horizontal; this means that the magnitude of stress gradient reaches a minimum, and the effect of peak stresses becomes small. Numerical simulation of different crack configurations shows that $E_s = E_0 / 3$ is a good choice for modifying the crack tip elements. This also can be explained as follows (Adibi-Asl and Seshadri, 2007):

Consider a crack configuration (Figure 5.3) for which the stresses at the crack tip can be expressed as

$$\sigma_{xx} = \sigma_{yy} = \sigma_{\max} \tag{5.4}$$

$$\sigma_{zz} = \begin{cases} 0 & \rightarrow \textit{Plane stress} \\ 2\nu\sigma_{\max} & \rightarrow \textit{Plane strain} \end{cases}$$

where $\sigma_{\max} = \dfrac{K_I}{\sqrt{2\pi r}} = \dfrac{Y\sigma_n\sqrt{\pi a}}{\sqrt{2\pi r}}$ and σ_n is remote field stress and Y is crack configuration factor.

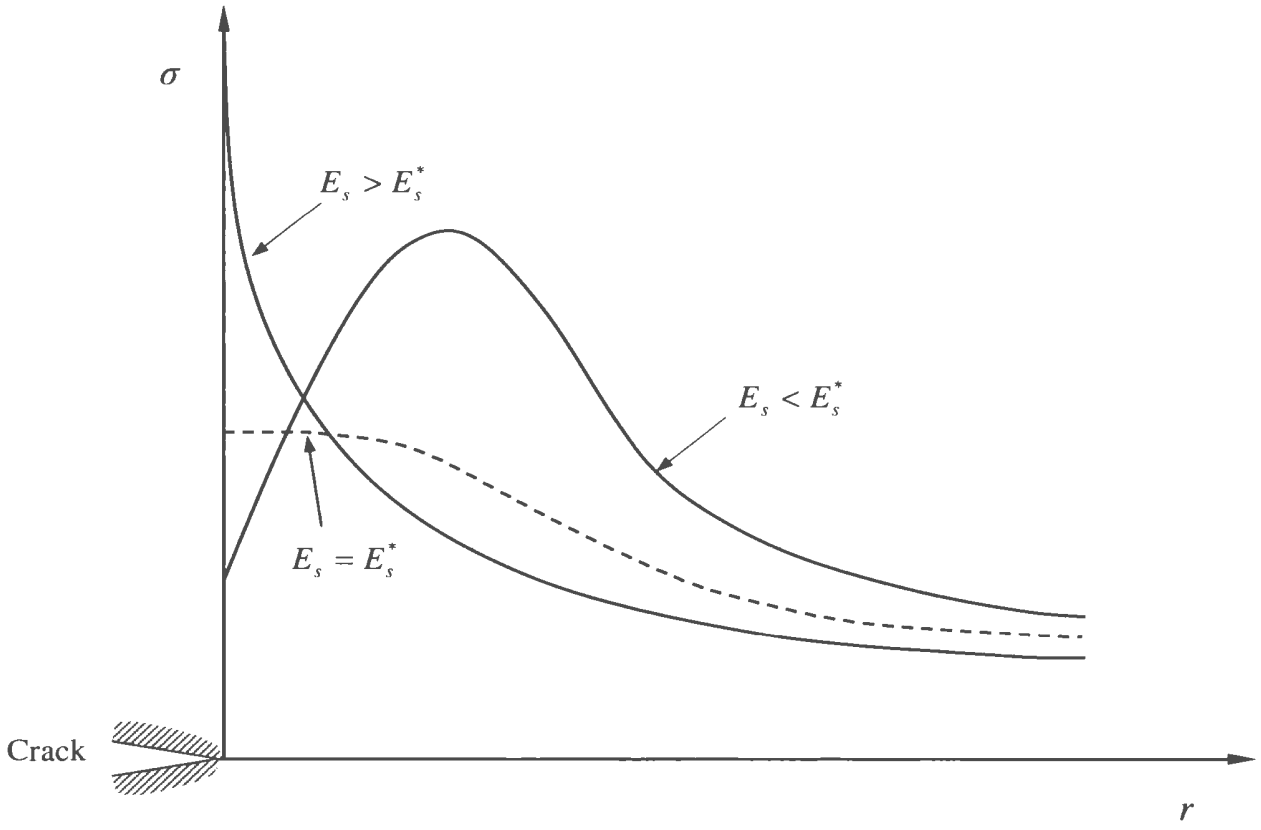

Figure 5.3 Elastic stress distribution ahead of the crack tip for different values of E_s (Adibi-Asl and Seshadri, 2007)

The above stresses are the principal stresses at the crack tip. The von-Mises criterion can be written as

$$[(\sigma_1-\sigma_2)^2+(\sigma_2-\sigma_3)^2+(\sigma_3-\sigma_1)^2]=2\sigma_{eq}^2 \tag{5.5}$$

Substituting the stresses from Eq. (5.4) into Eq. (5.5), the following expression can be obtained

$$\sigma_{eq}=A\sigma_{\max}=\frac{AY\sigma_n\sqrt{\pi\, a}}{\sqrt{2\pi\, r}} \tag{5.6}$$

where A=1 for plane stress and A= (1-2υ) for plane strain condition.

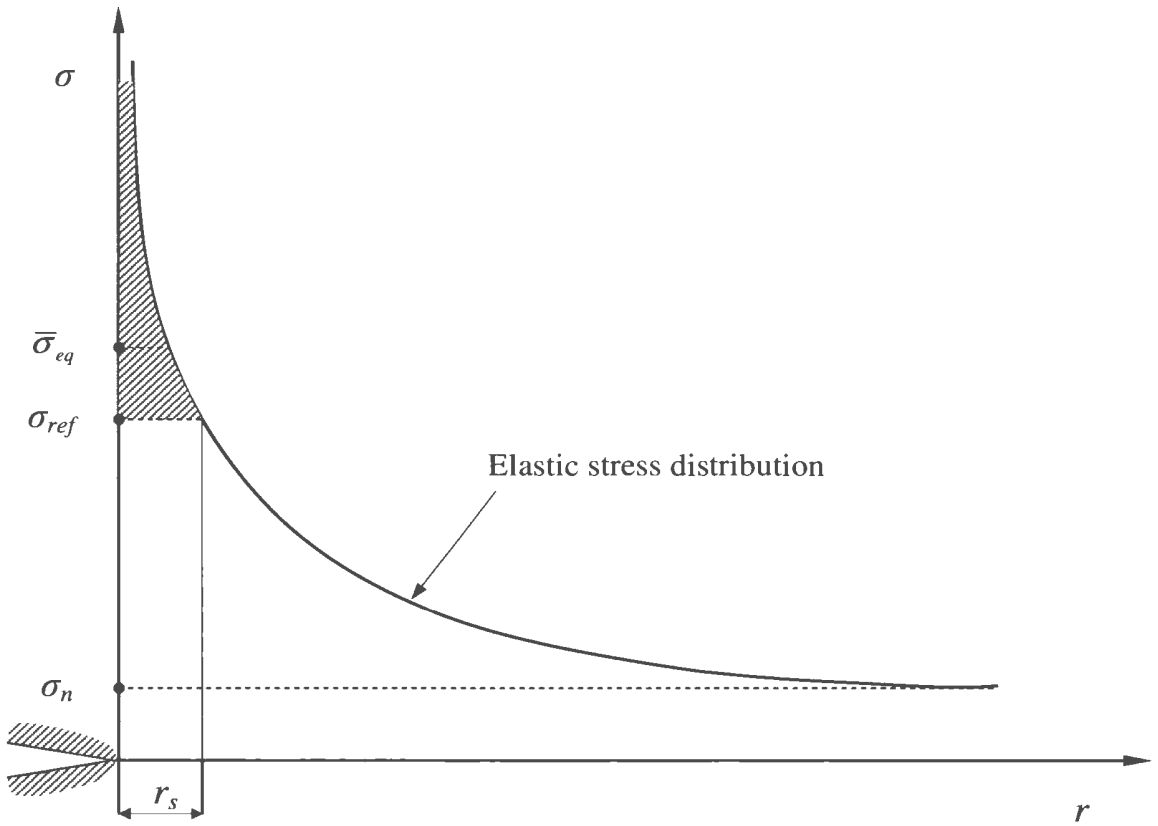

Figure 5.4 Elastic stress distribution ahead of the crack tip (Adibi-Asl and Seshadri, 20007)

The average stress along the crack orientation in the singularity domain can be calculated as

$$\overline{\sigma}_{eq} = \frac{\int_0^{r_s} \sigma_{eq}}{r_s} = \frac{2AY\sigma_n\sqrt{\pi\, a}}{\sqrt{2\pi\, r_s}} \tag{5.7}$$

Referring to Figure 5.4, at $r = r_s$ the equivalent stress is equal to the reference stress; thus,

$$\sigma_{eq} = A\sigma_{\max} = \frac{AY\sigma_n\sqrt{\pi\, a}}{\sqrt{2\pi\, r}} \tag{5.8}$$

Making use of Eq. (5.8), the relationship between the modified elastic modulus (E_s) and initial modulus of elasticity (E_0) can be written as

$$\frac{E_s}{E_0} = \left(\frac{\sigma_{ref}}{\overline{\sigma}_{eq}}\right)^q \tag{5.9}$$

The value of parameter "q" can be within the range of $1 \le q \le 2$ (Adibi-Asl and Seshadri, 2006). Applying the values $q = 1$ and $q = 2$, the E_s / E_0 will vary between 0.5 and 0.25, respectively. Based on numerous FEA on different crack configurations $E_s = E_0 / 3$ works out to be a good choice for modifying singular elements around a crack tip.

The modified elastic modulus of the singular elements around the crack tip can be obtained as $E_s = E_0 / 3$. A linear elastic FEA with $E_s / E_0 = 1/3$ for all adjacent elements

around the crack tip and with $E_s = E_0$ for all other elements of the component is carried out. The resulting parameters $(m^0/m,\ m^0/m_L)$ are used to locate B' (Figure 4.2).

5.3.2 Simplified Method for Cracked Components

Limit analysis is used to predict the load carrying capacity of cracked components and structures made up of sufficiently ductile material with high toughness. Local behavior of the structure is of considerable importance for components and structures with crack like flaws. Significant stress concentration is present at the crack tip. The peak stress due to the singular stress field needs to be blunted by artificially softening the material surrounding the crack tip, prior to applying the simplified method.

In this chapter of the thesis, the m_α-tangent method is extended in order to estimate the limit load of components and structures containing crack-like flaws. The proposed simplified method enables rapid determination of limit load based on a single linear elastic analysis. The method makes use of statically admissible stress field based on linear elastic finite element analysis. While using the m_α–tangent method, blunting of peak stresses are suggested to be performed in two stages if necessary. The detailed procedure is outlined in the following section of this chapter.

The steps to determine the limit load using the proposed m_α–tangent method are as follows: once the $R_\alpha^T = 1$ line is identified, the m_α^T value can be readily estimated by using the following relationship

$$m_\alpha^T = \frac{m^0}{1+0.2929(\zeta-1)} \tag{5.10}$$

and $$\zeta = \frac{m^0}{m_L} \tag{5.11}$$

The slope of the $R_\alpha^T = 1$ line is equal to $Tan(\theta) = \left(1 - \frac{1}{\sqrt{2}}\right)$. The value of m^0 and ζ can be determined from statically admissible distributions obtained from linear elastic FEA. With reference to Figure 4.4, the limit load multiplier m_α^T can be evaluated as follows:

Case-I: For $1.0 \le \zeta \le 1+\sqrt{2}$, point *A* (Figure 4.4) is assumed to lie on the $R_\alpha^T = 1$ line. The value of m_α^T can be obtained from Eq. (5.10). This case usually applies to pressure vessel components with negligible peak stresses.

Case-II: For $\zeta > 1+\sqrt{2}$, point *B* (Figure 4.4) is assumed to lie on the $R_\alpha^T = 1$ line. This case applies to components that develop flaws in service, or to components with sharp notches. The aim here is to blunt the peak stresses prior to evaluating m_α^T. With respect to Figure 4.4, the initial linear elastic FEA locates point *B* on the $R_\alpha^T = 1$ line and point B' on the TBM locus corresponding to $\zeta_i = \frac{m_i^0}{m_{L,i}}$. The subscript "*i*" refers to the initial point *B* and B'. The calculation procedure is as follows:

1. Perform a linear elastic analysis.

2. Locate point B and B'. Point B represents the combination of primary and secondary stresses whereas point B' represents the combination of primary, secondary and peak stresses.

3. Construct a horizontal line from point B to B'' signifying an invariant m_i^0 (blunting of peak stresses). Designate the value of m^0/m_L at B'' as ζ_f, which can be obtained by solving the equation

$$\frac{m_i^0}{m} = 1 + 0.2929(\zeta_i - 1) = \frac{\zeta_f^2 + 1}{2\zeta_f} \tag{5.12}$$

The roots of Eq. (5.12) are

$$\zeta_f = (1+C) \pm \sqrt{(1+C)^2 - 1} \tag{5.13}$$

where $C = 0.2929(\zeta_i - 1)$

4. The value of m_α^T can be evaluated by the equation

$$m_\alpha^T = \frac{m_i^0}{1 + 0.2929(\zeta_f - 1)} \tag{5.14}$$

5.3.3 Proposed Methodology

To estimate the limit load of cracked components and structures using the m_α-tangent method, the following procedure is proposed. In order to blunt the peak stresses due to the singular stress field at the crack tip, the elastic modulus of the singular elements around the crack tip in a finite element discretization scheme are modified as $E_s=E_0/3$,

where E_0 is the initial modulus and E_s is the modified modulus for the singular elements, while the rest of the component is specified a modulus of E_0.

From the statically admissible stress distribution obtained from a linear elastic FEA, inelastic parameters m^0 and ζ are obtained by using Eq. (5.10) and Eq. (5.11), respectively. If ζ is less than $1+\sqrt{2}$, the limit load multiplier (m_α^T) can be determined directly by using Eq. (5.10). However, if ζ is greater than $1+\sqrt{2}$, a second stage of softening is incorporated, and the value of m_α^T is obtained by using Eq. (5.14). It should be noted that BB'' (Figure 4.4) is designated in this thesis as "peak stress correction". In this section, we calculate limit load using three procedures:

- ***Procedure*-1:** Elastic analysis with E_s=E_0 and peak stress correction. This procedure is outlined in the previous section.

- ***Procedure*-2:** Elastic analysis with E_s=E_0/3 (singular elements) with no peak stress correction. This procedure simply modifies the singular elements without peak stress correction.

- ***Procedure*-3:** Elastic analysis with E_s=E_0/3 (singular elements) with peak stress correction. This procedure modifies the singular elements and makes the peak stress correction as outlined in the previous section.

A number of example problems are worked out in order to demonstrate the above mentioned procedures and the results are compared with those obtained from the inelastic finite element analysis.

5.4 Applications

The determination of limit load of cracked components using the proposed method is demonstrated in this section by working out several example problems. The finite element model for all the examples are developed using ANSYS (2008). Inelastic finite element analyses are performed by assuming elastic-perfectly plastic material model. While modeling the cracked components using the finite elements, singular stress field ahead of the crack-tip is simulated by using singular elements.

5.4.1 Compact Tension (CT) Specimen

The compact tension specimen, which contains an axial force and a moment on the ligament ahead of the crack, is widely used in fracture toughness testing. A compact tension specimen (Figure 5.5) having a width W=100 mm (3.937 in.), height H=125 mm (4.921 in.), thickness t=3 mm (0.118 in.) and crack length a=46 mm (1.811 in.) is considered. The modulus of elasticity of the material is 206.85 GPa (30×10^6 psi), yield strength is 206.85 MPa (30×10^3 psi). and Poisson's ratio is 0.3. The specimen is subjected to a tensile load of 5 kN (0.725 psi).

Due to the symmetry of geometry, loading and boundary conditions, one half of the specimen is modeled in plane stress condition. The finite element model is developed using eight noded isoparametric quadrilateral elements with sixteen singular elements around the crack tip. Using the proposed methodology, limit load of the component is estimated as follows:

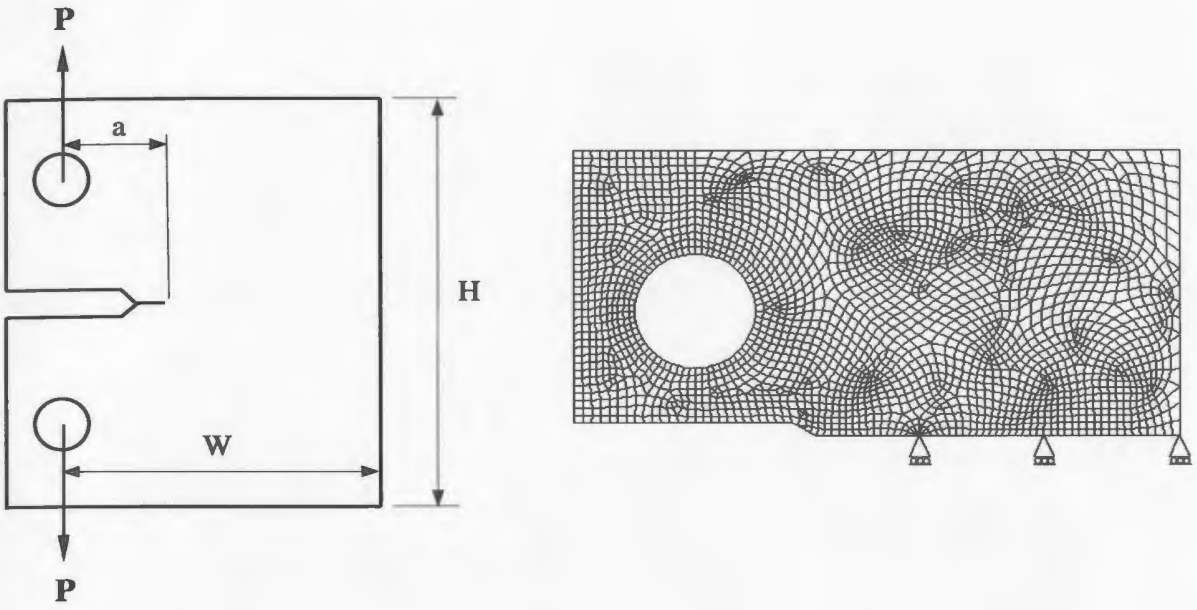

(a) (b)

Figure 5.5 Compact tension specimen (a) Geometry (b) Finite element model (half of the specimen)

Procedure-1: Linear elastic FEA for this component generates a statically admissible stress distribution, on the basis of which $m_i^0 = 2.603$, $m_{L,i} = 0.292$, and the corresponding ζ_i is equal to 8.906. Now $\zeta_i > 1+\sqrt{2}$ is represented by point *B*, as shown in Figure 4.4. Using Eq. (5.13), ζ_f is evaluated such that m^0 at *B* and B'' are equal. As a result, ζ_f =6.477 and m_α^T based on ζ_f, obtained from Eq. (5.14), is 0.9996.

Procedure-2: The singular stress field ahead of the crack tip is blunted by modifying the elastic modulus of the singular elements as E_s=E_0/3, where E_s is the modified elastic modulus of the singular elements and E_0 is the modulus of the rest of the elements of the

component. On the basis of a linear elastic FEA, $m_i^0 = 2.595$, $m_{L,i} = 0.494$, and the corresponding $\zeta_i = 5.258$ is obtained. Using Eq. (5.10), the value of m_α^T based on ζ_i is 1.155.

Procedure-3: The value of $\zeta_i = 5.258$ is obtained in Procedure-2, where $\zeta_i > 1+\sqrt{2}$ as represented by point *B*, shown in Figure 4.4. Therefore, peak stress correction is needed in this case. Using Eq. (5.13), ζ_f is evaluated such that m^0 at *B* and B'' are equal. As a result, $\zeta_f = 4.260$ and m_α^T based on ζ_f, obtained from Eq. (5.14), is 1.328. The corresponding elastic-plastic finite element estimate is 1.331. The results are shown in Table 5.1.

Table 5.1 Limit load multipliers for compact tension specimen

Procedure	m^0	m_L	ζ	m_α^T	m_{NFEA}
Procedure-1	2.603	0.292	6.477	1.000	1.331
Procedure-2	2.595	0.494	5.258	1.155	
Procedure-3	2.595	0.494	4.260	1.328	

5.4.2 Middle Tension Panel

Consider a thin middle tension panel (Figure 5.6) with the following dimensions: width, $2W$=250 mm (9.843 in.); thickness, t=3 mm (0.118 in.); length, $2L$= 600 mm (23.622 in.) and crack length, $2a$=50 mm (1.969 in.). The plate is subjected to a remote tensile load of 75 MPa (10.877×10^3 psi). The modulus of elasticity of the material is 206.85 GPa (30×10^6 psi), yield strength is 206.85 MPa (30×10^3 psi) and Poisson's ratio is 0.3. Due

to symmetry, only a quarter of the plate is modeled. The finite element model is developed with eight noded isoparametric quadrilateral elements with sixteen singular elements around the crack tip.

The model is first analyzed using *Procedure*-1. Based on the initial linear elastic FEA, the value of $m_i^0 = 2.715$, $m_{L,i} = 0.984$ and the corresponding $\zeta_i = 2.760$ is obtained. As $\zeta_i > 1+\sqrt{2}$, the peak stress correction is needed and therefore, the value of ζ_f is evaluated using Eq. (5.13) as 2.654. Based on ζ_f, the value of m_a^T is obtained from Eq. (5.14) as 1.829.

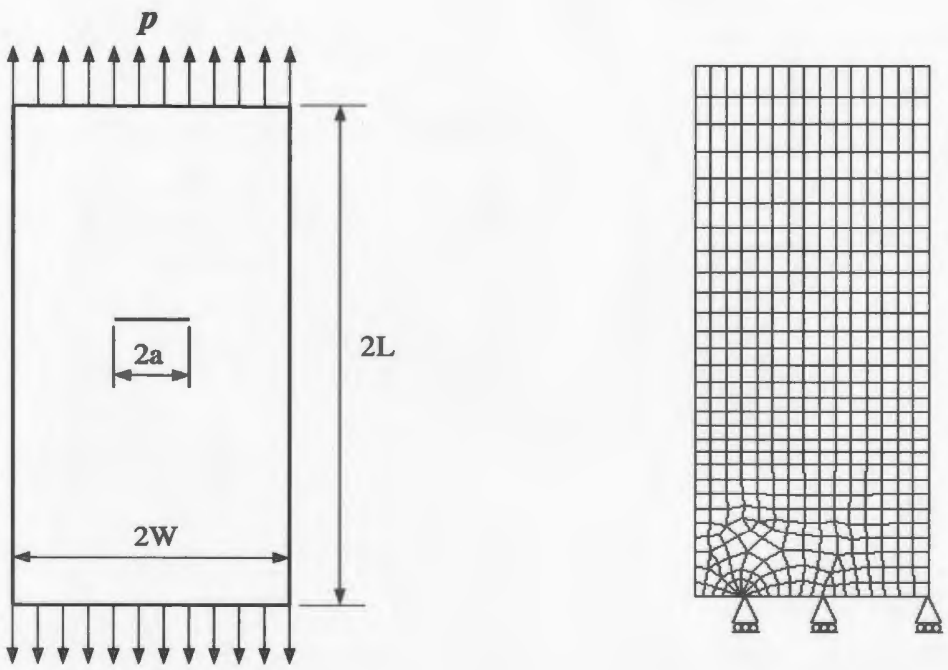

Figure 5.6 Middle tension panel (a) Geometry (b) Finite element model (quarter of the plate)

Table 5.2 Limit load multipliers for middle tension panel

Procedure	m^0	m_L	ζ	m_α^T	m_{NFEA}
Procedure-1	2.715	0.984	2.654	1.829	2.233
Procedure-2	2.713	1.369	1.981	2.107	
Procedure-3**	-	-	-	-	

** In this case, further peak stress correction is not needed since $\zeta_f < 1+\sqrt{2}$.

In order to estimate the limit load based on *Procedure*-2, the singular stress field ahead of the crack tip is blunted by modifying the elastic modulus of the singular elements as explained in the previous example. From the initial linear elastic FEA, the value m_i^0= 2.713 and $m_{L,i}$=1.369 is obtained. The corresponding ζ_i=1.981 lies within the m_α-triangle. Using Eq. (5.10) the value of the limit load multiplier is m_α^T= 2.107. Elastic-plastic FEA estimate the limit load multiplier m_{NFEA}=2.233. It should be noted that *Procedure-3* does not need to apply in this case as the value of $\zeta_i < 1+\sqrt{2}$. The results are shown in Table 5.2.

5.4.3 Plate with Multiple Cracks

A thin plate with multiple cracks (Figure 5.7) is considered in this example. The plate has one horizontal crack (length, 2*a*=20 mm (0.787 in.)) at the centre and four 45° inclined cracks (length, 2*b*=21.2 mm (0.835 in.)), symmetrically located on both sides of the horizontal and vertical lines of symmetry. The crack tips are spread vertically by *c*=30 mm (1.181 in.) and horizontally by *d*=60 mm (2.362 in.). The plate has a width, *W*=200 mm (7.874 in.); height, *H*=200 mm (7.874 in.) and thickness, *t*=3 mm (0.118 in.).

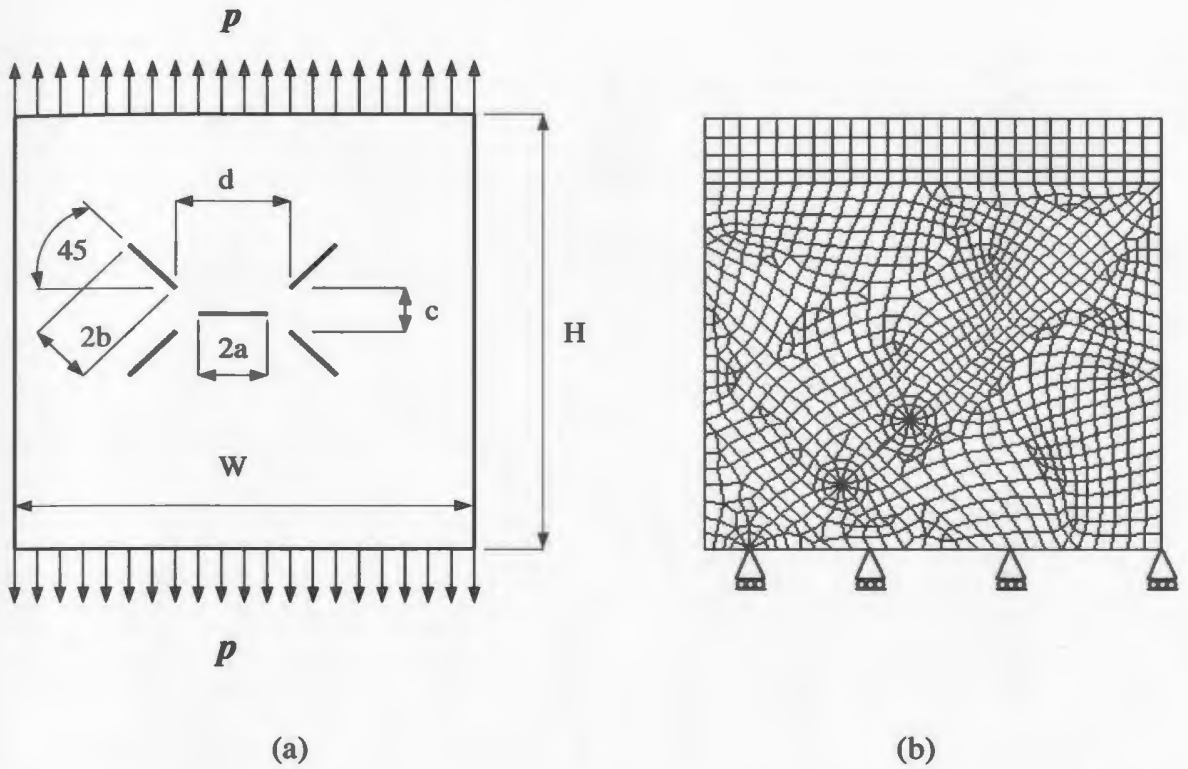

Figure 5.7 Plate with multiple cracks (a) Geometry (b) Finite element model (quarter of the plate)

The modulus of elasticity of the material is 262 GPa (38×10^6 psi), yield strength is 262 MPa (38×10^3 psi) and Poisson's ratio is 0.3. The plate is subjected to a remote tensile load of 75 MPa (10.878×10^3 psi). Only a quarter of the plate is modeled by taking advantage of symmetry.

Table 5.3 Limit load multipliers for plate with multiple cracks

Procedure	m^0	m_L	ζ	m_α^T	m_{NFEA}
Procedure-1	3.376	1.112	2.840	2.194	2.663
Procedure-2	3.369	1.389	2.426	2.377	
Procedure-3	3.369	1.389	2.423	2.378	

The model is first analyzed using *Procedure*-1. Based on the initial linear elastic FEA, the value of $m_i^0 = 3.376$, $m_{L,i} = 1.112$ and the corresponding $\zeta_i = 3.036$ is obtained. As $\zeta_i > 1+\sqrt{2}$, the peak stress correction is needed and therefore, the value of ζ_f is evaluated using Eq. (5.13) as 2.840. Based on ζ_f, the value of m_α^T is obtained from Eq. (5.14) as 2.194.

In order to estimate the limit load based on *Procedure*-2, the singular stress field ahead of the crack tip is blunted by modifying the elastic modulus of the singular elements as explained in the earlier example. From the initial linear elastic FEA, the value $m_i^0 = 3.369$ and $m_{L,i} = 1.389$ is obtained. The corresponding $\zeta_i = 2.426$ lies outside the m_α-triangle. Using Eq. (5.10), the value of m_α^T based on ζ_i is 2.377.

Then the limit load is estimated using *Procedure*-3. The value of $\zeta_i = 2.426$ is obtained in *Procedure*-2, where $\zeta_i > 1+\sqrt{2}$. Therefore, peak stress correction is needed in this case. Using Eq. (5.13), ζ_f is evaluated as 2.423 and corresponding m_α^T obtained from Eq. (5.14), is 2.378. The corresponding estimate based on elastic-plastic finite element analysis is 2.663. The results are shown in Table 5.3.

5.4.4 Pipe with an Extended Inner Axial Crack

A pipe with an extended inner axial crack (Figure 5.8) is considered in this example. The radius to thickness ratio of the pipe is R/t=2.5, the crack depth is a/t=0.4. The modulus of elasticity of the material is 262 GPa (38×10^6 psi) and yield strength is 262 MPa (38×10^3

psi). The structure is subjected to an internal pressure of 25 MPa (3.626×10^3 psi). Only a half of the pipe is modeled in plane strain condition due to the symmetry of geometry, loading and boundary conditions. Singular elements are used to simulate the singular stress field ahead of the crack tip.

The model is first analyzed using *Procedure*-1. Based on the initial linear elastic FEA, the value of $m_i^0 = 3.979$, $m_{L,i} = 1.077$ and the corresponding $\zeta_i = 3.695$ is obtained. As $\zeta_i > 1+\sqrt{2}$, the peak stress correction is needed and therefore, the value of ζ_f is evaluated using Eq. (5.13) as 3.274. Based on ζ_f, the value of m_a^T is obtained from Eq. (5.14) as 2.965.

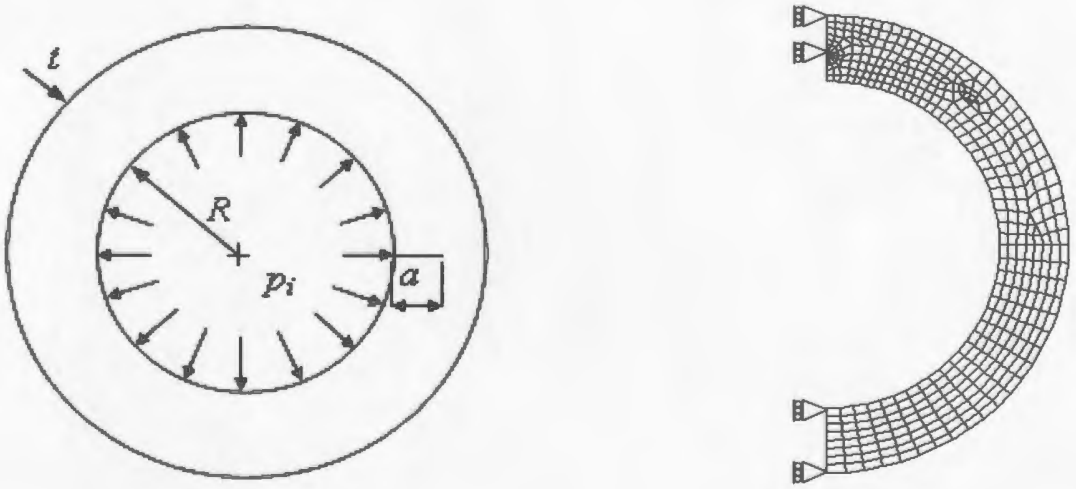

(a) (b)

Figure 5.8 Pipe with an extended inner axial crack (a) Geometry (b) Finite element model (half of the pipe).

Table 5.4 Limit load multipliers for pipe with an extended inner axial crack

Procedure	m^0	m_L	ζ_f	m_α^T	m_{NFEA}
Procedure-1	3.979	1.077	3.274	2.388	2.965
Procedure-2	3.972	1.695	2.344	2.850	
Procedure-3**	-	-	-	-	

** In this case, peak stress correction is not needed since $\zeta_f < 1+\sqrt{2}$.

In order to estimate the limit load based on *Procedure*-2, the singular stress field ahead of the crack tip is blunted by modifying the elastic modulus of the singular elements as explained in the earlier example. From the initial linear elastic FEA, the value $m_i^0 = 3.972$ and $m_{L,i} = 1.695$ is obtained. The corresponding $\zeta_i = 2.344$ lies inside the m_α-triangle. Using Eq. (5.10) the value of the limit load multiplier is $m_\alpha^T = 2.850$. Elastic-plastic FEA estimate the limit load multiplier $m_{NFEA} = 2.965$. It should be noted that *Procedure*-3 does not need to apply in this case as the value of $\zeta_i < 1+\sqrt{2}$. The results are tabulated in Table 5.4.

5.5 Discussion

The underlying feature of the m_α-tangent method is used in this chapter to develop a simplified method in order to estimate the limit load of mechanical components and structures containing crack-like flaws. By using the proposed method, reasonably accurate estimate of limit load of cracked components and structures can be obtained on the basis of a single linear elastic FEA. The proposed three procedures are applied to a

number of standard cracked component configurations. The capability of the method is further tested on more complicated practical component configuration. The results obtained are in good agreement with the respective inelastic FEA results. The method is suitable for level-2 "fitness-for-service" (FFS) assessment.

5.6 Closure

The m_α-tangent method has been extended in this chapter in order to estimate the limit load of mechanical components and structures containing crack-like flaws. The method is demonstrated through a number of example problems and the results are compared with the corresponding inelastic FEA results. In the next chapter, a linear elastic analysis based method is proposed to categorize the elastic stresses in pressure vessel components and structures. The method is considered as an attractive alternative over conventional techniques e.g., stress linearization and interaction / discontinuity analysis. The proposed method is applicable to components and structures subjected to both mechanical and thermal loads.

CHAPTER 6

STRESS CATEGORIZATION OF PRESSURE COMPONENTS

6.1 Introduction

Design by analysis (DBA) using the ASME stress categorization approach (Code Section III (2007), Subsection NB and Code Section VIII, Division 2 (2007)) is a direct application of linear elastic analysis results. The ASME Boiler and Pressure Vessel (B&PV) Code Section III (2007) (paragraph NB-3217 and Tables NB-3217-1 (for vessels) and NB-3217-2 (for piping)) and Section VIII Div. 2 (2007) (paragraph 5.2.2.2 and Table 5.6 [2]) provide guidelines for classifying the elastic stresses that could be obtained by finite element analysis. In these guidelines, the stresses are sorted into

different categories and allowable limits are imposed for each respective category and defined combinations of the same in order to guard against distinct type of failure modes. Although these guidelines cover a wide range of pressure vessel components and structures, they are sometimes difficult to use for three dimensional components with complex geometry.

Significant work has been reported over the decades in order to interpret the linear elastic stresses induced in pressure vessel components and structures. Kroenke (1974) developed a procedure to interpret two-dimensional stresses in axisymmetric structures along a predefined line called a stress classification line (SCL). Gordon (1976) proposed a procedure for evaluation of two-dimensional finite element stress resultants such that the evaluated stresses are comparable to the ASME Boiler and Pressure Vessel Code, Section III (Nuclear Power Plant Components, Division 1, 1974) stress requirements. Marriott (1998) investigated the issue of decomposition of load and deformation controlled stresses by using linear elastic FEA.

Seshadri and Marriott (1993) demonstrated that the reference stresses are load controlled stresses and are directly proportional to the applied loads. Seshadri and Marriott (1993) also attempted to relate the reference stress and limit load with the ASME stress categorization concepts. Hechmer and Hollinger (1997, 2000) have made significant contributions in developing the methods for categorization of the resultant stresses from various finite element analyses. Fanous and Seshadri (2006) implemented the redistribution node (r-node) method by using the elastic modulus adjustment procedure (EMAP) (Mackenzie et al., 1993), to identify the primary stresses in pressure vessel components. Stress classification lines or areas are not necessary in this method.

The categorization of linear elastic stresses in non-symmetric three dimensional components and structures is a challenging task despite the efforts mentioned above. In this thesis, a simplified method is proposed as an attempt to circumvent the difficulties in stress categorization of linear elastic stresses in complex three dimensional structures. The concepts underlying the m_α-tangent method, as discussed in Chapter 4, are used herein to categorize the linear elastic stresses in pressure vessel components and structures. The proposed method is a simplified tool for achieving the categorization of elastic stresses in two or three dimensional components with complex geometry.

The proposed simplified method is able to categorize the elastic stresses in pressure vessel components and structures, using a single linear elastic finite element analysis. The proposed method is based on approximate limit load multipliers and makes use of equivalent stresses (Tresca or von Mises) as a measure of the proximity to yield of the stress state or stress distribution. The proposed method is applicable to the components or structures subjected to both mechanical and thermal loads. The method is able to partition the elastic stresses into primary (P), primary plus secondary ($P+Q$), and peak (F) stress categories. The method is considered to be a direct and alternative approach over conventional approaches i.e., stress linearization and interaction / discontinuity analysis.

The method is first demonstrated by an example, a torispherical head subjected to internal pressure and thermal load (temperature gradient across the thickness of the wall). The method is further applied to several practical pressure vessel components and structures ranging from simple to relatively complex geometric configurations. The results compare well with those obtained by the conventional techniques. Therefore, the proposed method can be used as a tool for the categorization of linear elastic stresses induced in pressure

vessel components and structures, especially three dimensional components with complex geometric and loading conditions.

6.2 Stress Categories and Their Role in Pressure Component Design

The ASME Boiler and Pressure Vessel Code (2007) can be used to design pressure vessels and piping systems by analysis. Design by analysis (DBA) using the ASME stress categorization approach is a direct application of the linear elastic results. The main idea behind the stress categorization concept is that each category of stresses and their selective combinations are associated with distinct type of failure modes. Appropriate stress limits are imposed on each of these categories and their selective combinations in order to guard against the respective failure modes.

The ASME Boiler and Pressure Vessel Code (2007) provides guidelines for the classification of linear elastic stresses in pressure vessel components and structures into (a) primary, (b) secondary and (c) peak stress categories. The definition and basic characteristics of these stress categories and their role in practical pressure vessel component design is discussed below.

(a) Primary Stress

Primary stresses are set-up in a mechanical component or structure in order to equilibrate the applied external traction. The basic characteristic of the primary stress is that it is not

self-limiting. Primary stresses are set-up in a structure due to mechanical loads. Stresses developed by thermal load are not classified as primary stress. The definition of the primary stress that is spelled out in the Code (ASME B&PV Code, 2007) is as follows:

> *Primary stress is any normal stress or a shear stress developed by an imposed loading which is necessary to satisfy the laws of equilibrium of external and internal forces and moments.*

Primary stresses are subdivided into three categories: general primary membrane (P_m), local primary membrane (P_L) and primary bending (P_b) stress. The general primary membrane stress is the average stress across the thickness of a component or structure developed due to the mechanical loads. This stress is free from the effect of structural discontinuities. The local primary membrane stress is the average stress across the thickness of a component or structure developed due to the mechanical loads, and includes the effect of structural discontinuities.

The primary bending stress is the component of primary stress that is proportional to the distance from the centroid of the solid section, and is produced due to the mechanical loads. The local stress concentrations are not considered in the primary stresses. The primary stress limits are intended to prevent the plastic deformation and to provide a safety factor on the ductile bust pressure. If the primary stresses considerably exceed the yield strength of the material, the structure will be in the verge of collapse or, at least, in gross distortion.

(b) Secondary Stress

Secondary stress is developed in a component or structure in order to satisfy the geometric compatibility conditions. Secondary stresses are generally developed in the region of gross structural discontinuities due to internal and external constraints produced by the mechanical loads, and also due to differential thermal loads. The local stress concentrations are not considered in the secondary stresses. The definition of the secondary stress that is spelled out in the Code (ASME B&PV Code, 2007) is as follows:

> *Secondary stress is a normal stress or a shear stress developed by the constraint of adjacent material or by self-constraint of the structure.*

The basic characteristic of a secondary stress is that it is self-limiting. Local yielding and minor distortions can satisfy the conditions which cause the stress to occur and failure from one application of the stress is not to be expected. Secondary stresses are important for shakedown analysis. The primary plus secondary stress limits are intended to prevent the excessive plastic deformation leading to incremental collapse.

(c) Peak Stress

Peak stress is the highest stress in a component or structure produced by a notch or thermal gradient. The definition of the peak stress that is spelled out in the Code (ASME B&PV Code, 2007) is as follows:

Peak stress is that increment of stress which is additive to the primary plus secondary stresses by reason of local discontinuities or local thermal stress including the effects, if any, of stress concentrations.

Peak stresses are generally developed in the region of local structural discontinuities. The basic characteristic of a peak stress is that it does not cause any noticeable distortion in the component or structure and is objectionable only as a possible source of a fatigue crack or brittle fracture. The cumulative usage factor from all cycles of primary plus secondary plus peak stress is limited to a specific value, less than or equal to one to prevent fatigue failure.

6.3 Stress Categorization Approaches

6.3.1 Traditional Methods

Stress categorization in pressure vessel components and structures aims to isolate primary, secondary and peak stresses from the stress resultants of a linear elastic analysis. Traditionally, equilibrium and compatibility considerations between different elements of the component have been used for this purpose. Two of the methods that have been used to aid stress categorization are stress linearization and interaction / discontinuity analysis as per A-6200 of ASME B&PV Code, Section III (2007).

Stress linearization has been used to extract stresses that are similar to those from discontinuity analysis on the basis of linear elastic FEA. The finite element analysis as such provides total stresses, which can then be partitioned into membrane, bending and

peak stresses by linearization through the thickness as depicted in Figure 6.1. The membrane and bending stresses correspond to the force and moment transmitted by the wall. The dotted lines that appear in Figure 6.1 represent the linearized stress component distribution obtained from FEA across the thickness of a section for a given loading condition. The method works well for simple geometries such as axisymmetric pressure vessels. However, for complex three-dimensional geometric conditions, it can be very difficult (though not impossible) to identify the appropriate location and orientation of the stress linearization path. It should be noted that linearization does not explicitly categorize the stresses; categorization is dependent upon the analyst's interpretation of the rules contained within the respective ASME B&PV Codes (2007).

In a discontinuity analysis, the pressure vessel is decomposed into a finite number of interconnected blocks or elements. Primary stresses are then derived from the interacting forces and moments. Secondary stresses can be obtained by imposing displacement compatibility. Discontinuity analysis is particularly applicable to two dimensional axisymmetric pressure vessels. The method is generally not feasible for complex, asymmetric, three dimensional pressure vessels.

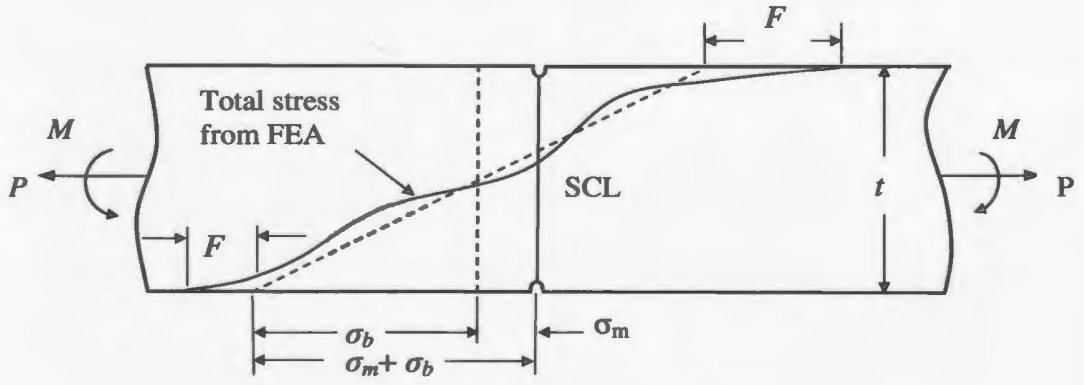

Figure 6.1 Finite element stress linearization

6.3.2 ASME Stress Categorization Procedure

ASME Boiler and Pressure Vessel Code Section III (2007) and Section VIII Div. 2 (2007) have provided guidelines to categorize linear elastic stresses based on the location, origin (e.g., pressure or thermal) and type (membrane, bending or peak) of the stresses. Each category of the stress is compared to the respective allowable limit. ASME has specified three different levels of allowable stresses, which are given as S_m, $1.5S_m$, and $3S_m$, where S_m is the allowable "stress intensity" based upon the material properties at the design temperature (here, stress intensity is the same as two times the maximum shear stress).

The main stress categories in pressure vessel components are general primary membrane (P_m), primary local membrane (P_L), primary bending (P_b), secondary (Q), and peak (F). ASME B&PV Code (2007) has provided allowable limit for each of these stress categories and their selective combinations: the primary membrane stress (P_m) is limited to S_m, the primary local membrane stress (P_L) and primary membrane plus bending stress (P_L+P_b) are limited to $1.5S_m$, the primary plus secondary stress range ($P+Q$) is limited to $3S_m$, and the cumulative usage factor from all cycles of ($P+Q+F$) is limited to a specified value less than or equal to one. Therefore, in order to apply the appropriate Code (ASME B&PV Code, 2007) limits in practice, it is necessary to develop a clear procedure to partition the total stresses obtained from FEA (or any other rigorous analysis method) into these predefined ASME B&PV Code (2007) stress categories.

6.3.3 Equivalent Stress Method

The ASME stress categorization guidelines work well for axisymmetric structures and thin shells. Guidelines have also been developed to address more complex three-dimensional geometries and non-symmetric loadings and boundary conditions, as previously discussed by Hechmer and Hollinger (1997, 2000). However, the basis for the application of stress linearization is much weaker than for axisymmetric structures, and in practical terms, the placement of classification lines becomes much more difficult to justify. Stress linearization can account for plastic stress redistribution (i.e. the redistribution of stress from the elastic state if plasticity occurs) through the thickness, but not for plastic stress redistribution in the plane of the shell. Local "hot spots" of high stress, e.g. within the attenuation length of a particular geometric discontinuity, near lugs or nozzles, require experience from the analyst in placing classification lines, or a very conservative evaluation will result. It is well recognized that stress classification may produce ambiguous results (Section 5.A.3 (c) [2]).

Alternative simplified concepts are utilized in the present work to categorize the elastic stresses induced in pressure vessel components and structures. The proposed method is based on approximate limit load multipliers and makes use of equivalent stresses (Tresca or von Mises) as a measure of the proximity to yield of the stress state or stress distribution. The proposed method is able to partition the elastic stresses into primary (P), primary plus secondary ($P+Q$), and peak (F) stress categories. It sidesteps some of the difficulties of the conventional stress categorization approaches, such as choosing suitable linearization locations. Therefore, the proposed method can be used as a tool for

the categorization of stresses for a general class of pressure vessel components, especially three dimensional components with complex geometries.

6.3.4 Post Processing of Linear Elastic FEA

Some of the currently available commercial finite element codes facilitate the linearization of stresses, resulting from a linear elastic FEA, through post-processing. The stress linearization is performed along a predefined path. The path is defined by two nodes (i.e., N_1 and N_2) across the section of interest as shown in Figure 6.2. The stress linearization tool available in commercial finite element codes, e.g. ANSYS (2008), enables the splitting of total stresses into membrane (constant), bending (linear), and peak categories through a predefined section.

The membrane stress for a given section of interest is computed as follows:

$$\sigma_i^m = \frac{1}{t}\int_{-t/2}^{t/2} \sigma_i dx_s \tag{6.1}$$

where t is the thickness of the section (length of the path), σ_i is the stress component, and x_s is the coordinate along the path. The magnitude of the bending stress at the extreme points of the path is calculated as follows:

$$\sigma_i^b = -\frac{6}{t^2}\int_{-t/2}^{t/2} \sigma_i x_s dx_s \tag{6.2}$$

The bending stress at the extreme fibers of the component will be equal in magnitude but opposite in sign.

Finally, the amount of peak stress, which usually occurs at the surface of the component, is the difference between the total stress and the sum of the linearized membrane and bending stresses. Therefore, the peak stress at any point along the path is given by

$$\sigma_i^F = \sigma_i - \left(\sigma_i^m + \sigma_i^b\right) \tag{6.3}$$

where σ_i is the total stress obtained from the results of the FEA.

It should be noted that ANSYS does not explicitly categorize the stresses; instead it linearizes them into membrane (σ_m), bending (σ_b) and peak (F) stresses. Therefore, additional effort is required to properly identify the different categories of stresses for Code (ASME B&PV Code Section III and Section VIII Div. 2, 2007) compliance.

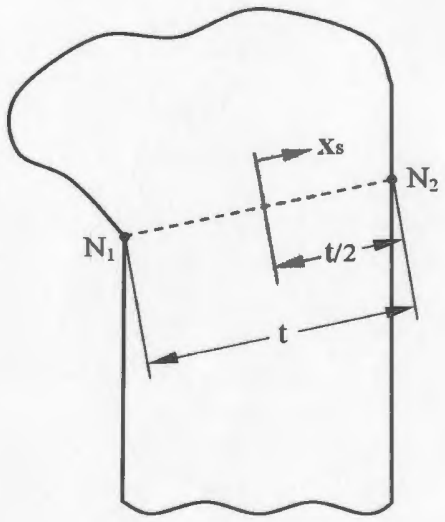

Figure 6.2 Coordinates of cross section

6.4 Concepts of Simplified Methods

The m_α–tangent method has been developed in this thesis in order to estimate the limit load of a general class of mechanical components and structures. The formulation of the m_α–tangent method is based on the variational principles in plasticity. The method has explicit dependency on the classical lower bound multiplier (m_L) and upper bound multiplier (m^0). The detail derivation of the m_α–tangent method is presented in Chapter 4 of this thesis. The underlying concepts of the two-bar model (TBM) and m_α-tangent method are invoked herein to categorize the linear elastic stresses in pressure vessel components and structures. The m_α–tangent method is briefly presented here in order to demonstrate the proposed stress categorization method in a more organized way.

6.4.1 Reference Two-Bar Model (TBM)

The Two-Bar Model is the simplest structure in which stress redistribution occurs after the onset of yielding. As such, it serves as a simplified representation of similar redistribution phenomena in general pressure vessel components. The geometry of the TBM can be adapted to best reflect the behavior of the component. General pressure vessel component configurations can be related to the reference two-bar structure by matching the point on the constraint map based on elastic analysis. Seshadri and Adibi-Asl (2006) have derived the "scaling equations" as follows (Figure 6.3):

$$\frac{m^0_{Comp}}{m_{L,Comp}} = \frac{m^0_{Bar}}{m_{L,Bar}} \left(= \frac{1}{\sqrt{\lambda}}\right) \tag{6.4}$$

where $\lambda = L_1/L_2 = \sigma_2/\sigma_1$.

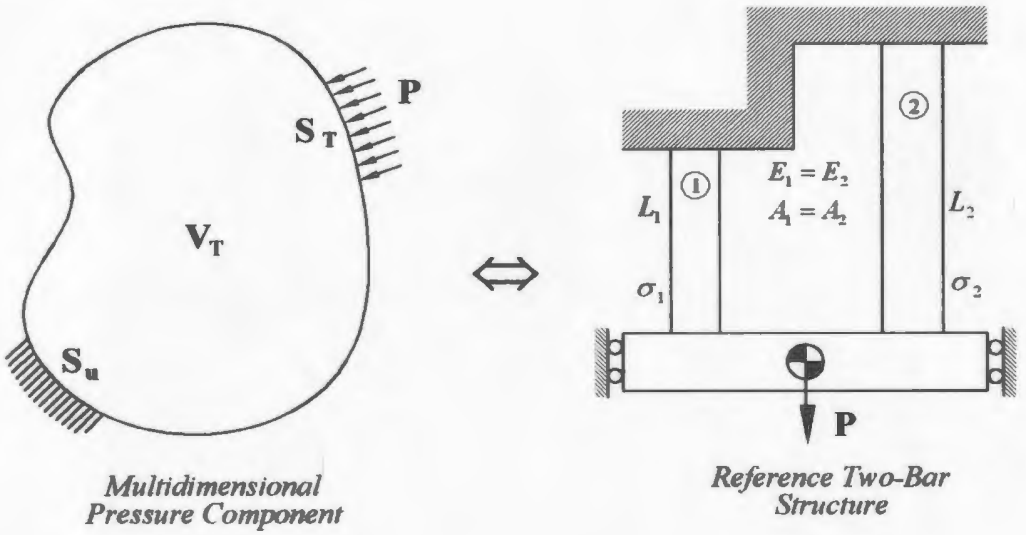

Figure 6.3 Reference two-bar structure (Seshadri and Adibi-Asl, 2006)

L_1 and L_2 are the lengths of the bars, and σ_1 and σ_2 are the respective stresses from elastic analysis. The cross sectional area and elastic modulus of the two bars are assumed to be the same. Therefore, the length ratio λ uniquely defines the stiffness ratio of the two bars. Without loss of generality, it is assumed that $\lambda \leq 1$. The yield strengths of both bars are the same, σ_y. Equation (6.4) serves to define the geometry parameter λ that best represents stress redistribution in the actual pressure vessel component. This is the reference TBM. Once m^0_{Comp} and $m_{L,Comp}$ are determined on the basis of a linear elastic FEA, the value of λ can be determined by using Eq. (6.4).

Based on this λ an estimate of m_{Comp} can be obtained using Eq. (6.4), which assumes that the ratios of m^0/m are the same for the actual component and the reference two-bar mechanism.

$$\frac{m^0_{Comp}}{m_{Comp}} = \frac{m^0_{Bar}}{m_{Bar}} \left(= \frac{\lambda+1}{2\sqrt{\lambda}} \right) \tag{6.5}$$

The limit load multiplier m is calculated analytically for the reference TBM as $m_{Bar} = \frac{2\sigma_y}{\sigma_1 + \sigma_2}$, where σ_1 is identified with the maximum equivalent stress, $(\sigma_e)_{\max}$. Therefore, the ratio $\left(\frac{m^0_{Bar}}{m_{Bar}} \right)$ will be a specific point representing combination of primary, secondary and peak stresses along the TBM trajectory. The entire TBM trajectory can be drawn by considering λ as a free parameter.

6.4.2 The m_α–Tangent Method

For a given pressure vessel component, a single elastic analysis will yield all the information that are needed to perform stress classification with the m_α–tangent method. The values of m^0 and ζ can be determined from statically admissible stress distributions obtained from linear elastic FEA of the component. The m^T_α value can then be readily estimated by using the following equations

$$m^T_\alpha = \frac{m^0}{1 + 0.2929(\zeta - 1)} \tag{6.6}$$

$$\text{and} \quad \zeta = \frac{m^0}{m_L} \tag{6.7}$$

The slope of the $R^T_\alpha = 1$ line is equal to $Tan(\theta) = \left(1 - \frac{1}{\sqrt{2}}\right)$.

Depending on the value of ζ, one of two cases needs to be considered:

Case-I: $\zeta \leq 1+\sqrt{2}$, (negligible peak stresses)

For this case, point *A* (Figure 4.4) is assumed to lie on the $R_\alpha^T = 1$ line. The value of m_α^T can be obtained from Eq. (6.6). This case usually applies to well-designed pressure vessel components with gentle geometric transitions.

Case-II: $\zeta > 1+\sqrt{2}$, (presence of peak stresses)

This case applies to components that develop flaws or cracks in service, or to components with sharp notches. The aim here is to blunt the peak stresses prior to evaluating m_α^T. With reference to Figure 4.4, the initial linear elastic FEA locates point *B* on the $R_\alpha^T = 1$ line and point B' on the TBM locus corresponding to $\zeta_i = \dfrac{m_i^0}{m_{L,i}}$. The subscript "*i*" refers to the initial point *B* and B'. The detailed calculation procedures are presented in Chapter 4 of this thesis.

6.5 Stress Categories in Pressure Components

The categorization of elastic stresses, induced in pressure vessel components, essentially means the decomposition of the stress resultants into primary (*P*), secondary (*Q*) and peak (*F*) stress. The primary stress could be either primary membrane (P_m) or primary bending (P_b) or combination of the two. Similarly, the secondary stress could be either secondary membrane (Q_m) or secondary bending (Q_b) or combination of the two.

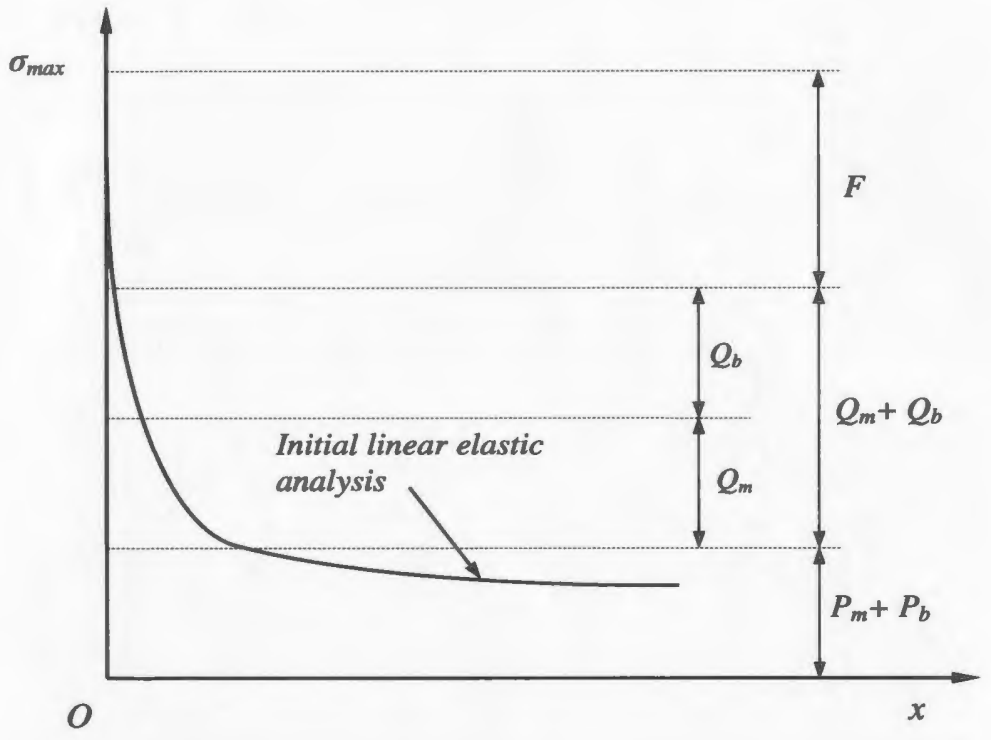

Figure 6.4 Stress distribution at the critical section of a component

Figure 6.4 represents the schematic stress distribution, based on initial linear elastic analysis, at the critical section of a component. The different categories of stresses are labeled in the figure in order to relate them with the linear elastic stress distribution. The stress distribution at the critical section of a component after the initial linear elastic FEA is shown by the "solid-line" in Figure 6.4, where σ_{max} represents the maximum stress in the component.

Practical pressure vessel components and structures usually experience combined mechanical and thermal loads. It should be noted that thermal load (due to through thickness temperature gradient) produces only secondary and peak stresses in the component or structure. These stresses are expected to disappear if the structure is allowed to expand (or contract) up to certain extent. These stresses are deformation-

controlled in nature. Most of the practical pressure vessel components and structures experience a certain extent of thermal load in their service life.

On the other hand, mechanical loading can produce primary, secondary and peak stress in the component or structure. Primary stresses are set-up in the structure in order to equilibrate the applied sustained loads. These stresses are statically admissible i.e., load controlled in nature. Mechanical loading can produce secondary stress due to the internal and external constraint of the structure. Peak stress in the structure is due to local structural discontinuity.

6.6 Stress Categorization Methodologies

For simple geometries, the tradeoff for considering the full membrane stress as load controlled primary stress (P) and full bending stress as deformation controlled secondary stress (Q) is usually workable (Hollinger and Hechmer, 2000). Therefore, for simple axisymmetric structures, primary plus secondary ($P+Q$) and peak (F) component of stresses could be obtained by using the stress linearization technique. For highly complex geometries, the Codes' (ASME B&PV Code, 2007) simplified assumption is to consider membrane stress as primary and bending stress as secondary (Hollinger and Hechmer, 2000).

It is well understood that the intensity of peak stress (F) is simply the difference between the total stress (σ_{max}) and the membrane plus bending stress ($\sigma_m + \sigma_b$), which could be obtained through stress linearization. On the other hand, primary plus secondary

stress $(P+Q)$ is the difference between the maximum total stress (σ_{max}) and the peak stress (F). Therefore, for simple axisymmetric structures, primary plus secondary $(P+Q)$ and peak (F) stress component could be obtained by using linearization technique within reasonable accuracy. As a result, the primary plus secondary stress $(P+Q)$ identified by the proposed method is compared with those obtained from the linearization technique for simple axisymmetric structures. The primary stress (P), identified by the proposed method is compared with elastic-plastic FEA results. It should be noted that the proposed method estimates the plastic limit load solution and, therefore, gives a primary stress (P), which is directly comparable with the S_m limit.

Inelastic FEA is considered to be an alternative tool to identify the primary stress. For complex three dimensional and especially nonsymmetric components and structures, inelastic FEA may not be effective in terms of computational effort and time. The proposed m_α-tangent method is able to identify the primary component of stresses using a single linear elastic analysis. The method is applicable to three dimensional components and structures with complex geometric and loading conditions. The step by step procedure for determining the primary, primary plus secondary and peak stress, using the proposed method, is outlined in the following section of this chapter.

6.6.1 Proposed Methodology (The m_α-Tangent Method)

The proposed method for categorization of stresses, using the m_α-tangent method, is applicable to both mechanical and thermal loads. Thermal load will generate secondary

and peak stresses but will not affect the primary stresses. For mechanical loading, the proposed method is as follows:

An initial linear elastic FEA is performed. The results of the initial FEA are used to evaluate classical lower bound multiplier (m_L) and upper bound multiplier (m^0) using Eq. (3.1) and Eq. (3.5), respectively.

(1) If m^0/m_L is less than $1+\sqrt{2}$ then only primary and secondary stresses are considered to be present in the component, and the magnitude of peak stresses is either zero or negligible. Then the limit load multiplier (m_α^T) is evaluated by using Eq. (6.6). The maximum stress in the component is $\sigma_{\max} = \sigma_y / m_L$. For mechanical load, the stresses are categorized as follows:

$$\left.\begin{array}{l} \text{Primary stress: } P = \sigma_y / m_\alpha^T \\ \text{Primary-plus-secondary stress: } P+Q = \sigma_{\max} \end{array}\right\} \qquad (6.8)$$

For combined mechanical and thermal loading, the stresses are categorized as follows:

$$\text{Primary-plus-secondary stress: } P+Q = \sigma_y / m_L \qquad (6.9)$$

Note that these stresses are within the m_α triangle. Therefore, peak stresses are either zero or negligible.

(2) If m^0/m_L is greater than $1+\sqrt{2}$ then all three categories of stresses are expected to be present in the component. Now ζ_f is obtained from Eq. (4.12). The value of $m_{L,f}$ corresponding to ζ_f can be evaluated as $m_{L,f} = m_i^0 / \zeta_f$. The limit load multiplier

(m_α^T), based on ζ_f, is evaluated by using Eq. (4.13). Then for mechanical loading, the stresses are categorized as follows:

$$\left.\begin{aligned} &\text{Primary stress: } P = \sigma_y / m_\alpha^T, \\ &\text{Primary-plus-secondary stress: } P + Q = \sigma_y / m_{L,f} \\ &\text{Peak stress: } F = \sigma_{\max} - \sigma'_{\max}, \text{ where } \sigma_{\max} = \sigma_y / m_{L,i} \text{ and } \sigma'_{\max} = \sigma_y / m_{L,f} \end{aligned}\right\} \quad (6.10)$$

For combined mechanical and thermal loading, the stresses are categorized as follows:

$$\left.\begin{aligned} &\text{Primary-plus-secondary stress: } P + Q = \sigma_y / m_{L,f} \\ &\text{Peak stress: } F = \sigma_{\max} - \sigma'_{\max}, \text{ where } \sigma_{\max} = \sigma_y / m_{L,i} \text{ and } \sigma'_{\max} = \sigma_y / m_{L,f} \end{aligned}\right\} \quad (6.11)$$

6.6.2 Finite Element Stress Linearization

The procedure for stress linearization using the post processor of finite element software (ANSYS) is as follows:

(1) An initial linear elastic FEA is performed.

(2) The results of the initial FEA are used in conjunction with the post processor of a finite element software to evaluate membrane (σ_m), membrane plus bending ($\sigma_m+\sigma_b$) and maximum (σ_{max}) stress.

(3) Then the maximum of (σ_m) and ($\sigma_m+ \sigma_b$)/1.5 is identified and considered to be the "equivalent stress" (S_{eq}) and the difference between the (σ_{max}) and ($\sigma_m+ \sigma_b$) is the peak stress (F) in the component.

It should be noted that stress linearization using ANSYS post processor, which gives membrane (σ_m), bending (σ_b) and peak (F) stress, is leaving it to the analyst and the rules provided in the Code (ASME B&PV Code, 2007) to decide about the primary and secondary component of stresses.

6.6.3 Nonlinear Finite Element Method (NFEM)

Limit analysis implicitly classifies the primary stresses in a component. In the present work, a complete elastic-plastic FEA is performed to compare the primary stress (P) obtained by the aforementioned methods.

6.7 Illustrative Example – Torispherical Head

The systematic procedure for the categorization of linear elastic stresses induced in pressure vessel components and structures is demonstrated in this section through an example. A typical pressure vessel component configuration, a torispherical head on a cylindrical vessel, is considered herein for the demonstration purpose. The geometry of the component is shown in Figure 6.5(a).

The torispherical head has the following dimensions: the ratio of the thickness to vessel diameter $t/D_s = 1/40$, toroidal radius to shell diameter $r/D_s = 0.12$, and head radius to shell diameter is $R_h/D_s = 0.8$. The modulus of elasticity of the material is 262 GPa (38×10^6 psi) and yield strength is 262 MPa (38×10^3 psi). The structure is subjected to an internal pressure of 5 MPa (725 psi).

In order to analyze the structure for combined (mechanical and thermal) loading, temperature gradient is applied through thickness of the structure, in addition to pressure loading. The thermal load that is applied to the structure is as follows: inside temperature of the head is $200^0 C$, outside temperature is $25^0 C$, and ambient temperature is $20^0 C$. Coefficient of thermal expansion of the material is considered to be 9.5×10^{-6} m/m.K. The finite element model of the structure is developed by taking advantage of symmetry.

(a) Load Case-I: Mechanical Loading (Internal Pressure)

The structure is first analyzed for mechanical loading (internal pressure). Then the proposed m_α-tangent method is applied to categorize the stresses. The detail procedure is as follows:

An initial linear elastic FEA is performed which gives a statically admissible stress distribution. From the results of the initial linear elastic FEA, m^0=3.0497; m_L=1.4047 is evaluated using Eq. (3.5) and Eq. (3.1), respectively. Then the corresponding ζ=2.171 is evaluated using Eq. (6.10). Since ζ is less then $1+\sqrt{2}$, the component has negligible amount of peak stress. The limit load multiplier based on the m_α-tangent method is estimated as m_α^T=2.271. The maximum stress in the component is $\sigma_{\max}$=186.52 MPa. From the results of the foregoing calculations, the stresses are categorized as follows:

Primary stress: P = 115.38 MPa

Primary-plus-secondary stress: $(P+Q)$ = 186.52 MPa

Peak stress: F = 0.

Note that peak stress $F = 0$ as ζ, corresponding to the initial linear elastic analysis, is within the m_α - triangle.

The structure is then analyzed for stress linearization using ANSYS Post Processor. The selection of appropriate location and orientation of the stress classification lines (SCL) is an important part in stress linearization process. In order to place the stress classification lines in appropriate locations, the collapse mechanism of the structure is studied from the available literature.

Seshadri and Fernando (1992) have discussed the collapse mechanism of the torispherical head on a cylindrical vessel. They have shown that the structure is expected to collapse after formation of three plastic hinges near the shell-head junction. Considering the shell-head junction as the most critical section of the component from design standpoint, stress classification lines (SCL) are placed arbitrarily at five different locations as shown in Figure 6.5(a).

On the basis of the initial linear elastic analysis for mechanical loading (internal pressure), the linearized stresses, i.e., membrane, membrane-plus-bending and peak stresses are evaluated through thickness of the shell at five different SCL locations. Note that the peak stress is simply the difference between the maximum stress and the membrane plus bending stress in the component for a given location. The maximum of (σ_m) and ($\sigma_m + \sigma_b$)/1.5 is identified and considered to be the "equivalent stress" (S_{eq}). The analysis results are shown in Table 6.1.

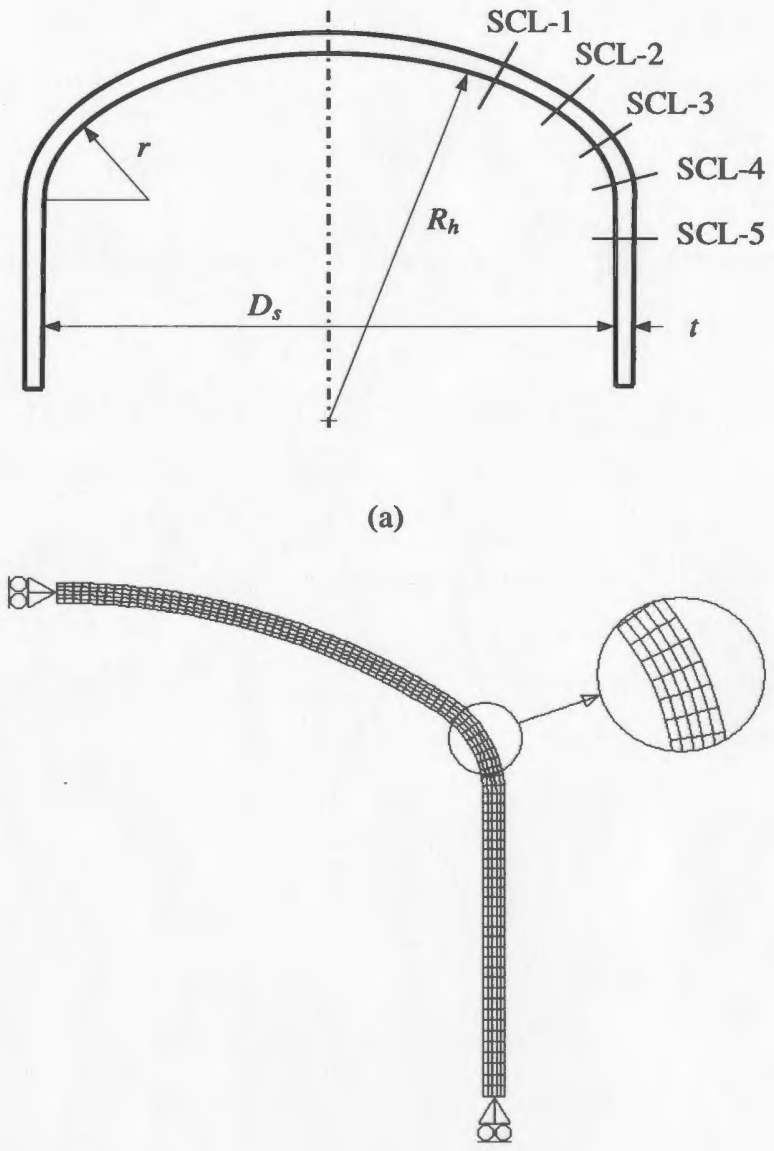

Figure 6.5 Torispherical head (a) Geometry, (b) Finite element model (axisymmetric)

It can be observed from the stress linearization results shown in Table 6.1 that SCL-3 is the maximum stress location and hence is considered to be the critical section to form the first "plastic hinge". The results also shows that the stress intensity gradually decreases in

either direction when we proceed from the first plastic hinge location (SCL-3). In order to complete the "collapse mechanism", the possible locations of other two plastic hinges are considered to be SCL-2 and SCL-4.

Therefore, from the above discussion it can be concluded that for mechanical loading (internal pressure), SCL-3 represents the most critical section of the component from design standpoint and hence the corresponding linearized stresses are compared with the results obtained from the m_α-tangent method.

Then a complete elastic-plastic FEA is performed which gives the primary stress P_{NFEM} = 93.90 MPa. The above mentioned results are compared in Table 6.2.

Table 6.1 ANSYS stress linearization for torispherical head under internal pressure

SCL Location	σ_m	$\sigma_m+\sigma_b$	σ_{peak}	S_{eq} *
SCL – 1	70.69	83.66	0	70.69
SCL – 2	85.58	156.34	2.44	104.23
SCL – 3	92.14	205.29	12.86	136.86
SCL – 4	82.44	178.49	11.26	118.99
SCL – 5	77.97	100.36	2.67	77.97

* S_{eq}= *Max.* (σ_m , ($\sigma_m+\sigma_b$) / 1.5); Note: All stresses are in MPa.

(b) Load Case-II: Combined Mechanical and Thermal Loading (Internal Pressure and Temperature Gradient)

The structure is then analyzed for combined mechanical (internal pressure) and thermal (temperature gradient) loading. Note that the thermal load will not contribute to the primary stress in the component and hence only primary plus secondary (P+Q) and peak

(F) stresses are evaluated in this case. The structure first analyzed by using the m_α-tangent method to extract the above mentioned categories of stresses. An initial linear elastic FEA is performed on the basis of which primary-plus-secondary stress $(P+Q)$ is evaluated using Eq. (6.9) as 353.77 MPa and peak stress, $F=0$. Note that these stresses are pseudo-elastic stresses.

Then linearization is performed for combined loading using the ANSYS post processor. The linearized membrane-plus-bending stress is evaluated at SCL-1 as $(\sigma_m+\sigma_b)$ = 371.53 MPa and peak stress as σ_{peak} = 7.96 MPa. The analyses results are compared in Table 6.2.

An important point should be noted here that for only mechanical loading (internal pressure), SCL-3 represents the most critical section (highest peak stress location) of the component as shown in Table 6.1. But the analysis shows that for combined mechanical (internal pressure) and thermal (temperature gradient) loading, the highest peak stress location shifts toward SCL-1 (Figure 6.5(a)), due to a non-uniform stress distribution in the component. Therefore, the linearized stresses are evaluated at SCL-1 in this case in order to compare with the results obtained from that of the m_α-tangent method.

Table 6.2 Stress categorization for torispherical head

Load Case	m_α-Tangent Method			ANSYS Stress Linearization*			NFEM
	P (MPa)	$P+Q$ (MPa)	F (MPa)	S_{eq} (MPa)	$\sigma_m+\sigma_b$ (MPa)	σ_{peak} (MPa)	P_{NFEM} (MPa)
Int. Pressure	115.38	186.52	0	136.86	205.29	12.86	93.90
Pr. + Thermal	-	353.77	0	-	371.53	7.96	

* These quantities are simply membrane, bending, or peak. The analyst using the rules provided in the Code (ASME B&PV, 2007) has to decide if these stresses are primary or secondary.

From the above discussion, it can be concluded that when loading condition changes, the maximum stress location might shift from its previous location. Therefore, for components having non-uniform stress distribution for combined loading might lead to an improper selection of class lines during the stress linearization process. Whereas the proposed m_α-tangent method gives only one value of the stress category irrespective of the loading condition. This is a very important advantage of using the m_α-tangent method for combined loading cases.

6.8 Applications

6.8.1 Thick Walled Cylinder

A thick-walled cylinder (Figure 6.6) with inner radius R=65 mm (2.56 in.) and wall thickness t=25 mm (0.984 in.) is modeled in plane-strain condition. The modulus of elasticity of the material is 200 GPa (29×10^6 psi) and yield strength is 300 MPa (43.51×10^3 psi). The cylinder is subjected to internal pressure of 50 MPa (7.252×10^3 psi). In addition to pressure loading, thermal load is applied to the structure as follows: inside temperature of the cylinder is 200^0C, outside temperature is 25^0C, and ambient temperature is 20^0C. Coefficient of thermal expansion of the material is considered to be 9.5×10^{-6} m/m.K.

The structure is first analyzed using the m_α-tangent method for mechanical (internal pressure) loading only. The initial linear elastic FEA leads to a statically admissible stress distribution, on the basis of which m_L=1.702; m^0=2.264 and corresponding ζ=1.33 is

evaluated using Eq. (3.5), Eq. (3.1) and Eq. (6.10), respectively. Since ζ is less than $1+\sqrt{2}$, there is negligible peak stress in the component and only primary and secondary stresses are expected to be present. Using Eq. (6.9), the corresponding limit load multiplier m_a^T =2.064 is evaluated. The maximum stress in the component is σ_{max}=176.26 MPa.

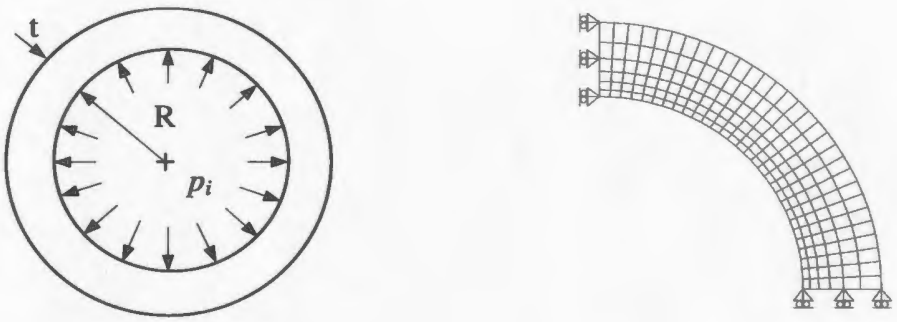

(a) (b)

Figure 6.6 Thick walled cylinder (a) Geometry, (b) Finite element model

From the results of the foregoing calculations, the stresses are categorized as follows:

Primary stress: P = 145.32 MPa

Primary-plus-secondary stress: $P+Q$ = 176.26 MPa

Note that peak stress $F=0$ as ζ, corresponding to the initial linear elastic analysis, is within the m_a - triangle.

The initial linear elastic FEA results are then used in conjunction with ANSYS post processor to obtain the linearized stresses which gives membrane stress σ_m = 130.98 MPa, membrane-plus-bending stress (σ_m+σ_b) = 155.62 MPa, and maximum stress σ_{max} = 182.39

MPa. The equivalent stress is evaluated as S_{eq} = 130.98 MPa. The peak stress is evaluated as 26.77 MPa.

It should be noted that the value of maximum stress obtained from the m_α-tangent method and the stress linearization method is slightly different. This is due to the fact that the m_α-tangent method makes use of the elemental values whereas the stress linearization method makes use of the nodal values provided by ANSYS. As the mesh size becomes smaller the difference is become negligible. Then a complete elastic-plastic FEA is performed which gives the primary stress P_{NFEM} = 133.04 MPa.

The structure is then analyzed for combined mechanical (internal pressure) and thermal (temperature gradient) loading. As thermal load will not contribute to the primary stress, primary-plus-secondary stress $(P+Q)$ is evaluated using Eq. (6.17) as 299.71 MPa and peak stress, $F=0$.

Then linearization is performed for combined loading using the ANSYS post processor. The linearized membrane-plus-bending stress is evaluated as $(\sigma_m+\sigma_b)$ = 327.16 MPa and peak stress as σ_{peak} = 37.26 MPa. Table 6.3 shows the comparison of the analysis results.

Table 6.3 Stress categorization for thick walled cylinder

Load Case	m_α-Tangent Method			ANSYS Stress Linearization*			NFEM
	P (MPa)	$P+Q$ (MPa)	F (MPa)	S_{eq} (MPa)	$\sigma_m+\sigma_b$ (MPa)	σ_{peak} (MPa)	P_{NFEM} (MPa)
Int. Pressure	145.32	176.26	0	130.98	155.62	26.77	133.04
Pr. + Thermal	-	299.71	0	-	327.16	37.26	

* These quantities are simply membrane, bending, or peak. The analyst using the rules provided in the Code (ASME B&PV, 2007) has to decide if these stresses are primary or secondary.

6.8.2 Reinforced Axisymmetric Nozzle

In this example, an axisymmetric cylindrical nozzle on a hemispherical head (Figure 6.8) is modeled. Inside radius of the head is R=914.4 mm (36 in.), and the nominal wall thickness is t=82.55 mm (3.25 in.). Inside radius of the nozzle is r=136.525 mm (5.375 in.) and nominal wall thickness is t_n=25.4 mm (1 in.). The required minimum wall thickness of the head and the nozzle are t_r=76.835 mm (3.025 in.) and t_{rn}=24.308 mm (0.957 in.), respectively.

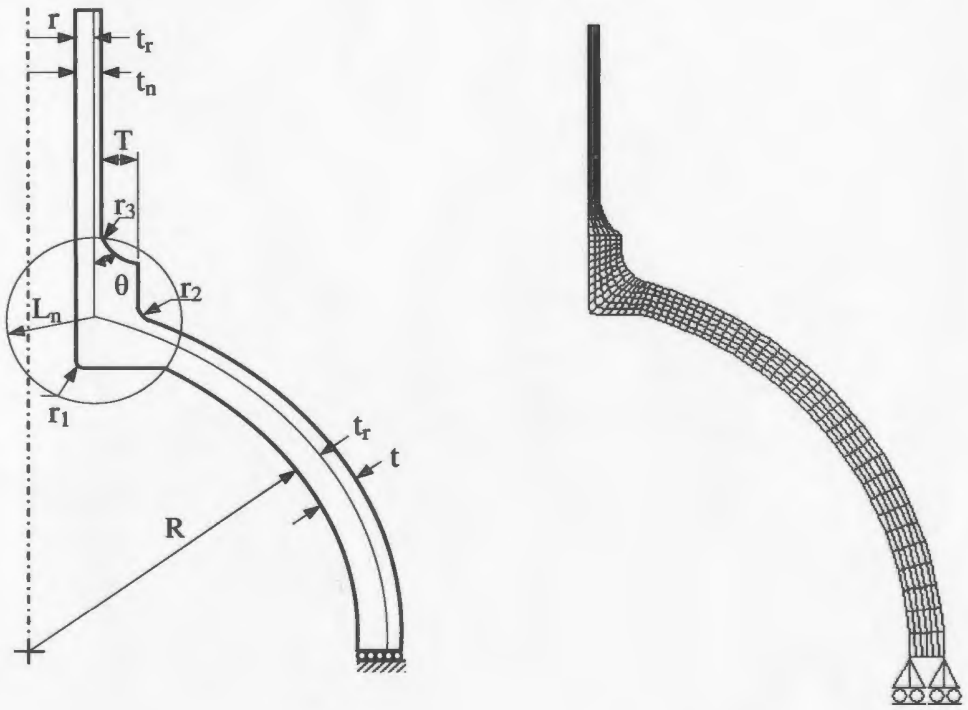

Figure 6.7 Reinforced nozzle on a hemispherical head (a) Geometry, (b) Finite element model

Table 6.4 Stress categorization for reinforced axisymmetric nozzle

m_α-Tangent Method			NFEM
P (MPa)	$P+Q$ (MPa)	F (MPa)	P_{NFEM} (MPa)
163.22	222.79	0	139.81

The nozzle is reinforced with an appropriate reinforcement scheme. The geometric transitions of the reinforcement are modeled with fillet radius, r_1=10.312 mm (0.406 in.), r_2= 83.312 mm, and r_3= 115.214 mm (4.536 in.). The other dimensions include, T_2=54.61 mm (2.15 in.) and θ=45°. The distribution of reinforcement is bounded by the reinforcement zone boundary specified by the circle of radius, L_n=143.51 mm (5.65 in.).

The modulus of elasticity of the material is 262 GPa (38×10^6 psi) and yield strength is 262 MPa (38×10^3 psi). The hemispherical head is restrained at the vessel end, away from the nozzle, in the meridional direction but allowed to move in the radial direction. The structure is subjected to an internal pressure of 24.132 MPa (3500 psi).

From the results of the initial linear elastic FEA, m^0=1.891 and m_L=1.176 is obtained. Since the value of ζ=1.608 is less than $1+\sqrt{2}$, the magnitude of peak stress is negligible. Now, the limit load multiplier m_α^T=1.605 is obtained. From the results of the foregoing calculations, the stresses are categorized as follows:

Primary stress: $P = 163.22$ MPa

Primary-plus-secondary stress: $P + Q = 222.79$ MPa

Peak stress: $F = 0$

Then a complete elastic-plastic finite element analysis is performed which gives primary stress P_{NFEM} = 139.81 MPa. The results are show in Table 6.4.

6.8.3 Oblique Nozzle

Limit load analysis of a vessel with oblique nozzle has been studied both experimentally and numerically by Sang. et al. (2005) to find the limit pressure. The geometry consists of a cylindrical vessel with a closed nozzle connected with an angle of 30 deg. The schematic diagram of the model and the finite element mesh is shown in Figure 6.9. The inside diameter of the vessel D_i=600 mm (23.622 in.) and outside diameter of the nozzle d_o=325 mm (12.795 in.). The wall thickness of both vessel and nozzle t=6 mm (0.236 in.). The length of the vessel L=2400 mm (94.488 in.) and the length of the nozzle along the centerline l=600 mm (23.622 in.). The dimensions of the heads of the vessel and the nozzle are H_i=175 mm (6.890 in.) and h_i=106 mm (4.173 in.), respectively. The saddles are located at a distance A=400 mm (15.748 in.).

Modulus of elasticity and yield strength of the material is 400 GPa (58.015×10^6 psi) and 339.4 MPa (49.226×10^3 psi), respectively. The structure is subjected to an internal pressure of 1.0 MPa (145 psi). The finite element model of the structure is developed by using three dimensional isoparametric solid elements. Due to the symmetry about the longitudinal plane, one-half of the vessel was modeled.

An initial linear elastic finite element analysis is performed. From the results of the initial elastic FEA, m^0=4.804; m_L=0.411 and σ_{max}=826.78 MPa is evaluated. Since ζ_i=11.688 is greater than $1+\sqrt{2}$, significant amounts of peak stresses are present in the structure.

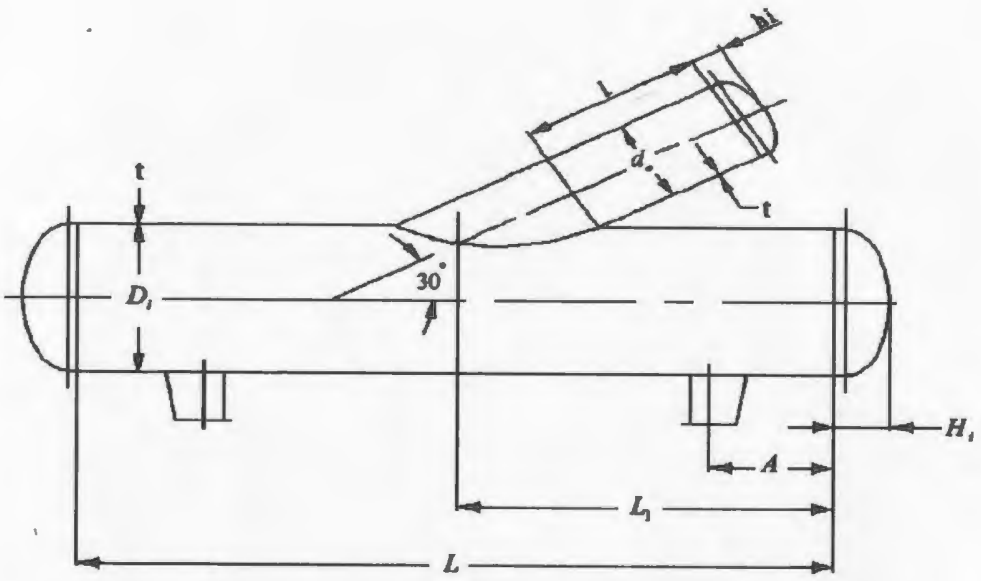

(a)

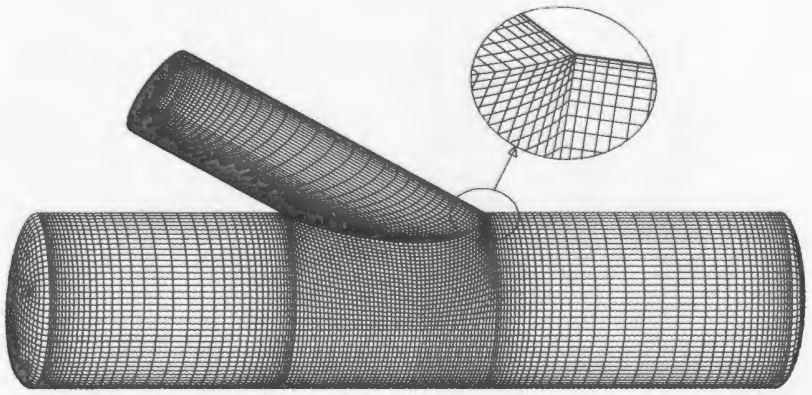

(b)

Figure 6.8 Oblique nozzle on a cylindrical vessel from Sang. et al. (2005) (a) Geometry, (b) Finite element model

Table 6.5 Stress categorization for oblique nozzle

m_α-Tangent Method			NFEM
P (MPa)	$P+Q$ (MPa)	F (MPa)	P_{NFEM} (MPa)
218.37	574.98	251.80	188.03

Now, ζ_f is evaluated so that m^0 at B and B^* are equal (Eq. (6.11)). The value of ζ_f = 8.1385 and the m_α^T based on ζ_f, as obtained from Eq. (6.13), is 1.5543. From the results of the foregoing calculations, the stresses are categorized as follows:

Primary stress: $P = 218.37$ MPa

Primary-plus-secondary stress: $P + Q = 574.98$ MPa

Peak stress: $F = 251.80$ MPa

Then a complete elastic-plastic finite element analysis is performed which gives primary stress $P_{NFEM} = 188.03$ MPa. It can be seen that the primary stress obtained from the proposed method is slightly conservative compared to the inelastic FEA. The peak stress is considerably high due to the sharp edges at the vessel-nozzle junction, which has not been rounded. Note that the stresses calculated above are pseudo-elastic stresses. The results are summarized in Table 6.5.

6.9 Discussion

The categorization of stresses by elastic FEA is a challenging task even with the finest computing facilities and advanced numerical techniques. The categorization of elastic

stresses in complex pressure vessels is involved and demands substantial skill. The purpose of the present work is to introduce a new stress categorization method based only on linear elastic FEA and demonstrate its application. The proposed method uses limit load multiplier estimates to decompose the elastic stresses into appropriate categories, using a single linear elastic FEA. The proposed method is able to identify the primary (P), primary plus secondary (P+Q) and peak (F) stress components for mechanical and thermal loads within reasonable accuracy. The results are directly comparable with the ASME B&PV Code (2007) limits. Notably, there is only a single primary stress to be evaluated against S_m, as opposed to separate limits for membrane and bending stress. Since the method delivers directly only a single bounding value for each stress category, its application is very convenient and straightforward.

Several example problems are worked out to demonstrate the method, including typical two and three dimensional pressure vessel components. The primary stresses obtained from the proposed method are in reasonably good agreement with the elastic-plastic FEA results. For simple axisymmetric pressure vessel (cylindrical vessel and torispherical head), the primary plus secondary stresses obtained from the proposed method are compared with those obtained from stress linearization method. The results are again in reasonably good agreement. The same approach is expected to work well for more complicated structures e.g., oblique nozzle on a cylindrical vessel.

The proposed method has several potential benefits over conventional stress categorization approaches. This method makes use of available FEA codes and currently requires a moderate amount of post-processing by the user, which could be automated. As a result, the method gives three numbers, namely the primary stress, primary plus

secondary stress, and peak stress. The method directly delivers the bounding values for the analyzed component. This sidesteps the potential difficulties encountered in justifying the appropriate location and orientation of the SCLs. The method is applicable to a wide range of pressure vessels including three dimensional vessel with complex geometry as shown in Example 7.4 in this paper. The proposed method is able to categorize the stresses for combined loading (pressure and thermal) without requiring two separate analyses. Therefore, the proposed method could be used as a tool for simplified stress categorization of pressure vessels with minimum computational effort.

6.10 Closure

A simplified method is proposed in this chapter to categorize the linear elastic stresses in pressure vessel components and structures. The method makes use of a single linear elastic finite element analysis to categorize the stresses. The proposed method is applicable to mechanical as well as thermal loading cases. The method is applied to a number of practical pressure vessel components and structures and the results are found to be in good agreement with those obtained from the conventional techniques. The next chapter discusses about the fitness-for-service assessment (FFS) of pressure vessels and piping systems. A simplified method is proposed for Level 2 FFS assessment of pressure vessels and piping systems containing thermal hot spot and corrosion damage.

CHAPTER 7

FITNESS-FOR-SERVICE (FFS) ASSESSMENT

7.1 Introduction

Integrity assessment of mechanical components and structures is a multidisciplinary effort. Structural integrity assessment is of considerable importance in many industrial sectors e.g., oil and gas, nuclear, and petrochemical industries. It is considered to be an essential tool for ensuring the safety and economy of an operating plant. It also aids in optimal maintenance and operation of the plants. Fitness-for-service (FFS) assessments are performed in order to demonstrate the structural integrity of aging components and structures containing defect. The common categories of defects in pressure vessel components and structures are blunt flaws, crack-like flaws, and mechanical or material

damage. In order to ensure the operational safety and structural integrity, all of these defects need to be identified and assessed properly.

In practice, FFS assessments are conducted periodically in order to determine the acceptability of in-service components and structures for continued service. Extended evaluations are often carried out as an effort to schedule routine inspection and estimate the remaining life of the component. A number of FFS assessment procedures are available in practice e.g., API 579 (2000), R5 and R6 procedure (2004), SINTAP (1999) etc. API 579 procedure is proposed by American Petroleum Institute and is widely used in North America, while R5 and R6 procedures are proposed by British Energy. SINTAP procedures are developed especially for European industry. These procedures are mostly semi-empirical and are based on extensive experimental data. In order to perform more precise assessment, advanced numerical simulation and analysis technique need to be incorporated, which will facilitate more accurate modeling and analysis of the real-life scenario. The above mentioned practices and procedures mostly address the fracture and plastic collapse type failure modes of in-service components and structures containing defect.

Thermal hot spot and corrosion are the typical of damages occurring in in-service pressure vessels and piping systems. FFS assessments of these components and structures need to be performed periodically in order to determine the suitability of the component for the prevailing operating conditions and for the assessment of remaining life. The so-called "remaining strength factor (RSF)" is generally used as a quantitative measure of the remaining strength of damaged components or structures. The RSF concept is very useful especially in case of thermal hot spot and corrosion damage. Significant effort has

been directed over the last two decades to study the structural integrity of aging pressure vessels and piping systems containing defect.

Sims et al. (1992) have studied the effect of thinned areas in pressure vessels and storage tanks as an effort to assess the remaining strength of the damaged structure. They have developed an empirical equation by curve fitting the inelastic finite element analysis (FEA) results. They have compared the results with ASME B31G (1984) criteria, which is commonly used for determining the remaining strength of corroded pipelines. They have shown that the results are in reasonably good agreement with ASME B31G (1984) especially for shells having relatively smaller diameter-to-thickness ratio.

Seshadri (2005) has studied the evaluation of thermal hot spot in cylindrical pressure vessels using variational principles in plasticity. A simplified formula for RSF is proposed to quantify the remaining strength of the vessel. Shell decay lengths are used in order to identify the "reference volume", which essentially represents the kinematically active portion of the component or structure that takes part in plastic action. Indermohan and Seshadri (2005) have extended the application of the concept to corrosion damage in cylindrical pressure vessels. A number of example problems are worked out to demonstrate the method.

Ramkumar and Seshadri (2005) have studied the internal and external corrosion in cylindrical pressure vessels using the concept of reference volume along with the m_α-multiplier. The results are compared with ASME B31G (1984) procedure and have shown that the proposed method gives improved estimate of the remaining strength of the structure. Tantichattanont et al. (2007) have studied the thermal hot spot and corrosion

damage in spherical pressure vessels. They have derived the expressions for decay lengths in spherical pressure vessels. RSF based on the m_α-multiplier has been proposed for FFS evaluation. The results are compared with the inelastic finite element analysis results.

In this thesis, a simplified method is developed for Level 2 FFS assessment (as described in API 579) of pressure vessels and piping systems containing thermal hot spot and corrosion damage. The method is based upon variational principles in plasticity, the m_α-tangent method (presented in Chapter 4 of this thesis), the concept of decay length and reference volume. The use of the m_α-tangent method extends the range of applicability of the proposed method to components and structures experiencing significant stress gradient in and around the damaged spot. The method is shown to provide a reasonably accurate estimate of the remaining strength of ageing pressure vessel components and structures. The method is demonstrated through an example and the results are compared with Level 3 inelastic finite element analyses.

7.2 Fitness-for-Service Assessment Procedure

Fitness-for-service assessments are performed in oil and gas, nuclear and petrochemical industries in order to demonstrate the integrity of in-service components and structures containing flaw or damage. For pressurized equipments in operating plants, API 579 has provided three levels of assessment for a given damage or flaw. Each of these assessment levels is based on the degree of conservatism, amount of inspection data required and

complexity of the analysis being performed. A brief overview of the three levels of assessment procedures is given below.

(a) Level 1 assessment procedure is primarily intended to provide conservative screening criteria that can be determined with a minimum quantity of inspection data or component information. This level of assessment is fairly easy and provides a relatively conservative estimate. Level 1 assessment is generally performed by the plant inspection or engineering personnel.

(b) Level 2 assessment procedure provides a more precise and detailed evaluation of the flawed component compared to that of Level 1 assessment procedure. In a Level 2 assessment, the amount of inspection and component data needed are similar to Level 1 assessment; however, more detailed evaluations are performed in this case. Level 2 assessment reduces the degree of conservatism found in a Level 1 assessment. Level 2 assessment is intended to perform by facilities or plant engineers, although some owner-operated organizations consider it more suitable for a central engineering evaluation.

(c) Level 3 assessment procedure is intended to provide the most precise and detailed assessment of the flawed components with a minimum degree of conservatism, compared to the other assessment procedures. Level 3 assessment procedures require the most detailed inspection and component information and advanced computational techniques such as finite element method. Level 3 assessments are intended to perform by experts of the relevant area.

The limitations that have been imposed on the Level 1 and Level 2 assessments are that the component is designed and constructed in accordance with a recognized Code or Standard and the metal loss area has a relatively smooth contour without any notch or crack. On the other hand, Level 3 assessment method facilitates the detailed evaluation through more accurate modeling of the contour of the damage spot. Level 3 assessment is proposed to be performed by using advanced computational techniques e.g., finite element and finite difference method. The evaluation may be based on a linear elastic stress analysis followed by stress categorization, or a nonlinear stress analysis determining plastic collapse load.

7.2.1 Flaw Acceptance Criterion

In API 579, the concept of remaining strength factor (RSF) is used to determine the acceptability of an in-service component for continued service. The assessment is based on limit or plastic collapse load of the structure. The remaining strength factor was originally proposed by Sims et al. (1992) to assess the locally thinned areas (LTA). The RSF is defined as the ratio of the plastic collapse load (pressure) of the damaged component (component with flaw or damage) to that of the undamaged component.

If the calculated RSF is greater than or equal to the allowable RSF, the component is considered to be suitable at current operating condition for continued service. If the calculated RSF is less than the allowable RSF, the component needs to be either rerated through standard procedures or needed to be repaired or replaced. Note that the

component is to be originally designed and constructed in accordance with a recognized design Code or Standard.

7.3 Corrosion Damage in Pressure Vessels and Piping

The metal loss in pressure vessels and piping systems due to corrosion can be divided into two main categories i.e., general metal loss and local metal loss. The detail definition of these flaws is spelled out in API 579 (2000) and different assessment methods are proposed for each of these categories. In order to distinguish between general metal loss and local metal loss, characteristics of the metal loss profile should be known in detail. The main difference between the assessment approaches of these two types of metal losses is that the amount and type of data that is required for the assessment. API 579 uses the thickness averaging approach to evaluate the general metal loss in the pressurized component. The present thesis focuses on the evaluation of local metal loss, which is generally termed as "locally thinned area" (LTA). Note that most of the criteria are developed to address the LTA's in piping and cylindrical pressure vessels.

7.3.1 Locally Thinned Area (LTA)

The local metal loss due to corrosion or erosion in pressure vessels and piping systems is generally termed as "local thin area" (LTA). A region of metal loss is classified as LTA when it satisfies the following criteria

$$\min(s, c) \geq 6\,(t_{rm} - t_{\min}) \tag{7.1}$$

where min (s, c) defines the minimum of the axial (s) and circumferential (c) extent of the LTA, and t_{rm} is the required minimum thickness of the component and t_{min} is the measured minimum thickness of the flaw as shown in Figure 7.1. This localized defected area, due to thickness reduction, is more susceptible to failure than the rest of the structure. The parameters that influence the behavior of LTA are applied loadings, component geometry, flaw geometry and material characteristics. In real-life, LTA occurs in an irregular shape and is generally represented by an equivalent standard area.

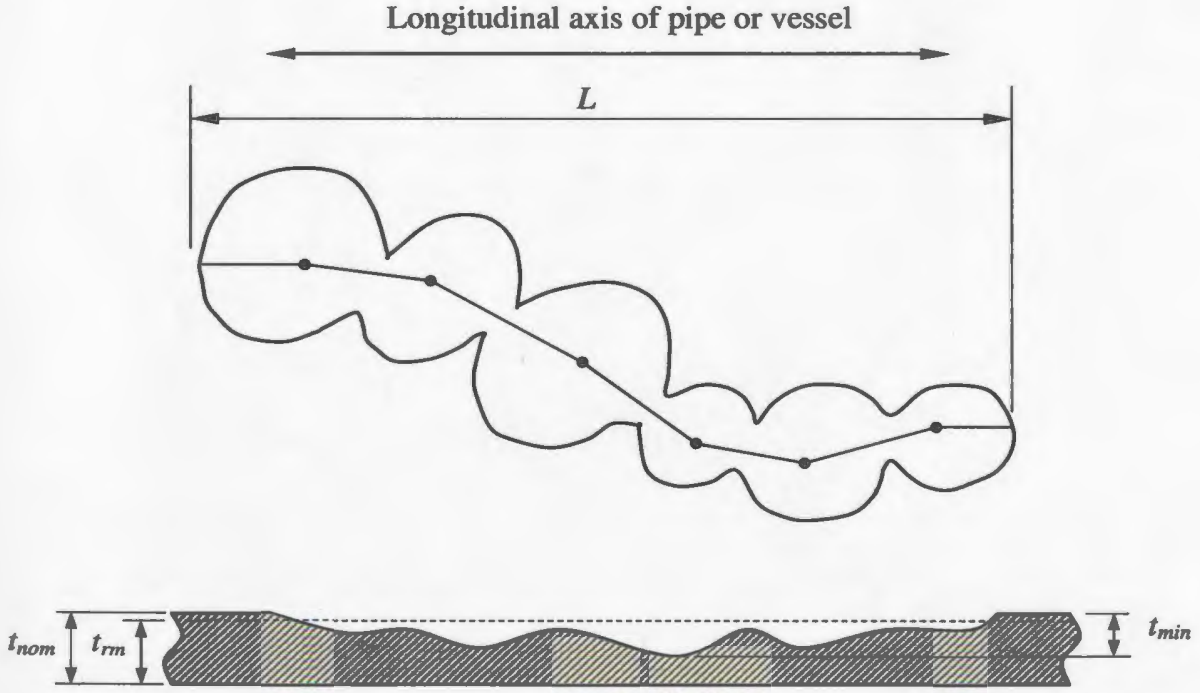

Figure 7.1 Schematic representation of metal loss in a pipe or in a cylindrical pressure vessel.

In case of cylindrical shells the damage profile is represented by an equivalent rectangular area. The irregular thickness profile is also represented by a standard profile following some standard procedures (API 579, 2000). The conservative one is to consider the maximum thickness loss as the effective thickness for the LTA. Due to thickness reduction by local metal loss, stiffness of the LTA will reduce. The reduction of stiffness depends on the remaining wall thickness, size of the LTA, material properties and the loading condition. The effective area method was developed based on the assumption that the strength loss due to corrosion is proportional to the amount of metal loss measured axially along the pipe (Figure 7.1).

Thinned areas due to metal loss generally act as stress raisers, thus leading to cracking, tensile instability, or bucking instability under compressive stresses. While tensile instability is the root-cause of failure, the LTA undergoes higher deformation than the surrounding undamaged region. This differential deformation of the structure is generally termed as "bulging". Excessive bulging in a pressurized component is undesirable and is a considerable threat to the structural integrity. In practice, Folias factor is used to quantify the bulging effect of an LTA in shell structures. The phenomenon exists in case of internal pressure and is more pronounced in shells with smaller diameter e.g., piping.

Due to the difference in thickness in the LTA and the surrounding shell, the LTA region bulges outward when the structure is subjected to internal pressure. In the LTA, stresses are considered to be purely primary and no redistribution occurs upon yield. Secondary bending stresses are induced at the edges of the LTA due to thickness misalignment near the edges of the LTA with the surrounding shell. However, the membrane stress is almost constant throughout the LTA.

The magnitude and significance of the bending stresses depends on the size and relative thickness of the LTA compared to the surrounding wall thickness. If the thickness of the LTA is very less compared to the surrounding wall thickness, then the effect of the edge bending moment becomes significant. The proximity of the LTA to major structural discontinuity is important. In this thesis, it is assumed that the LTA is not affected by the structural discontinuity. In a component or structure containing LTA, local failure occurs due to net section collapse and it is controlled by imposing maximum section strain or maximum point strain on the thin area of the defect.

7.3.2 Factors Influencing the Behaviour of LTA

Locally thinned areas (LTA) are local structural defects caused by corrosion or erosion. The parameters that contribute to the failure of LTA are the applied loadings, pipe or vessel geometry, flaw geometry and material characteristics. The interaction of these parameters is schematically shown in Figure 7.2.

The shell geometry, material characteristics and flaw geometry directly influence the stress and strain field in and around the LTA. The left side of the equation (Figure 7.2) represents the driving forces that contribute to the failure of the flaw or damage and the right side represents the material resistance to failure. The failure occurs when the stresses and strains, induced by the driving forces, exceeds the material resistance.

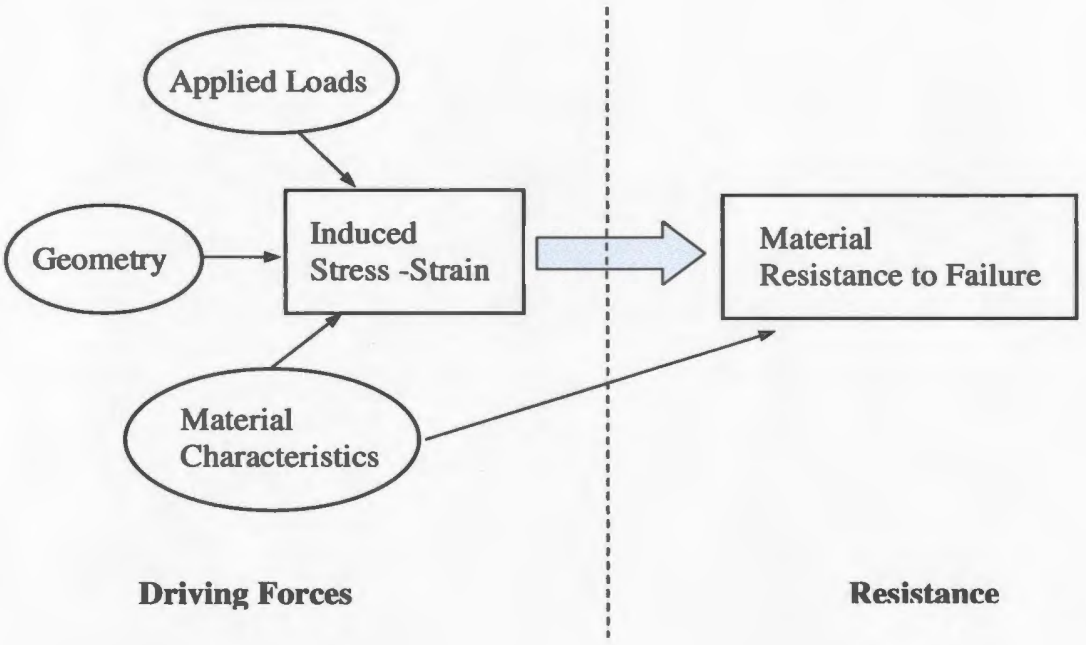

Figure 7.2 Schematic diagram of the primary factors controlling the behaviour of LTA's (Osage et al., 2001).

7.3.3 Evaluation of LTA

The evaluation of volumetric type flaw e.g., local thinning due to corrosion are performed on the basis of amount and distribution of metal loss and strength of the material. In addition, thermal and environmental effects on the material properties need to be taken into account. The evaluation of LTA in pipelines, pressure vessels and storage tanks are slightly different. The factors influencing the evaluation are the internal pressure loading and the corresponding response of the structure, which includes gross sectional effect and the effect of localized bending. Generally, the internal pressure capacity is the main focus of the evaluation process. The need for a practical and technically sound FFS assessment procedure is paramount.

Assessment of LTA using inelastic FEA is very attractive as the user has an opportunity to reduce the degree of conservatism of the assessment by using the advanced modeling and computational techniques. The evaluation using inelastic FEA gives more accurate (less conservative) result compared to the semi-empirically based methods proposed in available practices and procedures e.g., API 579. But the inelastic FEA is expensive in terms of computational effort and time as it requires detail flaw and material data as well as advanced computational techniques.

An alternative option is proposed in the inspection Codes' to evaluate LTA by stress analysis using linear elastic FEA. The approach is based on categorization of linear elastic stresses as described in ASME B&PV Code, Section VIII, Division 2 (2007). The two step process includes stress linearization followed by stress categorization. This approach becomes difficult to apply in FFS assessment as categorization of stresses is a very challenging task for practical three dimensional components and structures.

In this thesis, an attempt has been made to develop a method for Level 2 FFS assessment of pressure vessel components and structures containing LTAs. A simplified method based strength parameter has been proposed. The method is shown to rapid and easy to implement by the plant engineers. The proposed method can be applied to the pressure vessel components and structures experiencing significant stress gradient in and around the damaged spot (LTA). The analysis results obtained from the proposed method are compared with Level 3 inelastic finite element analysis results. The details of the proposed method will be discussed later in this chapter.

7.4 Thermal Hot Spots in Pressure Vessels and Piping

Thermal hot spots in pressure vessels, piping systems or storage tanks are considered as "damage". Therefore, the mechanical integrity of the components and structures containing thermal hot spot is of considerable importance. Thermal hot spots are setup in pressure vessels and piping systems due to the loss of refractory lining inside the vessel wall. The additional causes include the effect of higher temperature on the outside wall of the vessel or pipe and also the mal-distribution of flow containing reactive or catalytic fluids.

Due to temperature differential in the hot spot region, the material get softer and more flexible compared to the surrounding cold region. At higher temperature, the material properties of the hot spot changes and hence the damaged spot becomes more susceptible to failure than the rest of the structure. As a result, the structure fails locally. The difference in deformation of the damaged and undamaged region of the vessel or pipe is observed due to the difference in material properties at different temperatures. The membrane (primary) stress is same throughout the damage region of the component. In this thesis, only primary membrane stresses are considered in the assessment of hot spot.

7.4.1 Evaluation of Hot Spots

Currently there is no standard procedure for FFS assessment of thermal hot spots. In this thesis, an attempt has been made to develop a method for Level 2 FFS assessment of pressurized components and structures of cylindrical shape subjected to internal pressure

and contain thermal hot spot. A simplified method based strength parameter has been proposed to perform the assessment. The method is shown to rapid and easy to implement by the plant engineers. The analysis results obtained from the proposed method are compared with Level 3 inelastic finite element analysis results. The details of the proposed method will be discussed later in this chapter.

7.5 The Concept of Decay Length and Reference Volume

The concepts of decay length and reference volume have been discussed by Seshadri (2005) in order to identify the kinematically active portion of the shell that takes part in plastic action. During local plastic collapse, in case of LTA and local hot spot, the plastic flow is assumed to occur in a localized region as shown in Figure 7.3. Therefore, these localized effects are accounted for by using the concept of reference volume. These concepts are used here to demonstrate the integrity of the structures containing thermal hot spot and corrosion damage.

7.5.1 Decay Length for Cylindrical Shell

The localized effect of discontinuities due to thermal hot spot and corrosion damage in pressurized components is represented by introducing the concept of decay length. The decay length is defined as the distance from the applied force or moment to the point where the effect of the force is almost completely dissipated or becomes negligible.

To deduce the expression for decay lengths in the axial direction, consider a cylindrical shell subjected to axisymmetric loading. Seshadri (2005) has discussed the concept of decay lengths for pressure vessels and piping. The decay length in axial direction for cylindrical shell is

$$x_l = 2.5\sqrt{Rh} \tag{7.2}$$

The decay length in circumferential direction for cylindrical shell is (Seshadri 2005)

$$x_c = 6.10(R^3 h)^{1/4} \tag{7.3}$$

Since the extent of decay length in shells is highly dependent on the shell curvature, the decay lengths in circumferential and axial directions are different.

7.5.2 Reference Volume for Cylindrical Shell

When damage occurs in a pressurized component, a part of the component adjacent to the damage participates in the failure mechanism. A reference volume is the sum of the volume of damaged portion of the vessel (LTA) and the adjacent volume affected by the damaged portion. The adjacent volume is the effective undamaged volume outside the damaged area that participates in plastic action and is part of the reference volume. The dimensions of the adjacent volume are calculated by using the decay lengths.

An equivalent rectangular shape is utilized to represent the irregular shape of a hot spot or corrosion damage in cylindrical shell. Although the thickness of the corrosion is irregular in practice, uniform depth is considered. Maximum corrosion depth is a

conservative assumption. For a damaged area of width $2a$ in circumferential direction and length $2b$ in longitudinal direction of a cylindrical shell (Figure 7.3), the volume of the damaged spot V_D can be calculated as,

$$V_D = 4abh_D \tag{7.4}$$

where h_D is the thickness of the damaged area. The adjacent volume is the strip around the damaged volume that participates in plastic action and is bounded by decay lengths of cylindrical shells. Therefore, the adjacent volume is given by,

$$V_U = 4h\,[(x_c + a)(x_l + b) - ab] \tag{7.5}$$

where x_l and x_c are decay lengths of cylindrical shells in axial and circumferential directions, respectively. The reference volume is therefore the sum of the above volumes

$$V_R = V_D + V_U \tag{7.6}$$

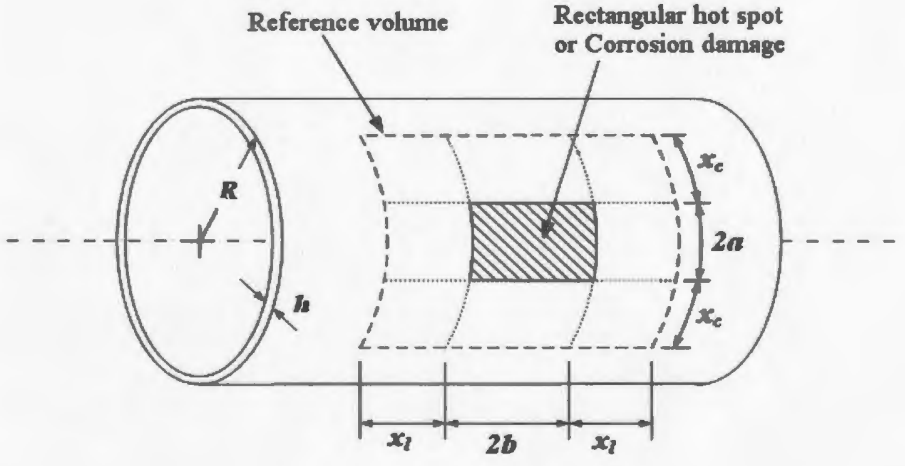

Figure 7.3 Decay length and reference volume dimensions for cylindrical shell

7.6 Structural Integrity Considerations

Structural integrity assessment essentially implies serviceability assessment as well as the remaining life assessment. In order to meet the minimum serviceability requirement, the theoretical limiting stress in the damaged spot should be the same as the limiting stress for the undamaged component. Seshadri (2005) introduced the variational concepts in plasticity in order to assess the integrity of pressure vessel components and structures. The integral mean of yield criterion is used to assess the damage.

The behavior of a structure under internal pressure due to thermal hot spot and corrosion damage is slightly different although both of these damages possess the similar type of failure mechanism. In both cases, the structure fails locally due to stiffness reduction in the damaged area. For corrosion damage, the stiffness of the LTA reduces due to the thickness reduction, whereas hot spot region looses its stiffness due to the softening of the material at higher temperature. In both cases, excessive plastic deformation is the primary cause of failure.

7.6.1 Integral Mean of Yield Criterion for Integrity Assessment

The integral mean of yield criterion was originally used in conjunction with the total volume of the component or structure. In pressure vessel components containing thermal hot spot or corrosion damage, failure occurs locally. Therefore, the assessment of the kinematically active portion of the volume that takes part in plastic action is of considerable interest. In order to use the integral mean of yield criterion in structural integrity assessment of components and structures containing local damage, the criterion

should be applied to the reference volume instead of the whole volume of the structure. The integral mean of yield criterion can be rewritten for reference volume as

$$\int_{V_R} \mu^0 \left[f(\bar{s}_{ij}^0) + (\varphi^0)^2 \right] dV = 0 \tag{7.7}$$

where $\bar{s}_{ij}^0$ is the statically admissible deviatoric stress for impending plastic flow; φ^0 is a point function which takes on a value of zero if $\bar{s}_{ij}^0$ is at yield and remains positive below yield, and V_R is the reference volume.

The Tresca and von Mises yield criteria can be expressed as

$$f(s_{ij}^0) = m_d^0 \sigma_e - \sigma_y = 0 \tag{7.8}$$

$$f(s_{ij}^0) = (m_d^0 \sigma_e)^2 - \sigma_y^2 = 0 \tag{7.9}$$

where m_d^0 is the upper bound limit load multiplier for the damaged component, σ_e is the statically admissible equivalent stress, and σ_y is the temperature dependent yield stress of the material.

(a) Corrosion Damage. For components containing corrosion damage, the integral mean of yield criterion using Tresca yield criterion can be expressed as

$$[(m_d^0 \sigma_{eU}) - \sigma_y]\ V_U + [(m_d^0 \sigma_{eC}) - \sigma_y]\ V_C = 0 \tag{7.10}$$

where suffix U refers to the uncorroded region of the reference volume and suffix C refers to the corroded region, σ_{eU} is the equivalent stress in the original shell and σ_{eC} is the equivalent stress in the corroded area of the shell.

Rearranging Eq. (7.10), the upper bound limit load multiplier for the damaged component can be obtained as

$$m_d^0 = \frac{\sigma_y V_R}{\sigma_{eU} V_U + \sigma_{eC} V_C} \tag{7.11}$$

Similarly, for components containing corrosion damage, the integral mean of yield using von Mises yield criterion can be expressed as

$$[(m_d^0 \sigma_{eU})^2 - \sigma_y^2]\ V_U + [(m_d^0 \sigma_{eC})^2 - \sigma_y^2]\ V_C = 0 \tag{7.12}$$

Rearranging Eq. (7.12), the upper bound limit load multiplier for the damaged component can be obtained as

$$m_d^0 = \sqrt{\frac{\sigma_y^2 V_R}{\sigma_{eU}^2 V_U + \sigma_{eC}^2 V_C}} \tag{7.13}$$

(b) Thermal Hot Spot. The integral mean of yield criterion, using Tresca yield criterion, can be expressed as

$$[(m_d^0 \sigma_{eU}) - \sigma_{yU}]\ V_U + [(m_d^0 \sigma_{eH}) - \sigma_{yH}]\ V_H = 0 \tag{7.14}$$

where suffix U refers to the uncorroded region of the reference volume and suffix H refers to the hot spot region, σ_{eU} is the equivalent stress in the original shell and σ_{eH} is the equivalent stress in the hot spot area of the shell.

Note that, as the shell thickness is constant throughout the structure, the membrane stresses in the hot spot and surrounding region are same i.e., $\sigma_{eU} = \sigma_{eH} = \sigma_e$. The upper bound limit load multiplier for the damaged spot can now be obtained as

$$m_d^0 = \frac{\sigma_{yU} V_U + \sigma_{yH} V_H}{\sigma_e V_R} \tag{7.15}$$

Similarly, for components containing hot spot, the integral mean of yield criterion using von Mises yield criterion can be expressed as

$$[(m_d^0 \sigma_{eU})^2 - \sigma_{yU}^2]\ V_U + [(m_d^0 \sigma_{eH})^2 - \sigma_{yH}^2]\ V_H = 0 \tag{7.16}$$

By applying $\sigma_{eU} = \sigma_{eH} = \sigma_e$ and rearranging Eq. (7.16), the upper bound limit load multiplier for the damaged spot can now be obtained as

$$m_d^0 = \sqrt{\frac{\sigma_{yU}^2 V_U + \sigma_{yH}^2 V_H}{\sigma_e^2 V_R}} \tag{7.17}$$

In the following sections of the chapter, m_d^0 based on the von Mises yield criterion will be discussed.

7.6.2 The Remaining Strength Factors (RSF)

As already been discussed, the remaining strength factor (RSF) is a parameter used for quantitative assessment of damaged components and structures. The RSF is a dimensionless parameter and is based on the primary load carrying capacity of the structure. The RSF can be defined as the ratio of the collapse load (pressure) of the damaged component to that of the undamaged component. Two RSFs are considered next for evaluation of pressure vessel components and structures containing thermal hot spot and corrosion damage.

(a) RSF Based on the m_α Multiplier: The first RSF is obtained by using the m_α multiplier proposed by Seshadri and Mangalaramanan (1997), which can be expressed as follows

$$RSF_\alpha = \frac{m_\alpha}{m_u^0} \tag{7.18}$$

where m_u^0 $(=\sigma_{yU}/\sigma_{eU})$ is the upper bound multiplier for undamaged vessel. Note that the m_α multiplier is dependent on the upper bound multiplier m^0 and the classical lower bound multiplier m_L. The m_α multiplier can be evaluated by using Eq. (3.25), where classical lower bound multiplier can be evaluated as $m_L = m_{Ld} = \sigma_y/\sigma_{eC}$ for corrosion damage and $m_{Ld} = \sigma_{yH}/\sigma_e$ for thermal hot spot; and the upper bound multiplier $m^0 (= m_d^0)$, based on the von Mises yield criterion, can be obtained by using the Eq. (7.13) for corrosion damage and Eq. (7.17) for thermal hot spot.

(b) RSF Based on the m_α-Tangent Multiplier: The second RSF is based on the m_α-tangent multiplier (m_α^T) proposed in Chapter 4 of this thesis. The proposed RSF can be expressed as

$$RSF_T = \frac{m_\alpha^T}{m_u^0} \tag{7.19}$$

The value of m_α^T can be obtained by using Eq. (4.10), where $\zeta = m_d^0 / m_{Ld}$; and m_{Ld} and m_d^0 have their usual meaning as mentioned above. The RSF based on the m_α-tangent method (RSF_T) is of considerable relevance from a structural integrity standpoint.

Note that the first RSF, based on the m_α multiplier, is applicable only if m^0/m_L is within the m_α - triangle i.e., $1 \le m^0 / m_L \le 1+\sqrt{2}$ (Figure 4.1). On the other hand, the second RSF, based on the m_α-tangent method, is simple and is applicable even if the value of m^0/m_L lies outside the m_α - triangle i.e., $m^0 / m_L > 1+\sqrt{2}$. This can be the case when the damaged spot experiences significant stress gradient. Therefore, the m_α-tangent method is capable of taking on any value of m^0/m_L (=ζ) while evaluating the corresponding multiplier. If the value of ζ is greater than $(1+\sqrt{2})$ then the m_α-tangent multiplier (m_α^T) needs to be evaluated using Eq. (4.13), instead of Eq. (4.10).

7.6.3 Allowable Remaining Strength Factor

The allowable RSF for a given pressurized component or structure may vary depending upon the application. Different procedures use different assumptions regarding the stress

at failure and hence result in different allowable RSF as shown in Table 7.1. For example, ASME B31G assumes 1.1*SMYS (specified minimum yield strength) as the flaw stress in order to predict the plastic flow of the material at the damaged spot. Hence the allowable RSF is turned out to be 0.909. This approach assumes that the structure with flaw or damaged fails when the stresses in the damaged spot reaches to the flow stress of the vessel or pipe material.

On the other hand, modified B31G and RSTRENG criterion assumes a less conservative assumption of the flow stress, which is SMYS+10,000 psi, and for Grade B pipe (SMYS = 35,000 psi) the allowable RSF turn out to be 0.778. Note that it increases the degree of conservatism when applied to relatively higher strength materials. API 579 has recommended the value of RSF equal to 0.90 for typical process equipments. This value implies that the strength of the damaged component or structure cannot be less than the 90 percent of the strength of the original design.

The allowable RSF is defined as the ratio of the required minimum thickness to the nominal thickness of the undamaged component. The required minimum thickness is the thickness that is required to resist the applied internal pressure and can be calculated according to appropriate design Codes. In this thesis, the required minimum thickness is calculated based on the ASME Boiler and Pressure Vessel Code, Section VIII Division 1 (2007). If the evaluated RSF is lower than the allowable RSF, then the component or structure can still be accepted to continue service upon rerating for MAWP.

Table 7.1 Comparison of allowable RSF for different criteria

Sl. No.	Criterion / Procedure	Allowable RSF
1	ASME B31G	0.91
2	Modified B31G*	0.78
3	RSTRENG*	0.78
4	API 579 Level 1	0.90
5	API 579 Level 2	0.90
6	API 579 Level 3	0.90

* Based upon Grade B pipe specifications

7.6.4 Remaining Life Assessment

Structural integrity assessment essentially means the assessment of serviceability as well as the remaining life of the component. Once the strength parameter of the damaged component is evaluated, the decision on suitability of the component for continued service could be made. When the component is considered to be acceptable for continued service, it is required to estimate the remaining life of the component. Assessment of remaining life of the component or structure is important in order to establish the routine inspection schedule and / or establishing a monitoring plan.

Widespread research has not been carried out in assessing the remaining service life of aging pressure vessel components and structures. The issue has been addressed in different practices and procedures, e.g., API 579. The procedure for estimation of remaining life of aging components and structures is case dependent i.e., it depends on the characteristics of the flaw or damage. For example, in case of local wall thinning, where there is no possibility of cracking, a certain remaining life of the damaged

component can be established on the basis of the parameters like, remaining thickness of the LTA, future corrosion allowance, rate of change of size of the damage and the corrosion rate data.

API 579 (2000) recommended two approaches for remaining life assessment of pressurized components and structures with LTAs: thickness approach and maximum allowable working pressure (MAWP) approach. The thickness approach is applicable where the thickness of the LTA is uniform and the later one is applicable when the remaining thickness is characterized by a thickness profile. It should be noted that there are some uncertainties in these assessment approaches due to the possibility of inaccurate inspection data, change of material properties of the aging component, assessment level, as well as the assumptions that are made during the course of the evaluation.

7.7 Finite Element Modeling

Inelastic strength of the cylindrical pressure vessel containing thermal hot spot and corrosion damage (LTA) is determined by performing inelastic finite element analysis. This Level 3 assessment method is used to verify the results obtained from the proposed Level 2 FFS assessment method. Note that inelastic finite element analysis is very expensive in terms of computational effort and time and hence is not suitable for plant engineers to use in a daily basis. In the inelastic finite element analysis, a bilinear kinematic hardening material model is assumed as shown in Figure 7.4. This assumption is made due to the fact that structural materials possesses significant amount of reserve strength beyond their yield limit.

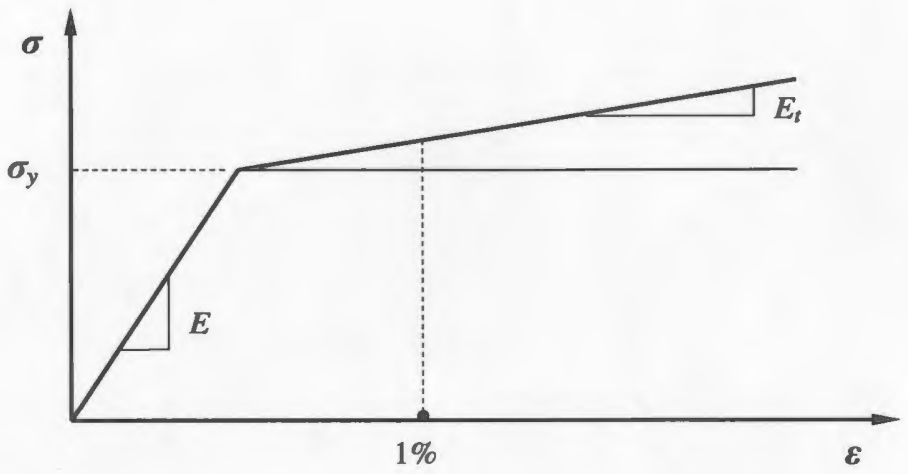

Figure 7.4 Material model for finite element analysis

Therefore, it is reasonable that a certain portion of the reserve strength could be taken into account while performing the assessment, given that the difference between the yield and ultimate strength of the material is considerably large. Note that there is an ongoing argument about the amount of reserve strength that could be taken into account beyond the yield limit. By adopting elastic-plastic material model and performing strain-based assessment, a portion of the reserve strength is taken into account, which reduces the conservatism in the assessment and hence avoids the unnecessary repair or replacement of the component.

Finite element models of the cylindrical vessels containing thermal hot spot and corrosion damage is developed using 3D 8-noded structural solid element. In order to account for the bending stresses, present at the edges of the LTA, a very fine mesh is generated in and around the LTA and four elements across the thickness. The relatively finer mesh helps in capturing the actual stress distribution in and around the damaged spot. Typical finite element mesh for a cylindrical vessel with LTA is shown in Figure 7.5.

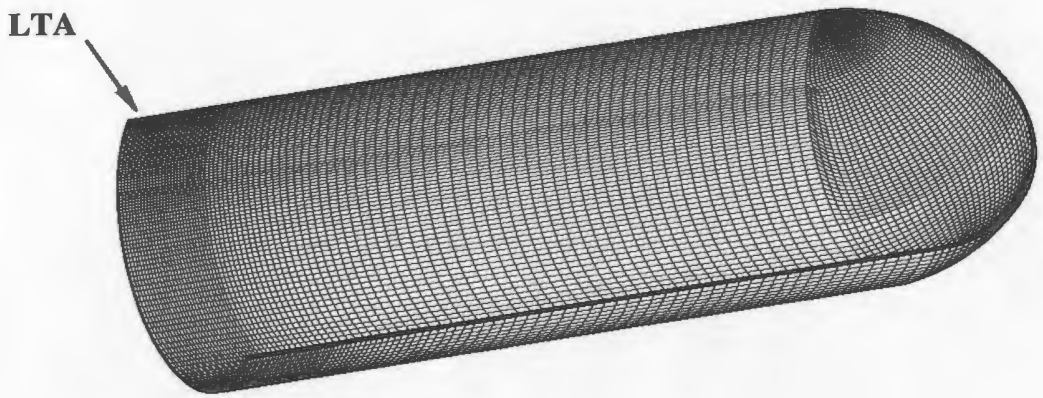

Figure 7.5 Finite element model of the cylindrical shell with local thin area (LTA)

The finite element model of the structure is developed by taking advantage of symmetry about the meridional and longitudinal plane. Therefore, one half of the structure is modeled and symmetric boundary conditions are applied to the edges of symmetry. The structure is subjected to internal pressure. The same procedure is applied for modeling and analyzing the cylindrical vessel with thermal hot spot except that the material properties of the hot spot region are different than that of the rest of the vessel due to relatively higher temperature.

7.7.1 Inelastic Finite Element Analysis

The strength parameters obtained by the proposed method is verified by Level 3 inelastic finite element analysis. Appropriate strain limits are used to obtain the collapse load of the structure. Sims et al. (1992) proposed a conservative limit on the amount of plastic strain in LTA based on numerous inelastic FEA. They argued that a limit of 2% plastic

strain at any location provides a reasonable and conservative estimate of the actual collapse load of the structure. They have shown that maximum plastic strain occurs at the centre of the LTA, which is the case when the structure is subjected to uniform internal pressure. It should be noted that the maximum allowable working pressure (MAWP) may not produce any plastic strain in the LTA.

In this thesis, 1% plastic strain at the middle fiber of the centre of the damaged spot (LTA or hot spot) is considered as the limit for plastic collapse load estimation. The approach is consistent with the work reported in (Seshadri, 2005; Indermohan and Seshadri, 2005; Ramkumar and Seshadri, 2005; Tantichattanont et al., 2007) on FFS assessment of thermal hot spot and corrosion damage. In case of pressure vessels and piping, maximum strain occurs at the centre of the LTA or hot spot due to uniform internal pressure. In case of LTA, it should be noted that the periphery of the LTA is assumed to be blended with an appropriate blend radius such that the maximum stress and strain occurs at the center of the LTA but not at the edges.

7.8 Illustrative Examples

In order to illustrate the proposed method for FFS assessment, a cylindrical vessel under internal pressure is considered. The basic dimensions of the shell including design considerations and operating conditions are given below. The values in the brackets are in SI units.

ASTM Material	:	SA 516 Grade 55
Shell inside radius (R_i)	:	33 in. (0.8382 m)
Operating pressure (p_o)	:	180 psig (1.24 MPa)
Design pressure (p_d)	:	220 psig (1.52 MPa)
Design temperature (T_l)	:	100 °F (37.78 °C)
Operating temperature	:	90 °F (32.22 °C)
Allowable stress (S)	:	13.7 ksi (94.46 MPa)
Corrosion allowance (CA)	:	1/16 in. (0.0016 m)
Joint efficiency (E_j)	:	1.0

Thickness Calculation: Design thickness for cylindrical shell can be calculated as $h_d = p_d R_i /(SE_j - 0.6p_d) = 0.535$ in. (0.014 m). Required thickness of the shell can be evaluated as $h = h_d$ + corrosion allowance (CA) = 0.598 in. (0.015 m). Therefore, a plate of 5/8 in. (0.016 m) thickness is specified. The shell outside radius is evaluated as R_o= 33.625 in. (0.854 m) and shell thickness is evaluated as h = 0.625 in. (0.016 m). The allowable RSF based on design requirements is obtained as $RSF^* = h_d / h = 0.856$.

Calculation of Decay Length: Decay length in meridional direction is evaluated as $x_l = 2.50\sqrt{Rh} =$ 11.354 in. (0.288 m) and decay length in circumferential direction is evaluated as $x_c = 6.10(R^3h)^{1/4} = 74.677$ in. (1.897 m).

7.8.1 Rectangular LTA in Cylindrical Shell

Assume that 1/3 of the shell thickness has undergone corrosion. The remaining thickness of the corroded shell h_C (=$2h/3$) = 0.417 in. (0.011 m) and the corroded radius R_{iC} = 33.208 in. (0.844 m).

Dimension of LTA: For the following calculation, circumferential and longitudinal dimension of the LTA (Figure 7.3) is considered as $2a$ = 20 in. (0.508 m); $2b$ = 20 in. (0.508 m), respectively. The aspect ratio of the damaged area (b/a) = 1.0.

Evaluation of Reference Volume: Volume of LTA is evaluated as $V_D = (4ab)\ h_C$ = 166.680 in.^{3} (0.003 m^3) and volume of the remaining shell that takes part in plastic action is calculated as $V_U = 4h\ [(x_c + a)\ (x_l + b) - ab]$ = 4270.402 in.^{3} (0.070 m^3). Therefore, the reference volume $V_R = (V_U + V_D)$ = 4437.082 in.^{3} (0.073 m^3).

Evaluation of Stresses for the LTA: Hoop stress is evaluated as $\sigma_{hC} = p_d R_{iC} / h_C$ = 17.533 ksi (120.884 MPa) and longitudinal stress is evaluated as $\sigma_{lC} = p_d R_{iC} / 2h_C$ = 8.766 ksi (60.442 MPa). Therefore, von Mises equivalent stress is calculated as $\sigma_{eC} = \sqrt{\sigma_{hC}^2 + \sigma_{lC}^2 - \sigma_{hC}\sigma_{lC}}$ = 15.184 ksi (104.688 MPa).

Evaluation of Stresses for the Remaining Shell: Hoop stress is evaluated as $\sigma_h = p_d R_i / h$ = 11.616 ksi (80.090 MPa) and longitudinal stress is evaluated as $\sigma_l = p_d R_i / 2h$ = 5.808 ksi (40.045 MPa). Therefore, von Mises equivalent stress is calculated as $\sigma_{eU} = \sqrt{\sigma_h^2 + \sigma_l^2 - \sigma_h\sigma_l}$ = 10.060 ksi (69.36 MPa).

Table 7.2 Comparison of RSF for corrosion damage; $h_C = 2h/3$

Case No.	*a* (in.)	. *b* (in.)	RSF_{α}	RSF_{T}	$RSF_{inelastic}$
1	5.0	5.0	0.808	0.866	0.978
2	7.5	7.5	0.806	0.862	0.871
3	10.0	10.0	0.805	0.857	0.844
4	12.5	12.5	0.803	0.853	0.837
5	15.0	15.0	0.801	0.848	0.830
6	20.0	20.0	0.797	0.839	0.821

Evaluation of Multipliers: Upper bound multiplier for the undamaged shell is evaluated as $m_U^0 = \sigma_y / \sigma_{eU} = 2.982$; lower bound multiplier for the damaged shell is calculated as $m_{Ld} = \sigma_y / \sigma_{eC} = 1.976$ and upper bound multiplier for the damaged shell is evaluated as $m_d^0 = \sqrt{\sigma_y^2 V_R / (\sigma_{eC}^2 V_C + \sigma_{eU}^2 V_U)} = 2.913$. The m_α multiplier for the damaged shell could be obtained by using Eq. (3.25) as $(m_\alpha)_d = 2.399$; where $m^0 = m_d^0$ and $m_L = m_{Ld}$. The m_α-tangent multiplier for the damaged shell could be obtained by using Eq. (4.10) as $(m_\alpha^T)_d = m_d^0 / (1 + 0.2929(\zeta - 1)) = 2.558$; where $\zeta = m_d^0 / m_{Ld}$.

Evaluation of RSF: Using Eq. (7.18), the RSF based on m_α multiplier is evaluated as $RSF_\alpha = (m_\alpha)_d / m_u^0 = 0.805$. Using Eq. (7.19), the RSF based on m_α-tangent multiplier is evaluated as $RSF_T = (m_\alpha^T)_d / m_u^0 = 0.857$. A number of LTAs are considered further with different aspect ratios to obtain the behavior of the evaluated Level 2 RSFs. The results are shown in Table 7.2.

Level 3 Inelastic Analysis: In order to verify the value of the Level 2 RSF obtained from the above mentioned methods, inelastic FEA is conducted. Plastic modulus of 50×10^4 psi

(3.45×10^9 Pa) is used to account for the strain hardening effect. The RSF is calculated from the ratio of the limit pressure at 1% membrane strain in the centre of the LTA to the limit pressure of the vessel without LTA. For this example, inelastic strength parameter, $RSF_{inelastic}$ is evaluated as 0.844. The same procedure is applied to LTA with different aspect ratios and corresponding results are shown in Table 7.2.

Discussion: The results in Table 1 show that the RSF based on the m_α method (RSF_α) is conservative compared to that of the m_α–tangent method (RSF_T). For relatively bigger LTAs, the RSF_T slightly exceeds the inelastic strength parameter $RSF_{inelastic}$. Extensive investigation revealed that this is a reference volume issue, not the method itself. Moreover, in the present analysis, RSF is calculated from the limit pressure at 1% membrane strain in the centre of the LTA, which is a conservative assumption compared to Sims (1992) assumption as 2% membrane strain (refer to Section 7.7.1 of this thesis for further detail). However, the maximum difference between the value of RSF_T and $RSF_{inelastic}$, as shown in Table 7.2, is about 2%, which is acceptable.

7.8.2 Rectangular Hot Spot in Cylindrical Shell

A rectangular hot spot of temperature 600 °F (316 °C) is considered for evaluation. The material properties of carbon steel for a temperature range of 100-600 °F (37.8 - 316 °C) are listed in Table 7.3. The basic dimensions of the shell including design considerations and operating conditions are as before. Dimension of the hot spot is the same as the dimension of the LTA.

Evaluation of Reference Volume: Volume of the damaged spot is evaluated as $V_D = (4ab)$ $h = 250.00$ in.^{3} (0.004 m^3) and volume of the remaining shell that takes part in plastic action is calculated as $V_U = 4h\ [(x_c + a)\ (x_l + b) - ab] = 4270.402$ in.^{3} (0.070 m^3). Therefore, the reference volume $V_R = (V_U + V_D) = 4520.402$ in.^{3} (0.074 m^3).

Calculation of Elastic Stresses: Hoop stress is evaluated as $\sigma_h = p_d R_i / h = 11.616$ ksi (80.09 MPa) and longitudinal stress is evaluated as $\sigma_l = p_d R_i / 2h = 5.808$ ksi (40.045 MPa). Therefore, von Mises equivalent stress: $\sigma_e = \sqrt{\sigma_h^2 + \sigma_l^2 - \sigma_h \sigma_l} = 10.060$ ksi (69.360 MPa).

Evaluation of Multipliers: Upper bound multiplier for the undamaged shell is evaluated as $m_U^0 = \sigma_{yU} / \sigma_e = 2.982$; lower bound multiplier for the damaged shell is calculated as $m_{Ld} = \sigma_{yH} / \sigma_e = 2.207$, and upper bound multiplier for the damaged shell is evaluated as $m_d^0 = \sqrt{(\sigma_{yH}^2 V_H + \sigma_{yU}^2 V_U) / \sigma_e^2 V_R} = 2.945$.

The m_α multiplier for the damaged shell could be obtained by using Eq. (3.25) as $(m_\alpha)_d = 2.593$; where $m^0 = m_d^0$ and $m_L = m_{Ld}$. The m_α-tangent multiplier for the damaged shell could be obtained by using Eq. (4.10) as $(m_\alpha^T)_d = m_d^0 / (1 + 0.2929(\zeta - 1)) = 2.682$; where $\zeta = m_d^0 / m_{Ld}$.

Table 7.3 Material properties for SA 516 Gr. 55

Temperature (°F)	100 (37.8 °C)	200 (93.3 °C)	300 (149 °C)	400 (204 °C)	500 (260 °C)	600 (316 °C)
E($\times 10^6$) psi	29.3	28.8	28.3	27.7	27.3	26.7
α($\times 10^{-6}$) in./in. °F	5.53	5.89	6.26	6.61	6.91	7.17
σ_y($\times 10^3$) psi	30.0	27.3	26.6	25.7	24.5	22.2

Evaluation of RSF: Using Eq. (7.18), the RSF based on m_α multiplier is evaluated as $RSF_\alpha = (m_\alpha)_d / m_u^0 = 0.869$. Using Eq. (7.19), the RSF based on m_α-tangent multiplier is evaluated as $RSF_T = (m_\alpha^T)_d / m_u^0 = 0.899$. A number of hot spots are considered further with different aspect ratios. The results are shown in Table 7.4.

Level 3 Inelastic Analysis: The same procedure is applied here to evaluate the inelastic strength parameter, where $RSF_{inelastic}$ is the ratio of the limit pressure at 1% membrane strain in the hot spot to the limit pressure of the vessel without hot spot. For this example, $RSF_{inelastic}$ is evaluated as 0.953. The same procedure is applied to hot spots with different aspect ratios and the results are shown in Table 7.4.

Table 7.4 Comparison of RSF for thermal hot spot; $T_H = 600$ °F

Case No.	*a* (in.)	. *b* (in.)	RSF_α	RSF_T	$RSF_{inelastic}$
1	5.0	5.0	0.872	0.904	0.989
2	7.5	7.5	0.871	0.902	0.981
3	10.0	10.0	0.869	0.899	0.953
4	12.5	12.5	0.868	0.897	0.918
5	15.0	15.0	0.866	0.894	0.902
6	20.0	20.0	0.863	0.889	0.893

Calculation of Thermo-elastic Stresses: Elastic modulus at average temperature of T_{avg} =350 °F (176.8 °C) is 28.0×10^6 psi (193.05×10^9 Pa) and coefficient of thermal expansion at T_{avg} is 6.435×10^{-6} in./in.°F (11.6×10^{-6} mm/mm °C). Therefore, the thermo-elastic stresses are evaluated as $\sigma_1 = (p_d R_i / h) - (E\alpha\Delta T / 2)$ = -33.429 ksi (-230.49 MPa) and $\sigma_2 = (p_d R_i / 2h) - (E\alpha\Delta T / 2)$=-39.237 ksi (-270.54 MPa). These stresses are compressive as the thermal stresses are dominating and developed in a cylindrical structure. Therefore, von Mises equivalent stress: $\sigma_e = \sqrt{\sigma_1^2 + \sigma_2^2 - \sigma_1\sigma_2}$ = 36.680 ksi (252.910 MPa), which is grater than the yield stress of the material at 600 °F (316 °C). Therefore, the hot spot will yield. Since the stresses are membrane compressive stress, there is a possibility of local buckling (Seshadri 2005).

Discussion: It can be observed from the tabulated results (Table 7.4) that the value of RSF_T, based on the m_α-tangent method, is in good agreement with the Level 3 inelastic FEA results ($RSF_{inelastic}$). Therefore, RSF_T is recommended for integrity assessment of pressure vessels and piping systems containing thermal hot spot.

7.9 Conclusion and Recommendation

Level 2 FFS assessment method is proposed in this Chapter to estimate the strength parameters for evaluating pressure vessels and piping systems containing thermal hot spot and corrosion damage. The integral mean of yield criterion in conjunction with the m_α-tangent method is used to develop the proposed method. The RSF obtained by using the m_α-tangent method is shown to be in good agreement with the Level 3 inelastic FEA

results. The RSF based on the m_a method (RSF_a) is found to be conservative compared to the RSF_T, which is based on the m_a-tangent method.

A significant advantage of using the m_a-tangent method (based RSF_T), over m_a method (based RSF_a), is that the former one is applicable to the damages experiencing high stress gradient in and around the damaged spot. By using the proposed m_a-tangent method based RSF, reasonably accurate assessment can be achieved for a wide range of damaged pressure vessel components and structures. Therefore, the proposed method is suggested as a simplified tool for achieving the FFS assessment of pressure vessels and piping systems containing thermal hot spot and corrosion damage.

7.10 Closure

The fitness-for-service (FFS) assessment of mechanical components and structures based on simplified method is presented in this chapter. The theoretical background, formulation and potential application areas of the proposed method are presented in a systematic way. The method is applicable to structures containing thermal hot spot and corrosion damage. In addition, the method is applicable if there is a significant stress gradient in and around the damaged spot. Illustrative examples are included in order to demonstrate the application of the method.

CHAPTER 8

CONCLUSIONS AND FUTURE RESEARCH

8.1 Summary and Conclusions

Design and integrity assessments of mechanical components and structures are of paramount importance in many industrial sectors. Evaluation of load carrying capacity is an important goal in structural design and structural integrity assessment. Limit analysis is particularly important as it provides a guaranteed margin of safety against load carrying capacity of the structure and simplifies the analysis by assuming an elastic perfectly plastic material model. Limit analysis is recognized by the available codes and standards, e.g., ASME B&PV Code (2007), as an acceptable tool to estimate the limit load. Limit analysis is widely used to identify primary stresses in the mechanical components and structures. It also plays an important role in integrity assessment of

aging mechanical components and structures. Therefore, the development of a robust and simplified method for limit analysis is of considerable interest from structural design and structural integrity assessment standpoint.

In practice, limit load can be determined by using analytical method, numerical method, experimental method, or by using simplified method. Use of simplified method is of considerable interest, over the conventional methods, as it is very effective in terms of computational effort and time; and is applicable to a wide range of practical component configurations including three dimensional components with complex geometry. In this thesis, a simplified method, called the m_α-tangent method, has been developed to estimate the limit load of a general class of mechanical components and structures. The underlying features of the m_α-tangent method enabled its application into three major areas which includes: analysis of cracked components, stress categorization and fitness-for-service assessment.

(a) The m_α-Tangent Method. The m_α-tangent method has been developed in this thesis as an alternative method over conventional limit analysis methods. The proposed method is based on variational principles in plasticity. It makes use of statically admissible stress field based on a single linear elastic analysis to estimate the limit load. The method makes use of the "limiting tangent" in order to relate the initial elastic state of a component or structure to that of the exact limit state.

The m_α-tangent method has several potential advantages over the conventional methods. It is particularly beneficial as it overcomes the potential numerical difficulties of the conventional inelastic FEA and cost effective compared to the experimental methods.

The proposed method is applicable to a wide range of practical components and structures with complex geometric configurations and loading conditions. The underlying feature of the m_α-tangent method enabled its application to components and structures experiencing significant amount of peak stresses. The method is shown to be quick and easy to implement in practice. The proposed method is economically viable to use on a daily or regular basis. This method can also be considered as an independent verification tool for conventional limit analysis techniques. The m_α-tangent method is applied to a number of mechanical components and structures, ranging from simple to relatively complex geometric configurations, and the results compare well with those obtained from the corresponding analytical and inelastic finite element analysis results.

(b) Analysis of Cracked Components. There is a growing interest in the quantitative assessment of the integrity of mechanical components and structures containing crack like flaws, which might lead to a catastrophic failure. Limit analysis plays an important role in integrity assessment of cracked components and structures. In this thesis, the proposed m_α-tangent method is extended to estimate the limit load of components and structures containing crack like flaws.

In a cracked body, significant amount of peak stresses are developed due to singular stress field ahead of the crack-tip. In order to apply the proposed m_α-tangent method, peak stresses ahead of the crack-tip are blunted in two stages. The method makes use of a single linear elastic finite element analysis to estimate the limit load. Three different procedures are proposed. A number of example problems are worked out in order to

demonstrate the method. The results are found to be in good agreement with the corresponding inelastic finite element analysis results.

(c) Stress Categorization of Pressure Components. The design of mechanical components and structures by elastic analysis essentially means the splitting of elastic stresses into primary, secondary and peak stress categories and then apply the appropriate stress limits for each of these categories and appropriate combinations of the same. The complete categorization of stresses is a challenging task even with the on-hand computing facilities and numerical techniques. An attempt has been made in this thesis to categorize the elastic stresses induced in pressure vessel components and structures by using simplified method, in light of available codes and standards (ASME B&PV Code, 2007). The proposed method is based on approximate limit load multiplier estimates to decompose the elastic stresses into appropriate categories, using a single linear elastic FEA. The proposed method is able to identify primary, primary plus secondary, and peak stress components for mechanical and thermal loads within reasonable accuracy.

The potential benefits of the proposed method over conventional methods are that the proposed method makes use of available FEA codes and requires a moderate amount of post-processing by the user, which could be automated; it does not require to make use of SCLs and hence is suitable for components with complex geometry. The proposed method is able to categorize the stresses for combined loading (mechanical and thermal) without requiring two separate analyses. The method is demonstrated by a number of example problems ranging from simple to relatively complex pressure vessel component configurations. The results are compared well with those obtained from the conventional

techniques. Therefore, the proposed method can be used as a tool for simplified stress categorization of pressure vessel components and structures with minimum computational effort.

(d) Fitness-for-Service (FFS) Assessment. Damage tolerance or fitness-for-service (FFS) assessments are performed in operating plants in order to demonstrate the structural integrity of the in-service components and structures undergoing damage. The concepts underlying the m_α-tangent method along with the concept of decay length and reference volume are used in this thesis to assess the remaining strength of corroded areas and thermal hot spots. The proposed method gives an improved estimate of the remaining strength of the aging pressure vessel components and structures. The method is applicable to a wide range of practical pressure vessel components and structures including damages experiencing significant stress gradient in and around the damaged spot. The method is demonstrated through a number of examples and the results are found to be in reasonably good agreement with the corresponding Level 3 inelastic finite element analysis results. The proposed method is economically viable to use by the plant engineers on a daily or regular basis.

8.2 Original Contributions

The original contributions to this thesis are as follows:

- A robust simplified method, designated as the m_α-tangent method, is proposed in order to estimate the limit load of a general class of mechanical components

and structures. The method makes use of statically admissible stress field based on a single linear elastic analysis in order to estimate the limit load. The m_α–tangent method can take practically any value of m^0 / m_L, which extended the domain of application of the proposed method beyond the "m_α triangle". The method is shown to be rapid and easy to implement in practice.

- The m_α-tangent method is extended to estimate the limit load of mechanical components and structures containing crack-like flaws. The method is able to estimate the limit load using a single linear elastic analysis. Three different procedures are proposed.

- A relationship is identified using the m_α-method (1997) and the reference two-bar structure method (2006) proposed by Seshadri et al., which signifies the importance of $1+\sqrt{2}$ as a threshold for peak stresses.

- A simple procedure is proposed to categorize the elastic stresses in pressure vessel components and structures into primary, secondary and peak stress components. The proposed method makes use of statically admissible stress field based on a single linear elastic analysis to categorize the stresses induced by both mechanical and thermal loads. The method is considered as a direct and alternative approach over conventional approaches e.g., stress linearization and interaction / discontinuity analysis.

- Simplified method based remaining strength factor (RSF) is proposed for fitness-for-service (FFS) assessment of pressure vessels and piping systems

containing thermal hot spot and corrosion damage. The proposed method is applicable to the damaged components or structures even when significant amount of peak stresses are present.

8.3 Recommendations for Future Research

Recommendations for future research are as follows:

1. The m_α-tangent method is proposed in this thesis for estimation of limit load of a general class of mechanical components and structures containing crack like flaws and those without flaws. The method has been applied to a wide range of pressure vessel components and structures ranging from simple to relatively complex three dimensional structures; and the results are found to be in good agreement with the corresponding analytical and inelastic FEA results. The method has also been applied to a number of standard example problems as well as typical pressure component configuration with crack like flaws and the results are found to be in good agreement with the corresponding analytical and inelastic FEA results. It will be beneficial to apply this method to three dimensional FE models with crack like flaws.

2. A linear elastic analysis based simplified method has been proposed in this thesis for categorization of linear elastic stresses induced in pressure vessel components and structures. The primary stress obtained from the proposed method is compared with the corresponding analytical and inelastic finite element analysis results and primary-plus-secondary stress for simple structures has been compared with those obtained

from the conventional techniques. It will be beneficial if the primary-plus-secondary stresses could further be verified by performing shakedown analysis.

3. In this thesis, simplified method based Level 2 FFS assessment method is proposed for FFS assessment of thermal hot spot and corrosion damage. The following recommendations are proposed for future research:

    - Current API 579 rules for FFS assessment covers LTA remote from major structural discontinuities. Therefore, evaluation of LTA near structural discontinuities will be useful. In addition, interaction of LTAs could be considered for future research.

    - FFS assessment of LTA based on linear elastic analysis using stress categorization approach can be considered for future research.

    - The method is currently applied to cylindrical shells. The domain of application of the proposed method could be extended to other practical components and structures such as elbows and conical transitions.

REFERENCES

ASME Boiler and Pressure Vessel Code, 2007, Section III, American Society of Mechanical Engineers, New York, USA

ASME Boiler and Pressure Vessel Code, 2007, Section VIII, American Society of Mechanical Engineers, New York, USA.

Mendelson, A., 1968, *Plasticity: Theory and Application*, Macmillan, New York.

Calladine, C. R., 2000. *Plasticity for Engineers: Theory and Application*. Chichester: Horwood Publishing.

Hill, R., 1950. *The mathematical Theory of Plasticity.* London: Oxford University Press.

Kachanov, L. M., 1971. *Foundations of the Theory of Plasticity.* Amsterdam: North-Holland Publishing Company.

Mura, T. and Lee, S. L., 1963. "Application of Variational Principles to Limit Analysis". Quarterly of Applied Mathematics. **21(3)**, pp. 243-348.

Mura, T., Rimawi, W. H. and Lee, S. L., 1965. "Extended Theorems of Limit Analysis". Quarterly of Applied Mathematics, **23**, pp. 171-179.

Seshadri, R., and Mangalaramanan, S. P., 1997, "Lower Bound Limit Loads Using Variational Concepts: the m_α-method," Int. J. Pressure Vessels & Piping, **71**, pp. 93–106.

Reinhardt W. D., and Seshadri R., 2003, "Limit Load Bounds for the m_α-Multipliers," ASME J. Pressure Vessel Technol., **125**, pp.11– 18.

Webster, G., and Ainsworth, R. A., 1994, *High Temperature Component Life Assessment*, Chapman and Hall, London, UK.

Ainsworth, R. A., Dean, D. W., and Budden, P. J., 2000, "Development in Creep Fracture Assessments within the R5 Procedure," IUTAM Symposium on Creep in Structures, Nagoya, Japan, pp. 321–330.

Ainsworth, R. A., O'Dowd, N. P., 1995, "Constraint in the Failure Assessment Diagram Approach for Fracture Assessment," ASME J. Pressure Vessel Technol., **117**, pp. 260–267.

Seshadri, R., 1991, "The Generalized Local Stress Strain (GLOSS) Analysis— Theory and Applications," ASME J. Pressure Vessel Technol., **113**, pp. 219–227.

Jones, G. L., Dhalla A. K., 1981, "Classification of Clamp Induced Stresses in Thin Walled Pipe," ASME J. Pressure Vessel Technol., **81**, pp. 17-23.

Marriott, D. L., 1988, "Evaluation of Deformation or Load Control of Stress under Inelastic Conditions using Elastic Finite Element Stress Analysis," ASME J. Pressure Vessel Technol., **136**, pp. 3–9.

Seshadri, R., and Fernando, C. P. D., 1992, ''Limit Loads of Mechanical Components and Structures using the GLOSS R-Node Method, ''ASME J. Pressure Vessel Technol., **114**, pp. 201-208.

Mackenzie, D., and Boyle, J. T., 1993, "A Method of Estimating Limit Loads Using Elastic Analysis, I: Simple Examples," Int. J. Pressure Vessels & Piping, **53**, pp. 77–85.

Ponter, A. R. S., Fuschi, P., and Engelhardt, M., 2000, ''Limit Analysis for a General Class of Yield Conditions,'' Eur. J. Mech. A / Solids, **19**, pp. 401–421.

Ponter, A. R. S., and Engelhardt, M., 2000, ''Shakedown Limit for a General Yield Condition,'' Eur. J. Mech. A / Solids, **19**, pp. 423–445.

Adibi-Asl, R., Fanous, I. F. Z. and Seshadri, R., 2006, ''Elastic Modulus Adjustment Procedures—Improved Convergence Schemes,'' Int. J. Pressure Vessels Piping, **83**, pp. 154-160.

Adibi-Asl, R., and Seshadri, R., 2007, "Simplified Limit Load Determination of Cracked Components Using the Reference Two-Bar Structure," ASME PVP, Paper No. PVP2007-26747, San Antonio, Texas, USA.

Kroenke, W. C., 1974, "Classification of Finite Element Stresses According to ASME Section III Stress Categories," ASME PVP Publications: Analysis and Computers, NY, pp. 107-140.

Gordon, J. L., 1976, "OUTCUR: An Automated Evaluation of Two-Dimensional Finite Element Stresses According to ASME Section III Stress Requirements," ASME Winter Annual Meeting, Paper No. 76-WA/PVP-16, New York.

Seshadri, R., and Marriott, D. L., 1993, "On Relating the Reference Stress, Limit Load and the ASME Stress Classification Concepts," Int. J. Pressure Vessels & Piping, **56**, pp. 387–408.

Hechmer, J. L., and Hollinger, G. L., 1997, "*3D Stress Criteria: Guidelines for Application*," PVRC, Final Report.

Hollinger, G. L., and Hechmer, J. L., 2000, "Three-Dimensional Stress Criteria- Summary of the PVRC Project," ASME J. Pressure Vessel Technol., **122**, pp. 105-109.

Ihab, F. Z. Fanous, and Seshadri, R., 2006, "Stress Classification Using the R-Node Method," ASME PVP, Paper No. PVP2006-ICPVT-11, Vancouver, BC, Canada.

Seshadri, R., and Adibi-Asl, R., 2007, "Limit Loads of Pressure Components Using the Reference Two-Bar Structure," ASME J. Pressure Vessel Technol., **129**, pp.280–286.

ANSYS, 2008, University Research Version, 11.0, SAS IP, Inc.

Sang, Z. F., Lin, Y. J., Xue, L.P., and Widera, G. E. O, 2005, "Limit and Burst Pressures for a Cylindrical Vessel With a 30 deg – Lateral ($d/D \geq 0.5$)," ASME J. Pressure Vessel Technol., **127**, pp. 61–69.

Adibi-Asl, R., and Reinhardt, W., 2008, "Elastic Modulus Adjustment Procedure (EMAP) for Shakedown," ASME PVP, Paper No. PVP2008-61641, Chicago, Illinois, USA.

American Petroleum Institute (API), 2000. *Fitness-for-Service*, API 579. Washington, D.C.

R6, *Assessment of the Integrity of Structures Containing Defects*, Nuclear Electric, Berkeley Nuclear Laboratories, 1995.

Seshadri, R., 2005. "Integrity Assessment of Pressure Components with Local Hot Spots," ASME J. Pressure Vessel Technol., **127**, pp. 137-142.

Indermohan, H. and Seshadri, R., 2005. "Fitness-for–service Methodology based on Variational Principles in Plasticity," ASME J. Pressure Vessel Technol., **127**, pp. 92-97.

SINTAP, 1999, "Structural Integrity Assessment Procedure for European Industry," Project BE95-1426. Final Procedure, British Steel Report, Brussels: Brite Euram Programme.

Kiefner J. F, Vieth, P. H, 1989, "A Modified Criterion for Evaluating the Remaining Strength of Corroded Pipe (with RSTRENG)," American Gas Association, Catalogue L51609, PR3-805.

Ramkumar, B. and Seshadri R., June 2005. "Fitness for Service Assessment of Corroded Pipelines based on Variational Principles in Plasticity". Journal of Pipeline Integrity, **2**, pp. 99-116.

Harrison, R. P., Loosemore, K., and Milne, I., 1976, "Assessment of the Integrity of Structures Containing Defects," CEGB Report R/H/R6, Berkeley, U.K.

Sims, J. R., Hantz, B. F., Kuehn, K. E., 1992, "A Basis for the Fitness for Service Evaluation of Thin Areas in Pressure Vessels and Storage Tanks," Pressure Vessel Fracture, Fatigue, and Life management, ASME PVP, **233**, pp. 51-8.

Tantichattanont, P., Adluri, S. M. R, and Seshadri, R., 2007, "Fitness-for-Service Assessment of Spherical Pressure Vessels with Hot Spots." Int. J. Pressure Vessels & Piping, **84**, pp. 762–772.

Tantichattanont, P., Adluri, S. M. R, and Seshadri, R., 2007, "Structural Integrity for Corrosion in Spherical Pressure Vessels." Int. J. Pressure Vessels & Piping, **84**, pp. 749–761.

Tantichattanont, P., Adluri, S., and Seshadri, R., 2006, "Integrity Assessment of Spherical Pressure Components with Local Corrosion and Hot Spots." ASME PVP, Paper No. PVP2006-ICPVT-11-93513, Vancouver, BC, Canada.

Osage, D. A., Janelle, J., Henry, P. A., 2000, "Fitness-for-Service Local Metal Loss Assessment Rules in API 579" Service Experience and Fitness-for-Service in Power and Petroleum Processing, PVP Vol. 411, pp. 143-176.

ASME, 1984. *Manual for Determining the Remaining Strength of Corroded Pipelines*, American National Standards Institute (ANSI)/ American Society of Mechanical Engineers (ASME) B31G.

Zhu, X. K. and Leis, B. N., 2005, "Influence of Yield-to-Tensile Strength Ratio on Failure Assessment of Corroded Pipelines," ASME J. Pressure Vessel Technol., **127**, pp. 436–441.

Flugge, W., A., 1973, *Stresses in Shells*, Second Edition, Springer-Verlag, New York.

Bednar, H. H., 1985, *Pressure Vessel Design Handbook*, Second Edition, Van Nostrand Reinhold Company, New York.

Donnell, L. H., 1993, "Stability of Thin-Walled Tubes Under Torsion" Report National Advisory Committee for Aeronautics, **479**, pp. 95-116.

Harvey, J. F. 1991, *Theory and Design of Pressure Vessels*, Second Edition, Chapman and hall, New York.

Kiefner, J. F. 1990, "*The Remaining Strength of Corroded Pipe*," API Pipeline Conference, API, April 1990.

Mura, T. and Koya, T., 1992, *Variational Methods in Mechanics*, Oxford University Press, New York.

Osage, D. A., 1997, "New Development in PI 579," Int. J. Pressure Vessels & Piping, **71**, pp. 93–106.

Pan, L. and Seshadri. R., 2002, "Limit Load Estimation Using Plastic Flaw Parameter in Repeated Elastic Finite Element Analysis," ASME J. Pressure Vessel Technol., **124**, pp. 433–439.

Timoshenko, S., 1970, *Theory of Plates and Shells*, Second Edition, McGraw-Hill, Inc., New York.

Ugural, A. C., 1999, *Stresses in Plates and Shells*, Second Edition, McGraw-Hill, Inc., New York.

Walker, A. C., and Williams, K. A. J., 1995, "Strain Based Design of Pipelines," *Pipeline Technology,* OMAE, 5, pp. 345-350.

Anderson, T. L., and Osage, D. A., 2000, "API 579: a Comprehensive Fitness-for-Service Guide," Int. J. Pressure Vessels & Piping, **77**, pp. 953–963.

Milne, I., Ainsworth, R. A., Dowling, A. R., and Stewart, A. T., 1988, "Assessment of the Integrity of Structure Containing Defects," Int. J. Pressure Vessels & Piping, **32**, pp. 3–104.

Miller, A. G., 1988, "Review of Limit Loads of Structures Containing Defects," Int. J. Pressure Vessels & Piping, **32**, pp. 197–327.

Sang, Z. F., Wang, H. F., Xue, L. P., and Widera, G. E. O., 2006, "Plastic Limit Loads of Pad Reinforced Cylindrical Vessels Under Out-of-Plane Moment of Nozzle," ASME J. Pressure Vessel Technol., **128**, pp. 49–56.

Newman, R. C. and Marcus, P., 2002, *Stress Corrosion Cracking Mechanisms*, Corrosion Mechanisms in Theory and Practice, Second Edition, Marcel Dekker, New York.

Szilard, R., 2004, *Theories and Applications of Plate Analysis: Classical, Numerical and Engineering Methods*, John Wiley, New Jersey.

Kraus, H., 1967, *Thin Elastic Shell*, John Wiley, New York.

APPENDIX A

ANSYS Command Listing

ANSYS batch files are used to perform the finite element analysis of different mechanical components and structures. The analysis type includes both elastic and inelastic finite element analysis. Typical input files of a number of example problems, used in Chapter 4, 5, 6 and 7, are provided in this section. The examples include standard example problem to typical pressure component configuration.

A.1 Thick Walled Cylinder Subjected to Internal Pressure

```
/TITLE, Thick Walled Cylinder under Internal Pressure

! Cylinder dimensions (m)
*SET,Ri,65e-3
*SET,Ro,90e-3
*SET,Rm,(Ro+Ri)/2
*SET,Thick,(Ro-Ri)

*AFUN,DEG
*SET,Pi,3.1416
```

```
! Applied internal pressure
*SET,Prs,50e6

! Material model
*SET,YS,300e6
*SET,EM,200e9
*SET,Pois,0.3

! Enter preprocessor
/PREP7
ET,1,PLANE82,,,2
MP,EX,1,EM
MP,NUXY,1,Pois

! Modeling geometry
K,10
K,1,,RI
K,2,RI
LARC,1,2,10,RI
K,3,,Ro
K,4,Ro

LARC,3,4,10,Ro
L,1,3
L,2,4
AL,1,2,3,4

! Meshing
*SET,m,0.25
ARC=(Pi*90*Rm)/180
*SET,THKdiv,Thick*1e3*m
*SET,CIRdiv,ARC*1e3*m

LESIZE,3,,,THKdiv,3
LESIZE,4,,,THKdiv,3
```

```
LESIZE,1,,,CIRdiv
LESIZE,2,,,CIRdiv
AMESH,ALL

! Boundary conditions
DL,3,1,SYMM
DL,4,1,SYMM
ALLSEL

! Apply load
SFL,1,PRES,Prs
ALLSEL
SBCTRAN
FINISH

! Enter into the solver
/SOLU
ANTYPE,0
SOLVE
SAVE
FINISH

! Post Processing
/POST1
ETABLE,Sig,S,EQV
ETABLE,Vol,VOLU
*GET,Emax,ELEM,0,COUNT

*SET,Vtot,0
*DO,kk,1,Emax
*GET,Evol,ELEM,kk,ETAB,Vol
Vtot=Vtot+Evol
*ENDDO

! Evaluate multipliers
```

```
*SET,SumRef,0

*DO,kk,1,Emax
*GET,SigEq,ELEM,kk,ETAB,Sig
*GET,Evol,ELEM,kk,ETAB,Vol
SumRef=SumRef+((SigEq**2)*Evol)
*ENDDO

SIGref=SQRT(SumRef/Vtot)

m0_1=(YS/SIGref)
*SET,m_0,m0_1

ESORT,ETAB,Sig,0
*GET,SIGmax,SORT,0,MAX
m_L=(YS/SIGmax)

*SET, Jeta, (m_0/m_L)
*SET, Tan_theta, 0.2929
m_tangent=m_0/(1+(Jeta-1)*Tan_theta)

! Open file
*CFOPEN,m_TWcylinder,,,APPEND
*CFWRITE,m0,m_0
*CFWRITE,mL,m_L
*CFWRITE,m0_by_mL,Jeta
*CFWRITE,m_tangent,m_tangent
*CFCLOS
FINISH
```

A.2 Plate with a Centre Hole

```
/TITLE, Plate with a Centre Hole
```

```
! Plate dimension
*SET,R,20e-3
*SET,W,150e-3
*SET,L,300e-3
*AFUN,DEG
*SET,Pi,3.1416

! Material model
*SET,YS,150e6
*SET,EM,150e9
*SET,Pois,0.3

! Loading
*SET,Prs,100e6

! Enter Preprocessor
/PREP7
ET,1,PLANE82,,,0
MP,EX,1,EM
MP,NUXY,1,Pois

! Geometry
K,1,0,0
K,2,R,0
K,3,0,R
K,4,L/2,0
K,5,0,W/2
K,6,L/2,W/2

LARC,2,3,1,R
L,2,4
L,3,5
L,4,6
L,5,6
```

```
LDIV,1,1.5,,,0
LDIV,5,L/W,,,0

K,9,L/4
L,7,8
L,8,9
LCSL,2,9

AL,1,10,9,8
AL,8,5,3,6
AL,9,11,4,7

! Meshing
*SET,m,0.5
*SET,ARClen,(Pi*45*R)/180
*SET,ARCdiv,(ARClen*1e3)*m
*SET,ACLdiv,((L/4-R)*1e3/2)*m

LESIZE,1,,,ARCdiv
LESIZE,9,,,ARCdiv
LESIZE,6,,,ARCdiv
LESIZE,5,,,ARCdiv

LESIZE,10,,,ACLdiv,3
LESIZE,8,,,ACLdiv,3
LESIZE,3,,,ACLdiv,3

LESIZE,11,,,ARCdiv*1,1/2
LESIZE,7,,,ARCdiv*1,2
LESIZE,4,,,ARCdiv
AMESH,ALL

! Load & Boundary conditions
DL,3,2,SYMM
DL,10,1,SYMM
```

```
DL,11,3,SYMM
ALLSEL


! Loading
SFL,4,PRES,-Prs
ALLSEL
SBCTRAN
FINISH

! Solution
/SOLU
ANTYPE,0
SAVE
SOLVE
FINISH

! Enter Postprocessor
/POST1
ETABLE,Sig,S,EQV
ETABLE,Vol,VOLU
*GET,Emax,ELEM,0,COUNT

*SET,Vtot,0
*DO,kk,1,Emax
*GET,Evol,ELEM,kk,ETAB,Vol
Vtot=Vtot+Evol
*ENDDO

! Evaluate the multipliers
*SET,SumRef,0
*DO,kk,1,Emax
*GET,SigEq,ELEM,kk,ETAB,Sig
*GET,Evol,ELEM,kk,ETAB,Vol
SumRef=SumRef+((SigEq**2)*Evol)
```

```
*ENDDO

SIGref=SQRT(SumRef/Vtot)

m0_1=(YS/SIGref)
*SET,m_0,m0_1

ESORT,ETAB,Sig,0
*GET,SIGmax,SORT,0,MAX
m_L=(YS/SIGmax)

*SET,Jeta,(m_0/m_L)
*SET,Tan_theta,0.2929
m_tangent=m_0/(1+(Jeta-1)*Tan_theta)

! Open file
*CFOPEN,m_PlateHole13000
*CFWRITE,m0,m_0
*CFWRITE,mL,m_L
*CFWRITE,m_tangent,m_tangent
*CFCLOS
FINISH
```

A.3 Indeterminate Beam

```
/TITLE, Indeterminate beam

! Beam Dimensions (m)
*SET,H,25.4e-3
*SET,D,25.4e-3
*SET,Len,508e-3

! Loading
*SET,Prs,1.0e6
```

```
! Material model
*SET,YS,206.85e6
*SET,EM,206.85e9
*SET,Pois,0.3

! Enter preprocessor
/PREP7
ET,1,PLANE82,,,3
R,THK,D

MP,EX,1,EM
MP,NUXY,1,Pois

! Modeling geometry
K,1
K,2,,H/2
K,3,,H
K,4,Len
K,5,Len,H/2
K,6,Len,H

L,1,2
L,2,3
L,1,4
L,4,5
L,5,6
L,6,3
L,2,5

AL,1,3,4,7
AL,7,5,6,2

! Meshing
*SET,m,20
```

```
*SET,Hdiv,(1/2)*m
*SET,Ldiv,20*m

LESIZE,1,,,Hdiv,1/1
LESIZE,2,,,Hdiv,1
LESIZE,4,,,Hdiv,1/1
LESIZE,5,,,Hdiv,1

LESIZE,3,,,Ldiv,1/1
LESIZE,7,,,Ldiv,1/1
LESIZE,6,,,Ldiv,1
AMESH,ALL

! Boundary conditions
LSEL,S,LINE,,1
LSEL,A,LINE,,2
DL,ALL,,UX,0
ALLSEL

LSEL,S,LINE,,1
LSEL,A,LINE,,2
DL,ALL,,UY,0
ALLSEL

*GET,X4,KP,4,LOC,X
NSEL,S,LOC,X,X4,X4+1
D,ALL,UY,0
ALLSEL

! Loading
LSEL,S,LINE,,6
SFL,ALL,PRES,Prs
ALLSEL
SBCTRAN
FINISH
```

```
! Solving
/SOLU
ANTYPE,0
SOLVE
SAVE
FINISH

! Enter postprocessor
/POST1
ETABLE,Sig,S,EQV
ETABLE,Vol,VOLU
*GET,Emax,ELEM,0,COUNT

*SET,Vtot,0
*DO,kk,1,Emax
*GET,Evol,ELEM,kk,ETAB,Vol
Vtot=Vtot+Evol
*ENDDO

! Evaluate multipliers
*SET,SumRef,0

*DO,kk,1,Emax
*GET,SigEq,ELEM,kk,ETAB,Sig
*GET,Evol,ELEM,kk,ETAB,Vol
SumRef=SumRef+((SigEq**2)*Evol)
*ENDDO

SIGref=SQRT(SumRef/Vtot)

m0_1=(YS/SIGref)
*SET,m_0,m0_1

ESORT,ETAB,Sig,0
```

```
*GET,SIGmax,SORT,0,MAX
m_L=(YS/SIGmax)

*SET,Jeta,(m_0/m_L)
*SET,Tan_theta,0.2929
m_Tangent=m_0/(1+(Jeta-1)*Tan_theta)
FINISH
```

A.4 Unreinforced Nozzle on Hemispherical Head

```
/TITLE, Unreinforced Nozzle on Hemispherical Head

! Head dimension (in.)
*SET,Rhi,(36*0.254)
*SET,Th,(3.25*0.254)
*SET,Trh,(3.025*0.254)

*SET,Rhbs,Rhi+Trh
*SET,Rh0,Rhi+Th

! Nozzle dimension
*SET,Rni,(5.375*0.254)
*SET,Tn,(1.00*0.254)
*SET,Trn,(0.957*0.254)

*SET,Rnbs,Rni+Trn
*SET,Rn0,Rni+Tn

*SET,Len,10*SQRT(Rnbs*Trn)

! Loading
*SET,Prs,24.132e6

! Material  model
```

```
*SET,YS,262e6
*SET,EM,262e9
*SET,Pois,0.3

*AFUN,DEG
*SET,Pi,3.1416

! Enter preprocessor
/PREP7
ET,1,PLANE82,,,1,,1
MP,EX,1,EM
MP,NUXY,1,Pois

! Geometry
K,100
K,1,,Rhi
K,2,Rhi
LARC,1,2,100,Rhi

K,3,,Rh0
K,4,Rh0
LARC,3,4,100,Rh0

K,5,Rni,Rh0+Len
K,6,Rnbs,Rh0+Len
K,7,Rni,Rhi/2
K,8,Rnbs,Rhi/2

L,5,7
L,6,8
L,5,6

LCSL,1,3
LCSL,7,4
LCSL,2,8
```

```
LCSL,7,3

LDELE,4,,,1
LDELE,6,,,1
LDELE,9,,,1
LDELE,10,,,1
L,2,4

LDELE,14,,,1
LDELE,15,,,1
L,9,12
LCOMB,12,13,0
LCOMB,1,11,0

LDIV,12,0.80
LANG,8,1,90
LDIV,2,0.96
L,100,7
LCSL,1,11
LDELE,16,,,1

AL,5,12,9,8
AL,9,6,4,7
AL,4,15,14,10
AL,14,13,3,2

! Meshing
*SET,m,20*(3/4)
*SET,Arc,(Pi*90*Rhi)/180

*SET,NlnDiv,Len*m*0.20
LESIZE,8,,,NlnDiv,1/2
LESIZE,12,,,NlnDiv,1/2
LESIZE,6,,,NlnDiv*0.30,1/1.5
LESIZE,7,,,NlnDiv*0.30,1/2
```

```
*SET,HcirDiv,Arc*m/5
LESIZE,10,,,HcirDiv*0.15,1/3
LESIZE,15,,,HcirDiv*0.15,1/2

LESIZE,13,,,HcirDiv,1/6
LESIZE,2,,,HcirDiv,1/6

*SET,CirThk,Trh*m*0.4
LESIZE,3,,,CirThk
LESIZE,14,,,CirThk
LESIZE,4,,,CirThk
LESIZE,9,,,CirThk
LESIZE,5,,,CirThk
AMESH,ALL

! Load & boundary conditions
DL,3,3,UY,0

LSEL,S,LINE,,13
LSEL,A,LINE,,15
LSEL,A,LINE,,6
LSEL,A,LINE,,12
SFL,ALL,PRES,Prs
ALLSEL
SBCTRAN
FINISH

! Solving
/SOLU
ANTYPE,0
SOLVE
SAVE
FINISH
```

```
! Enter postprocessor
/POST1
ETABLE,Sig,S,EQV
ETABLE,Vol,VOLU
*GET,Emax,ELEM,0,COUNT

*SET,Vtot,0
*DO,kk,1,Emax
*GET,Evol,ELEM,kk,ETAB,Vol
Vtot=Vtot+Evol
*ENDDO

! Evaluate multipliers
*SET,SumRef,0

*DO,kk,1,Emax
*GET,SigEq,ELEM,kk,ETAB,Sig
*GET,Evol,ELEM,kk,ETAB,Vol
SumRef=SumRef+((SigEq**2)*Evol)
*ENDDO

SIGref=SQRT(SumRef/Vtot)

m0_1=(YS/SIGref)
*SET,m_0,m0_1

ESORT,ETAB,Sig,0
*GET,SIGmax,SORT,0,MAX
m_L=(YS/SIGmax)

*SET,Jeta,(m_0/m_L)
*SET,Tan_theta,0.2929
m_tangent=m_0/(1+(Jeta-1)*Tan_theta)

! Open file
```

```
*CFOPEN,m_PlateHole13100
*CFWRITE,m0,m_0
*CFWRITE,mL,m_L
*CFWRITE,m_tangent,m_tangent
*CFCLOS
FINISH
```

A.5 Torispherical Head

```
/TITLE, Torispherical Head

! Torispherical head dimension
*SET,Rs,1000
*SET,Ts,50
*SET,Rk,240
*SET,Rh,1600

*SET,Hh,(Rs/2.118)
*SET,Ls,750

*AFUN,DEG
*SET,Pi,3.1416

! Loading
*SET,Prs,5e6

! Material model
*SET,YS,262e6
*SET,EM,262e9
*SET,Pois,0.3

! Enter Preprocessor
/PREP7
```

```
ET,1,PLANE82,,,1,,1
MP,EX,1,EM
MP,NUXY,1,Pois

! Geometry
K,100
K,1,Rs
K,2,(Rs+Ts)
K,3,Rs,(-L)
K,4,(Rs+Ts),(-Ls)

L,1,2
L,1,3
L,3,4
L,4,2

K,110,(Rs-Rk)
K,10,(Rs-Rk),Rk
K,20,(Rs-Rk),(Rk+Ts)
LARC,1,10,110,Rk
LARC,2,20,110,(Rk+Ts)

K,7,,Hh
K,8,,(Hh+Ts)
L,7,8
K,170,,-(R-Hh)
K,1700,Rs,-(R-Hh)
CSKP,11,SPHE,17,170,7

K,70,Rh
K,80,(Rh+Ts)
LARC,7,70,170,Rh
LARC,8,80,170,(Rh+Ts)
CSYS,0
```

```
LCSL,5,8
LCSL,6,9
LDELE,13,,,1
LDELE,17,,,1
LDELE,12,,,1

LDELE,16,,,1
LDELE,14,,,1
LDELE,18,,,1

LCOMB,5,19,0
LCOMB,10,15,0
L,6,11

AL,6,8,7,11
AL,6,10,1,5
AL,1,2,3,4

! Meshing
*SET,m,2
*SET,THKdiv,2.5*m

LESIZE,7,,,THKdiv
LESIZE,6,,,THKdiv
LESIZE,1,,,THKdiv
LESIZE,3,,,THKdiv

*SET,CIRdiv,25*m
LESIZE,8,,,CIRdiv
LESIZE,11,,,CIRdiv

*SET,TORIdiv,6*m
LESIZE,5,,,TORIdiv,1
LESIZE,10,,,TORIdiv,1
```

```
*SET,SHLdiv,15
LESIZE,2,,,SHLdiv,1
LESIZE,4,,,SHLdiv,1
AMESH,ALL
! Boundary Conditions
DL,7,1,UX,0
DL,3,2,UY,0
ALLSEL

! Loading
LSEL,S,LINE,,1
LSEL,A,LINE,,10
LSEL,A,LINE,,2
SFL,ALL,PRES,Prs
ALLSEL
SBCTRAN
FINISH

! Enter Solver
/SOLU
ANTYPE,0
SOLVE
SAVE
FINISH

! Enter Postprocessor
/POST1
ETABLE,Sig,S,EQV
ETABLE,Vol,VOLU
*GET,Emax,ELEM,0,COUNT

*SET,Vtot,0
*DO,kk,1,Emax
*GET,Evol,ELEM,kk,ETAB,Vol
Vtot=Vtot+Evol
```

```
*ENDDO

! Evaluate Multipliers
*SET,SumRef,0
*DO,kk,1,Emax
*GET,SigEq,ELEM,kk,ETAB,Sig
*GET,Evol,ELEM,kk,ETAB,Vol
SumRef=SumRef+((SigEq**2)*Evol)
*ENDDO

SIGref=SQRT(SumRef/Vtot)

m0_1=(YS/SIGref)
*SET,m_0,m0_1

ESORT,ETAB,Sig,0
*GET,SIGmax,SORT,0,MAX
m_L=(YS/SIGmax)

! Evaluate Multipliers
*SET,Jeta,(m_0/m_L)
*SET,Tan_theta,0.2929
m_Tangent=m_0/(1+(Jeta-1)*Tan_theta)
FINISH

! Enter Postprocessor
/POST1
PATH,ToriH03,2,,4
PPATH,1,13
PPATH,2,100
PDEF,ToriH3,S,EQV,AVG
PLPATH,ToriH0
PLSECT,S,EQV,(Rs+Ts),1

PATH,ToriH02,2,,40
```

```
PPATH,1,1
PPATH,2,2
PDEF,ToriH0,S,EQV,AVG
PLPATH,ToriH2
PLSECT,S,EQV,(R+T/2),1
FINISH
```

A.6 Compact Tension (CT) Specimen

```
/TITLE, Compact Tension (CT) Specimen

! Compact Tension (CT) Specimen Dimensions (m)
*SET,W,100e-3
*SET,H,(1.25*W)
*SET,Wtot,(1.25*W)

*SET,B,3e-3
*SET,a,46e-3

*SET,Wtaper,80e-3
*SET,Wcrack,75e-3
*SET,Htaper,3e-3

*SET,LCCy,(0.275*W)
*SET,R,(0.125*W)

! Loading
*SET,Load,5e3

! Material Model
*SET,YS,206.85e6
*SET,EM,206.85e9
*SET,Es,(EM/3)
*SET,Pois,0.3
```

```
*AFUN,DEG
*SET,Pi,3.1416

! Enter Preprocessor
/PREP7
ET,1,PLANE82,,,3
R,1,B

MP,EX,1,EM
MP,EX,2,Es
MP,NUXY,1,Pois

! Geometry
K,1,a
K,2,W
K,3,W,H/2
K,4,,H/2

K,5,(W-Wtot),H/2
K,6,(W-Wtot),Htaper
K,7,,Htaper
K,8,(W-Wtaper),Htaper
K,9,(W-Wcrack)

K,10,,LCCy
K,11,,LCCy,LCCy
CIRCLE,10,R,11,4,,64
L,1,2
*REPEAT,8,1,1
L,9,1
L,4,12
L,7,44

KSEL,S,LOC,X,-1e-6,1
```

```
LSLK,S,1
AL,ALL

KSEL,S,LOC,X,-1,1e-6
LSLK,S,1
AL,ALL
KSEL,ALL
LSEL,ALL

! Meshing
ESIZE,a/12
KSCON,1,a/18,1.0,8
*SET,Hdiv,36
*SET,Wdiv,14

LESIZE,69,,,Hdiv
LESIZE,74,,,14
LESIZE,75,,,8

LESIZE,68,,,Wdiv
LESIZE,70,,,Wdiv
LESIZE,71,,,12
LESIZE,72,,,4

LESIZE,73,,,12
LESIZE,65,,,32
AMESH,ALL

! Modify elastic modulus of the singular elements
NSEL,S,NODE,,182
ESLN,S,0,ALL
EMODIF,ALL,MAT, 2
ALLSEL

! Displacement Boundary Conditions
```

```
LSEL,S, LINE,,65
DL, ALL, ,SYMM
ALLSEL

! Loading
P=Load/256
FK,27,FY,P*1
FK,26,FY,P*2
FK,25,FY,P*3

FK,24,FY,P*4
FK,23,FY,P*5
FK,22,FY,P*6
FK,21,FY,P*7

FK,20,FY,P*8
FK,19,FY,P*9
FK,18,FY,P*10
FK,17,FY,P*11

FK,16,FY,P*12
FK,15,FY,P*13
FK,14,FY,P*14
FK,13,FY,P*15
FK,12,FY,P*16

FK,75,FY,P*15
FK,74,FY,P*14
FK,73,FY,P*13
FK,72,FY,P*12

FK,71,FY,P*11
FK,70,FY,P*10
FK,69,FY,P*9
FK,68,FY,P*8
```

```
FK,67,FY,P*7
FK,66,FY,P*6
FK,65,FY,P*5
FK,64,FY,P*4

FK,63,FY,P*3
FK,62,FY,P*2
FK,61,FY,P*1
ALLSEL
SBCTRAN
FINISH

! Solving
/SOLU
ANTYPE, 0
SOLVE
SAVE
FINISH

! Enter Post Processor
/POST1
ETABLE,Sig,S,EQV
ETABLE,Vol,VOLU
*GET,Emax,ELEM,0,COUNT

*SET,Vtot,0
*DO,kk,1,Emax
*GET,Evol,ELEM,kk,ETAB,Vol
Vtot=Vtot+Evol
*ENDDO

! Evaluate Multipliers
*SET,SumRef,0
```

```
*DO, kk, 1, Emax
*GET,SigEq,ELEM,kk,ETAB,Sig
*GET,Evol,ELEM,kk,ETAB,Vol
SumRef=SumRef+((SigEq**2)*Evol)
*ENDDO
SIGref=SQRT(SumRef/Vtot)

m0_1=(YS/SIGref)
*SET,m_0,m0_1

ESORT,ETAB,Sig,0
*GET,SIGmax,SORT,0,MAX
m_L=(YS/SIGmax)

! Evaluate Multipliers
*SET,Jeta,(m_0/m_L)
*SET,Tan_theta,0.2929
m_Tangent=m_0/(1+(Jeta-1)*Tan_theta)
FINISH
```

A.7 Plate with a Centre Crack

```
/TITLE, Plate with a Centre Crack

! Plate Dimensions (m)
*SET,W,125e-3
*SET,L,300e-3
*SET,B,3e-3
*SET,a,25e-3

*AFUN,DEG
*SET,Pi,3.1416

! Loading
```

```
*SET,Prs,75e6

! Material
*SET,YS,206.85e6
*SET,EM,206.85e9
*SET,Es,(EM/3)
*SET,Pois,0.3

! Enter Preprocessor
/PREP7
ET,1,PLANE82,,,3
R,1,B
MP,EX,1,EM
MP,EX,2,Es
MP,NUXY,1,Pois

! Quarter geometry
K,1,a
K,2,W
K,3,W,L
K,4,,L
K,5

L,1,2
L,2,3
L,3,4
L,4,5
L,5,1

LDIV,2,1/4,20,,0
LANG,4,20,90,40
AL,1,2,8,7,5
AL,8,6,3,4

! Meshing
```

```
ESIZE,a/3
KSCON,1,a/2.5,1.0,8

*SET,LCdiv,30
*SET,Ldiv,20
*SET,Wdiv,30
AMESH,1

LESIZE,4,,,Ldiv,1/2.5
LESIZE,6,,,Ldiv,2.5
AMESH,2

! Modify material of the singular element
NSEL,S,NODE,,1
ESLN,S,0,ALL
EMODIF,ALL,MAT,2
ALLSEL

! Displacement Boundary Conditions
LSEL,S,LINE,,1
DL,ALL,,SYMM
ALLSEL

LSEL,S,LINE,,4
LSEL,A,LINE,,7
DL,ALL,,SYMM
ALLSEL

! Loading
LSEL,S,LINE,,3
SFL,ALL,PRES,-Prs
ALLSEL
SBCTRAN
FINISH
```

```
! Solving
/SOLU
ANTYPE,0
SOLVE
SAVE
FINISH

! Evaluate Multipliers
/POST1
ETABLE,Sig,S,EQV
ETABLE,Vol,VOLU
*GET,Emax,ELEM,0,COUNT

*SET,Vtot,0
*DO,kk,1,Emax
*GET,Evol,ELEM,kk,ETAB,Vol
Vtot=Vtot+Evol
*ENDDO

! Evaluate multipliers
*SET,SumRef,0

*DO,kk,1,Emax
*GET,SigEq,ELEM,kk,ETAB,Sig
*GET,Evol,ELEM,kk,ETAB,Vol
SumRef=SumRef+((SigEq**2)*Evol)
*ENDDO

SIGref=SQRT(SumRef/Vtot)
m0_1=(YS/SIGref)
*SET,m_0,m0_1

ESORT,ETAB,Sig,0
*GET,SIGmax,SORT,0,MAX
m_L=(YS/SIGmax)
```

```
*SET,Jeta,(m_0/m_L)
*SET,Tan_theta,0.2929
m_Tangent=m_0/(1+(Jeta-1)*Tan_theta)
m_Pro=(2*YS)/(SIGmax+SIGref)
FINISH
```

A.8 Cylinder with Internal Corrosion

```
/TITLE, Cylinder with Internal Corrosion

! Cylinder Dimensions (m)
*SET, pi, 3.14159265

! Basic inputs
*SET,Ri,33
*SET,h,0.625
*SET,Ro,(Ri+h)

*SET,Ln,100

! Corosion dimension
*SET,c,(h/3)
*SET,h_c,(h-c)
*SET,Rc,(Ri+c)

*SET,a,10
*SET,b,10
*SET,theta_c,(a/Ro)*(180/pi)

! Material model
*SET,EM,30E6
*SET,PM,50E4
*SET,Pois,0.3
```

```
*SET,YS,30E3

*SET,Temp,(100-32)*(5/9)

! Loading
*SET,Pd,220
*SET,P,(Pd*10)

*SET,SIG_lon,(Pd*Ri)/(2*h_c)

! Enter Preprocessor
/PREP7
/TITLE, Cylindrical shell, Solid 185
ET,1,SOLID185

! Material properties for temperature 100 deg. F
MP,EX,1,EM
MP,PRXY,1,Pois

TB,BKIN,1,,,1
TBTEMP,Temp
TBDATA,,YS,PM

! Arc length
*SET,ARC_o,(Ro*90)*(Pi/180)
*SET,ARC_c,(Rc*90)*(Pi/180)
*SET,ARC_i,(Ri*90)*(Pi/180)

*SET,ARC_co,(Ro*theta_c)*(Pi/180)
*SET,ARC_cc,(Rc*theta_c)*(Pi/180)
*SET,ARC_ci,(Ri*theta_c)*(Pi/180)

*SET,Ratio_o,ARC_co/ARC_o
*SET,Ratio_c,ARC_cc/ARC_c
*SET,Ratio_i,ARC_ci/ARC_i
```

```
! Geometry
K,100
K,1,,Rc
K,2,Rc
K,3,,-Rc

LARC,1,2,100,Rc
LARC,2,3,100,Rc

K,4,,Ro
K,5,Ro
K,6,,-Ro
K,7,,Ri
K,8,Ri
K,9,,-Ri

LARC,4,5,100,Ro
LARC,5,6,100,Ro
LARC,7,8,100,Ri
LARC,8,9,100,Ri

LDIV,3,Ratio_o,10,0
LDIV,1,Ratio_c,11,0
LDIV,5,Ratio_i,12,0

L,10,11
L,11,12
L,4,7
LCSL,1,12

L,5,2
L,2,8
L,6,3
L,3,9
```

```
AL,1,14,5,11
AL,1,10,3,13
AL,11,9,15,8
AL,8,12,7,10
AL,15,6,17,2
AL,12,2,16,4

K,111,,Rc,b
L,1,111
VDRAG,1,2,3,4,5,6,18

K,131,,Rc,50
L,13,131
VDRAG,11,15,19,22,26,29,48

VDELE,1,,,1
LDELE,18,,,1
LDELE,48,,,1

K,311,Rc,,Ln
L,31,311
VDRAG,34,38,42,45,49,52,5
LDELE,5,,,1

! MESHING
*SET,Hdiv,6
*SET,Hcdiv,3

*SET,LTAdiv_a,28
*SET,LTAdiv_b,28
*SET,CIRdiv_Xc,44
*SET,CIRxc_ratio,2

*SET,LENdiv_Xl,42
```

```
*SET,LENxl_ratio,1.5
*SET,CIRdiv_90,38
*SET,LENdiv_Xlad,38

LESIZE,1,,,LTAdiv_a
LESIZE,3,,,LTAdiv_a
LESIZE,24,,,LTAdiv_a
LESIZE,19,,,LTAdiv_a
LESIZE,29,,,LTAdiv_a

LESIZE,54,,,LTAdiv_a
LESIZE,49,,,LTAdiv_a
LESIZE,59,,,LTAdiv_a

LESIZE,79,,,LTAdiv_a
LESIZE,14,,,LTAdiv_a
LESIZE,84,,,LTAdiv_a

LESIZE,20,,,LTAdiv_b,LTA_ratio
LESIZE,30,,,LTAdiv_b,LTA_ratio
LESIZE,23,,,LTAdiv_b,LTA_ratio

LESIZE,21,,,LTAdiv_b,LTA_ratio
LESIZE,28,,,LTAdiv_b,LTA_ratio

LESIZE,33,,,LTAdiv_b,LTA_ratio
LESIZE,35,,,LTAdiv_b,LTA_ratio
LESIZE,38,,,LTAdiv_b,LTA_ratio

LESIZE,41,,,LTAdiv_b,LTA_ratio
LESIZE,43,,,LTAdiv_b,LTA_ratio
LESIZE,46,,,LTAdiv_b,LTA_ratio

LESIZE,7,,,CIRdiv_Xc,CIRxc_ratio
LESIZE,8,,,CIRdiv_Xc,CIRxc_ratio
```

```
LESIZE,9,,,CIRdiv_Xc,CIRxc_ratio

LESIZE,32,,,CIRdiv_Xc,CIRxc_ratio
LESIZE,36,,,CIRdiv_Xc,1/CIRxc_ratio
LESIZE,39,,,CIRdiv_Xc,1/CIRxc_ratio

LESIZE,62,,,CIRdiv_Xc,CIRxc_ratio
LESIZE,66,,,CIRdiv_Xc,1/CIRxc_ratio
LESIZE,69,,,CIRdiv_Xc,1/CIRxc_ratio

LESIZE,87,,,CIRdiv_Xc,CIRxc_ratio
LESIZE,91,,,CIRdiv_Xc,1/CIRxc_ratio
LESIZE,94,,,CIRdiv_Xc,1/CIRxc_ratio

LESIZE,4,,,CIRdiv_90
LESIZE,2,,,CIRdiv_90
LESIZE,6,,,CIRdiv_90

LESIZE,40,,,CIRdiv_90
LESIZE,44,,,CIRdiv_90
LESIZE,47,,,CIRdiv_90

LESIZE,70,,,CIRdiv_90
LESIZE,74,,,CIRdiv_90
LESIZE,77,,,CIRdiv_90

LESIZE,95,,,CIRdiv_90
LESIZE,99,,,CIRdiv_90
LESIZE,102,,,CIRdiv_90

LESIZE,60,,,LENdiv_Xl,LENxl_ratio
LESIZE,50,,,LENdiv_Xl,LENxl_ratio
LESIZE,55,,,LENdiv_Xl,LENxl_ratio

LESIZE,53,,,LENdiv_Xl,LENxl_ratio
```

```
LESIZE,51,,,LENdiv_Xl,LENxl_ratio
LESIZE,58,,,LENdiv_Xl,LENxl_ratio

LESIZE,63,,,LENdiv_Xl,LENxl_ratio
LESIZE,65,,,LENdiv_Xl,LENxl_ratio
LESIZE,68,,,LENdiv_Xl,LENxl_ratio

LESIZE,71,,,LENdiv_Xl,LENxl_ratio
LESIZE,73,,,LENdiv_Xl,LENxl_ratio
LESIZE,76,,,LENdiv_Xl,LENxl_ratio

LESIZE,85,,,LENdiv_Xlad
LESIZE,18,,,LENdiv_Xlad
LESIZE,80,,,LENdiv_Xlad

LESIZE,83,,,LENdiv_Xlad
LESIZE,25,,,LENdiv_Xlad
LESIZE,78,,,LENdiv_Xlad

LESIZE,88,,,LENdiv_Xlad
LESIZE,90,,,LENdiv_Xlad
LESIZE,93,,,LENdiv_Xlad

LESIZE,96,,,LENdiv_Xlad
LESIZE,98,,,LENdiv_Xlad
LESIZE,101,,,LENdiv_Xlad

LESIZE,13,,,Hdiv
LESIZE,10,,,Hdiv
LESIZE,27,,,Hdiv

LESIZE,31,,,Hdiv
LESIZE,12,,,Hdiv
LESIZE,37,,,Hdiv
```

```
LESIZE,16,,,Hdiv
LESIZE,45,,,Hdiv

LESIZE,61,,,Hdiv
LESIZE,57,,,Hdiv
LESIZE,67,,,Hdiv
LESIZE,75,,,Hdiv

LESIZE,11,,,Hcdiv
LESIZE,22,,,Hcdiv
LESIZE,26,,,Hcdiv

LESIZE,15,,,Hcdiv
LESIZE,34,,,Hcdiv
LESIZE,17,,,Hcdiv
LESIZE,42,,,Hcdiv

LESIZE,56,,,Hcdiv
LESIZE,52,,,Hcdiv
LESIZE,64,,,Hcdiv
LESIZE,72,,,Hcdiv

VMESH,ALL
*GET,EMAX,ELEM,0,COUNT

! Apply symmetric boundary conditions
ASEL,S,AREA,,2
ASEL,A,AREA,,3
ASEL,A,AREA,,4
ASEL,A,AREA,,5
ASEL,A,AREA,,6
DA,ALL,SYMM
ALLSEL

ASEL,S,AREA,,14
```

```
ASEL,A,AREA,,33
ASEL,A,AREA,,37
ASEL,A,AREA,,53
ASEL,A,AREA,,57
DA,ALL,SYMM
ALLSEL

ASEL,S,AREA,,24
ASEL,A,AREA,,27
ASEL,A,AREA,,47
ASEL,A,AREA,,50
ASEL,A,AREA,,67
ASEL,A,AREA,,70
DA,ALL,SYMM
ALLSEL

ASEL,S,AREA,,54
ASEL,A,AREA,,58
ASEL,A,AREA,,62
ASEL,A,AREA,,65
ASEL,A,AREA,,69
ASEL,A,AREA,,72
DA,ALL,UZ,0
ALLSEL

DK,43,UX,0
DK,43,UY,0

! Apply internal pressure
ASEL,S,AREA,,7
ASEL,A,AREA,,8
ASEL,A,AREA,,11
ASEL,A,AREA,,32

ASEL,A,AREA,,16
```

```
ASEL,A,AREA,,39
ASEL,A,AREA,,23
ASEL,A,AREA,,46

ASEL,A,AREA,,10
ASEL,A,AREA,,59
ASEL,A,AREA,,66
SFA,ALL,1,PRES,P
ALLSEL

ASEL,S,AREA,,2
ASEL,A,AREA,,3
ASEL,A,AREA,,4
ASEL,A,AREA,,5
ASEL,A,AREA,,6
SFA,ALL,,PRES,-SIG_lon
ALLSEL

DTRAN
SFTRAN
FINISH

! SOLVING
/SOLU
ANTYPE,0
PRED,ON,,ON

AUTOS,ON
NSUBST,500
OUTRESS,ALL,ALL

SOLVE
SAVE
FINISH
```

A.9 Cylinder with Thermal Hot Spot

```
/TITLE, Cylinder with Thermal Hot Spot

! Cylinder Dimensions (m)
*SET,pi,3.1416

! Basic inputs
*SET,Ri,33
*SET,h,0.625
*SET,Ro,(Ri+h)
*SET,Ln,100

! Corosion dimension
*SET,c,(h/3)
*SET,h_c,(h-c)
*SET,Rc,(Ri+c)

*SET,a,10
*SET,b,10
*SET,theta_c,(a/Ro)*(180/pi)

! Arc length
*SET,ARC_o,(Ro*90)*(Pi/180)
*SET,ARC_c,(Rc*90)*(Pi/180)
*SET,ARC_i,(Ri*90)*(Pi/180)

*SET,ARC_co,(Ro*theta_c)*(Pi/180)
*SET,ARC_cc,(Rc*theta_c)*(Pi/180)
*SET,ARC_ci,(Ri*theta_c)*(Pi/180)

*SET,Ratio_o,ARC_co/ARC_o
*SET,Ratio_c,ARC_cc/ARC_c
*SET,Ratio_i,ARC_ci/ARC_i
```

```
! Loading
*SET,Pd,(220*10)

! Preprocessor
/PREP7

! Geometry modeling
K,100
K,1,,Rc
K,2,Rc
K,3,,-Rc

LARC,1,2,100,Rc
LARC,2,3,100,Rc

K,4,,Ro
K,5,Ro
K,6,,-Ro
K,7,,Ri
K,8,Ri
K,9,,-Ri

LARC,4,5,100,Ro
LARC,5,6,100,Ro
LARC,7,8,100,Ri
LARC,8,9,100,Ri

LDIV,3,Ratio_o,10,0
LDIV,1,Ratio_c,11,0
LDIV,5,Ratio_i,12,0

L,10,11
L,11,12
L,4,7
```

```
LCSL,1,12

L,5,2
L,2,8
L,6,3
L,3,9

AL,1,14,5,11
AL,1,10,3,13
AL,11,9,15,8

AL,8,12,7,10
AL,15,6,17,2
AL,12,2,16,4

K,111,,Rc,b
L,1,111
VDRAG,1,2,3,4,5,6,18

K,131,,Rc,50
L,13,131
VDRAG,11,15,19,22,26,29,48

VDELE,1,,,1
LDELE,18,,,1
LDELE,48,,,1

K,311,Rc,,Ln
L,31,311
VDRAG,34,38,42,45,49,52,5
LDELE,5,,,1

K,101,,,Ln
K,102,,,(Ln+Ri)
LARC,42,102,101,Ri
```

```
VDRAG,62,65,,,,,5

LARC,39,49,101,Ri
LARC,7,48,101,Rc
LARC,41,53,101,Ro

AL,81,116,103,117
AL,86,117,115,118
AL,84,114,118
AL,14,104,117
AL,79,105,116

VA,58,83,84,80,85
VA,54,82,85,73,86

LARC,45,50,101,Ri
LARC,46,51,101,Rc
LARC,47,52,101,Ro
LDELE,5,,,1

AL,111,120,100,121
AL,108,119,97,120
AL,112,102,121
AL,109,99,120
AL,107,95,119

VA,87,78,89,72,90
VA,88,75,90,69,91
VDRAG,11,,,,,,23
VGLUE,2,24,3

AREVERSE,7
AREVERSE,23
AREVERSE,16
```

```
AREVERSE,39
AREVERSE,59
AREVERSE,46
AREVERSE,66
AREVERSE,74

AREVERSE,2
AREVERSE,3
AREVERSE,4
AREVERSE,5
AREVERSE,6

AREVERSE,33
AREVERSE,53
AREVERSE,82

AREVERSE,87
AREVERSE,88
AREVERSE,99

! Meshing
*SET,Hdiv,3
*SET,Hcdiv,2
*SET,LTAdiv_a,40
*SET,LTAdiv_b,40

*SET,CIRdiv_Xc,38
*SET,CIRxc_ratio,2.5
*SET,LENdiv_Xl,36
*SET,LENxl_ratio,3.5

*SET,CIRdiv_90,40
*SET,LENdiv_Xlad,34

LESIZE,1,,,LTAdiv_a
```

```
LESIZE,3,,,LTAdiv_a
LESIZE,130,,,LTAdiv_a

LESIZE,24,,,LTAdiv_a
LESIZE,19,,,LTAdiv_a
LESIZE,29,,,LTAdiv_a

LESIZE,54,,,LTAdiv_a
LESIZE,49,,,LTAdiv_a
LESIZE,59,,,LTAdiv_a

LESIZE,79,,,LTAdiv_a
LESIZE,14,,,LTAdiv_a
LESIZE,84,,,LTAdiv_a

LESIZE,20,,,LTAdiv_b
LESIZE,30,,,LTAdiv_b
LESIZE,127,,,LTAdiv_b

LESIZE,23,,,LTAdiv_b
LESIZE,21,,,LTAdiv_b
LESIZE,28,,,LTAdiv_b

LESIZE,33,,,LTAdiv_b
LESIZE,35,,,LTAdiv_b
LESIZE,38,,,LTAdiv_b
LESIZE,41,,,LTAdiv_b
LESIZE,43,,,LTAdiv_b
LESIZE,46,,,LTAdiv_b

LESIZE,127,,,LTAdiv_b

LESIZE,7,,,CIRdiv_Xc,CIRxc_ratio
LESIZE,8,,,CIRdiv_Xc,CIRxc_ratio
LESIZE,9,,,CIRdiv_Xc,CIRxc_ratio
```

```
LESIZE,32,,,CIRdiv_Xc,CIRxc_ratio
LESIZE,36,,,CIRdiv_Xc,1/CIRxc_ratio
LESIZE,39,,,CIRdiv_Xc,1/CIRxc_ratio

LESIZE,62,,,CIRdiv_Xc,CIRxc_ratio
LESIZE,66,,,CIRdiv_Xc,1/CIRxc_ratio
LESIZE,69,,,CIRdiv_Xc,1/CIRxc_ratio

LESIZE,87,,,CIRdiv_Xc,CIRxc_ratio
LESIZE,91,,,CIRdiv_Xc,1/CIRxc_ratio
LESIZE,94,,,CIRdiv_Xc,1/CIRxc_ratio

LESIZE,4,,,CIRdiv_90
LESIZE,2,,,CIRdiv_90
LESIZE,6,,,CIRdiv_90

LESIZE,40,,,CIRdiv_90
LESIZE,44,,,CIRdiv_90
LESIZE,47,,,CIRdiv_90

LESIZE,70,,,CIRdiv_90
LESIZE,74,,,CIRdiv_90
LESIZE,77,,,CIRdiv_90

LESIZE,95,,,CIRdiv_90
LESIZE,99,,,CIRdiv_90
LESIZE,102,,,CIRdiv_90

LESIZE,60,,,LENdiv_Xl,LENxl_ratio
LESIZE,50,,,LENdiv_Xl,LENxl_ratio
LESIZE,55,,,LENdiv_Xl,LENxl_ratio

LESIZE,53,,,LENdiv_Xl,LENxl_ratio
LESIZE,51,,,LENdiv_Xl,LENxl_ratio
```

```
LESIZE,58,,,LENdiv_Xl,LENxl_ratio

LESIZE,63,,,LENdiv_Xl,LENxl_ratio
LESIZE,65,,,LENdiv_Xl,LENxl_ratio
LESIZE,68,,,LENdiv_Xl,LENxl_ratio

LESIZE,71,,,LENdiv_Xl,LENxl_ratio
LESIZE,73,,,LENdiv_Xl,LENxl_ratio
LESIZE,76,,,LENdiv_Xl,LENxl_ratio

LESIZE,85,,,LENdiv_Xlad
LESIZE,18,,,LENdiv_Xlad
LESIZE,80,,,LENdiv_Xlad

LESIZE,83,,,LENdiv_Xlad
LESIZE,25,,,LENdiv_Xlad
LESIZE,78,,,LENdiv_Xlad

LESIZE,88,,,LENdiv_Xlad
LESIZE,90,,,LENdiv_Xlad
LESIZE,93,,,LENdiv_Xlad

LESIZE,96,,,LENdiv_Xlad
LESIZE,98,,,LENdiv_Xlad
LESIZE,101,,,LENdiv_Xlad

LESIZE,13,,,Hdiv
LESIZE,10,,,Hdiv
LESIZE,27,,,Hdiv
LESIZE,31,,,Hdiv

LESIZE,12,,,Hdiv
LESIZE,37,,,Hdiv
LESIZE,16,,,Hdiv
LESIZE,45,,,Hdiv
```

```
LESIZE,61,,,Hdiv
LESIZE,57,,,Hdiv
LESIZE,67,,,Hdiv
LESIZE,75,,,Hdiv

LESIZE,11,,,Hcdiv
LESIZE,22,,,Hcdiv
LESIZE,26,,,Hcdiv
LESIZE,15,,,Hcdiv
LESIZE,34,,,Hcdiv

LESIZE,17,,,Hcdiv
LESIZE,42,,,Hcdiv
LESIZE,56,,,Hcdiv

LESIZE,52,,,Hcdiv
LESIZE,64,,,Hcdiv
LESIZE,72,,,Hcdiv

LESIZE,107,,,CIRdiv_90
LESIZE,109,,,CIRdiv_90
LESIZE,112,,,CIRdiv_90

LESIZE,119,,,CIRdiv_90
LESIZE,120,,,CIRdiv_90
LESIZE,121,,,CIRdiv_90

LESIZE,114,,,LTAdiv_a
LESIZE,104,,,LTAdiv_a
LESIZE,105,,,LTAdiv_a

LESIZE,116,,,LTAdiv_a
LESIZE,117,,,LTAdiv_a
LESIZE,118,,,LTAdiv_a
```

```
LESIZE,106,,,CIRdiv_Xc,CIRxc_ratio
LESIZE,110,,,CIRdiv_Xc,1/CIRxc_ratio
LESIZE,113,,,CIRdiv_Xc,1/CIRxc_ratio

LESIZE,81,,,Hcdiv
LESIZE,86,,,Hdiv
LESIZE,48,,,Hcdiv

LESIZE,82,,,Hdiv
LESIZE,89,,,Hcdiv
LESIZE,92,,,Hdiv

LESIZE,103,,,Hcdiv
LESIZE,115,,,Hdiv
LESIZE,108,,,Hcdiv

LESIZE,111,,,Hdiv
LESIZE,97,,,Hcdiv
LESIZE,100,,,Hdiv

! Hot Spot material model
*SET, EM_h,26.7E6
*SET,Pois,0.3
*SET,FS_h,22.2917E3
*SET,PM_h,0
*SET,Temp_h,(600-32)*(5/9)

! Remaining shell material model
*SET,EM,29.3E6
*SET,Pois,0.3
*SET,FS,30.09E3
*SET,PM,0
*SET,Temp,(100-32)*(5/9)
```

```
/TITLE, Cylindrical shell, Solid185, Hot Spot
! Element type 1
ET,1,SOLID185
ET,2,SOLID185

! Material properties for temperature 600 deg. F
MP,EX,1,EM_h
MP,PRXY,1,Pois

TB,BKIN,1,,,1
TBTEMP,Temp_h
TBDATA,,FS_h,PM_h

! Material properties for temperature 100 deg. F
MP,EX,2,EM
MP,PRXY,2,Pois

TB,BKIN,2,,,1
TBTEMP,Temp
TBDATA,,FS,PM

! Meshing the hot spot region
TYPE,1
MAT,1
VSEL,S,VOLU,,2
VSEL,A,VOLU,,25
VMESH,ALL

! Meshing the hot region
TYPE,2
MAT,2
VSEL,ALL
VSEL,U,VOLU,,2
VSEL,A,VOLU,,25
VMESH,ALL
```

```
ALLSELL

! Apply symmetric boundary conditions
ASEL,S,AREA,,2
ASEL,A,AREA,,97
ASEL,A,AREA,,3

ASEL,A,AREA,,4
ASEL,A,AREA,,5
ASEL,A,AREA,,6
DA,ALL,SYMM
ALLSEL

ASEL,S,AREA,,14
ASEL,A,AREA,,98
ASEL,A,AREA,,33

ASEL,A,AREA,,37
ASEL,A,AREA,,53
ASEL,A,AREA,,57

ASEL,A,AREA,,82
ASEL,A,AREA,,83
ASEL,A,AREA,,81
ASEL,A,AREA,,77
DA,ALL,SYMM
ALLSEL

ASEL,S,AREA,,24
ASEL,A,AREA,,27
ASEL,A,AREA,,47

ASEL,A,AREA,,50
ASEL,A,AREA,,67
ASEL,A,AREA,,70
```

```
ASEL,A,AREA,,88
ASEL,A,AREA,,87
DA,ALL,SYMM
ALLSEL
DK,51,UX,0
DK,51,UY,0

! Loading
ASEL,S,AREA,,99
ASEL,A,AREA,,32
ASEL,A,AREA,,16
ASEL,A,AREA,,39

ASEL,A,AREA,,23
ASEL,A,AREA,,46
ASEL,A,AREA,,10

ASEL,A,AREA,,59
ASEL,A,AREA,,66

ASEL,A,AREA,,86
ASEL,A,AREA,,74
ASEL,A,AREA,,91

SFA,ALL,1,PRES,Pd
ALLSEL
DTRAN
SFTRAN
FINISH

! Enter solver
/SOLU
ANTYPE,0
PRED,ON,,ON
```

```
AUTOS,ON
NSUBST,1000
OUTRESS,ALL,ALL

SOLVE
SAVE
FINISH
```

APPENDIX B

MATLAB Files

MATLAB files are used in this thesis to perform the numerical analysis of different mechanical components and structures. Typical input files of a number of example problems used in this thesis are provided in this section. The examples include standard example problem to typical pressure component configuration.

B.1 RSF for Cylinder with Corrosion Damage

```
% RSF for Cylinder with Corrosion Damage

clear;
clc;

Ri = 33;
H = 0.625;
Ro = (Ri+h);

Pd = 220;
```

```
Sy = 30e3;

c = (h/3);
h_c = (h-c);
Rc = Ro-h_c;

Theta_c = 17.0396;
aBYb = 1.0;
a = 10
b = a/aBYb

% Calculation of decay lengths
Xc = 6.10*(Ro^3*h)^(1/4)
Xl = 2.50*sqrt(Ro*h)

% Calculation of reference volume
Vc = 4*a*b*h_c
Vu = 4*h*((a+Xc)*(b+Xl)-(a*b))
Vref = (Vc+Vu)

% Calculation of elastic stresses
Stc = (Pd*Rc)/h_c
Slc = (Pd*Rc)/(2*h_c)
Sec = sqrt(Stc^2 + Slc^2 - Stc*Slc)

St = (Pd*Ri)/h
Sl = (Pd*Ri)/(2*h)
Seu = sqrt(St^2 + Sl^2 - St*Sl)

% Evaluation of multipliers
mL_d = S_flow/Sec
Num = (S_flow^2*Vref);
Den = (Sec^2*Vc)+(Seu^2*Vu);
m0_d = sqrt(Num/Den)
m0_u = Sy/Seu
```

```
% Evaluation of m-alpha multiplier
Z = m0_d/mL_d
n1 = 2*Z^2;
n2 = Z*(Z-1)^2;
n3 = 1+sqrt(2)-Z;
n4 = Z-1+sqrt(2);
n1234 = n1+sqrt(n2*n3*n4);

d1 = Z^2+2-sqrt(5);
d2 = Z^2+2+sqrt(5);
d12=(d1*d2);
m_alpha_d = 2*m0_d*(n1234/d12)

% Evaluation of m-alpha tangent multiplier
jeta_i = m0_d/mL_d;
m_alpha_tangent_B = m0_d/(1+0.2929*(jeta_i-1))

% RSF calculation
RSF_U = m0_d/m0_u
RSF_mAlpha = m_alpha_d/m0_u
RSF_mAlpha_tangent = m_alpha_tangent_B/m0_u
RSF_L = mL_d/m0_u
Return
```

B.2 RSF for Cylinder with Thermal Hot Spot

```
% RSF for Cylinder with Thermal Hot Spot
clear;
clc;

% Inputs
Ri = 33;
h = 0.625;
```

```
Pd = 220;
Ro = (Ri+h);

Sy_h = 25.7E3;
Sy = 30.0e3;

% Decay length calculation
Xc = 6.10*(Ro^3*h)^(1/4);
Xl = 2.50*(Ro*h)^(1/2);

Theta_h = 50.95
aBYb = 2.0;

a = (Theta_h/180)*pi*Ro
b = a/aBYb

% Reference volume calculation
Vh = (2*a)*(2*b)*h;
V = (2*(a+Xc)*2*(b+Xl)-(2*a)*(2*b))*h;
V_ref = Vh+V;

% Evaluation of elastic stresses
Sc = (Pd*Ri)/h;
Sl = (Pd*Ri)/(2*h);
Seq = sqrt(Sc^2 + Sl^2 - Sc*Sl);

% Evaluation of multipliers
mL_d = Sy_h/Seq;
m0_d = sqrt((Sy_h^2*Vh + Sy^2*V)/(Seq^2*V_ref));
m0_u = Sy/Seq;

% Evaluation of m-alpha multiplier
Z = m0_d/mL_d;
n1 = 2*Z^2;
n2 = Z*(Z-1)^2;
```

```
n3 = 1+sqrt(2)-Z;
n4 = Z-1+sqrt(2);
n1234 = n1+sqrt(n2*n3*n4);

d1 = Z^2+2-sqrt(5);
d2 = Z^2+2+sqrt(5);
d12=(d1*d2);
m_alpha_d = 2*m0_d*(n1234/d12);

% Evaluation of m_alpha tangent multiplier
mL_i = mL_d;
m0_i = m0_d;
jeta_i = m0_i/mL_i;
m_alpha_tangent_B = m0_i/(1+0.2929*(jeta_i-1));

% for BB"
if jeta_i > 1+sqrt(2)
C = 0.2929*(jeta_i-1);
jeta_f1 = (1+C) + sqrt((1+C)^2-1);
jeta_f2 = (1+C) - sqrt((1+C)^2-1);

m0_f = m0_i;
jeta_f = jeta_f1;
m_alpha_tangent_C = m0_f/(1+0.2929*(jeta_f-1));
else
m_alpha_tangent_C = 0;
end

% RSF Calculation
RSF_d = m0_d/m0_u;
RSF1_m_alpha = m_alpha_d/m0_u
RSF3_m_alpha_tangent = m_alpha_tangent_B/m0_u
Return
```